Theses and Dissertations   1. Thesis and Dissertation Collection, all items

2009-12

How to detect the location and time of a covert chemical attack a Bayesian approach

See, Mei Eng Elaine.

Monterey, California: Naval Postgraduate School

http://hdl.handle.net/10945/4344

NAVAL POSTGRADUATE SCHOOL

MONTEREY, CALIFORNIA

THESIS

HOW TO DETECT THE LOCATION AND TIME OF A COVERT CHEMICAL ATTACK: A BAYESIAN APPROACH

by

Mei Eng Elaine See

December 2009

Thesis Advisor: Moshe Kress
Second Reader: Rachel Johnson

Approved for public release; distribution is unlimited

THIS PAGE INTENTIONALLY LEFT BLANK

REPORT DOCUMENTATION PAGE		*Form Approved OMB No. 0704-0188*
Public reporting burden for this collection of information is estimated to average 1 hour per response, including the time for reviewing instruction, searching existing data sources, gathering and maintaining the data needed, and completing and reviewing the collection of information. Send comments regarding this burden estimate or any other aspect of this collection of information, including suggestions for reducing this burden, to Washington headquarters Services, Directorate for Information Operations and Reports, 1215 Jefferson Davis Highway, Suite 1204, Arlington, VA 22202-4302, and to the Office of Management and Budget, Paperwork Reduction Project (0704-0188) Washington DC 20503.		
1. AGENCY USE ONLY *(Leave blank)*	**2. REPORT DATE** December 2009	**3. REPORT TYPE AND DATES COVERED** Master's Thesis
4. TITLE AND SUBTITLE How to Detect the Location and Time of a Covert Chemical Attack: A Bayesian Approach		**5. FUNDING NUMBERS**
6. AUTHOR(S) Mei Eng Elaine See		
7. PERFORMING ORGANIZATION NAME(S) AND ADDRESS(ES) Naval Postgraduate School Monterey, CA 93943-5000		**8. PERFORMING ORGANIZATION REPORT NUMBER**
9. SPONSORING /MONITORING AGENCY NAME(S) AND ADDRESS(ES) N/A		**10. SPONSORING/MONITORING AGENCY REPORT NUMBER**
11. SUPPLEMENTARY NOTES The views expressed in this thesis are those of the author and do not reflect the official policy or position of the Department of Defense or the U.S. Government.		
12a. DISTRIBUTION / AVAILABILITY STATEMENT Approved for public release; distribution is unlimited		**12b. DISTRIBUTION CODE** A

13. ABSTRACT (maximum 200 words)

In this thesis, we develop a Bayesian updating model that estimates the location and time of a chemical attack using inputs from chemical sensors and Atmospheric Threat and Dispersion (ATD) models. In bridging the critical gap between raw sensor data and threat evaluation and prediction, the model will help authorities perform better hazard prediction and damage control.

The model is evaluated with respect to settings representing real-world operations. Factors that affect the model's capability to accurately estimate the location and time of an attack are (i) the specific layout of the deployed sensors relative to the attack location; (ii) the number of false positive signals; and (iii) the number of false negative errors. An experimental design is used to evaluate the model against the factors identified. The dominant factor is the Expected Number of Correct Signals (ENCS), which depends on the specific layout of the deployed sensors relative to the attack location. From analyzing the effect of sensitivity (absence of false negative errors) and specificity (absence of false positive errors) of the sensors deployed, we conclude that it is more worthwhile to invest in sensitivity than specificity. We also obtain insights on sensor coverage.

14. SUBJECT TERMS Bayesian updating model, Atmospheric Threat and Dispersion model, Estimation of location and time of a chemical attack, Sensor placement			**15. NUMBER OF PAGES** 121
			16. PRICE CODE
17. SECURITY CLASSIFICATION OF REPORT Unclassified	**18. SECURITY CLASSIFICATION OF THIS PAGE** Unclassified	**19. SECURITY CLASSIFICATION OF ABSTRACT** Unclassified	**20. LIMITATION OF ABSTRACT** UU

THIS PAGE INTENTIONALLY LEFT BLANK

HOW TO DETECT THE LOCATION AND TIME OF A COVERT CHEMICAL ATTACK: A BAYESIAN APPROACH

Mei Eng Elaine See
Civilian, DSO National Laboratories
B.Eng. (Hons) (Chemical) National University of Singapore, 2000

Submitted in partial fulfillment of the
requirements for the degree of

MASTER OF SCIENCE IN OPERATIONS RESEARCH

from the

**NAVAL POSTGRADUATE SCHOOL
December 2009**

Author: Mei Eng Elaine See

Approved by: Moshe Kress
                   Thesis Advisor

                   Rachel Johnson
                   Second Reader

                   Robert F. Dell
                   Chairman, Department of Operations Research

THIS PAGE INTENTIONALLY LEFT BLANK

ABSTRACT

In this thesis, we develop a Bayesian updating model that estimates the location and time of a chemical attack using inputs from chemical sensors and Atmospheric Threat and Dispersion (ATD) models. In bridging the critical gap between raw sensor data and threat evaluation and prediction, the model will help authorities perform better hazard prediction and damage control.

The model is evaluated with respect to settings representing real-world operations. Factors that affect the model's capability to accurately estimate the location and time of an attack are (i) the specific layout of the deployed sensors relative to the attack location; (ii) the number of false positive signals; and (iii) the number of false negative errors. An experimental design is used to evaluate the model against the factors identified. The dominant factor is the Expected Number of Correct Signals (ENCS), which depends on the specific layout of the deployed sensors relative to the attack location. From analyzing the effect of sensitivity (absence of false negative errors) and specificity (absence of false positive errors) of the sensors deployed, we conclude that it is more worthwhile to invest in sensitivity than specificity. We also obtain insights on sensor coverage.

THIS PAGE INTENTIONALLY LEFT BLANK

TABLE OF CONTENTS

LIST OF FIGURES

LIST OF TABLES

EXECUTIVE SUMMARY

In the aftermath of the catastrophic events of September 11, 2001, and the international anthrax and Sarin nerve gas scare, it has become clear that no reliable method currently exists to protect ordinary citizens from chemical and biological agents that are dispersed in the air. The challenge involves both the detection and identification of possible contamination sources in the shortest time possible. Therefore, a goal of paramount importance for international security agencies is to infer in near real-time the existence of an air-contaminating event; to determine its source location and time of release, and subsequently to respond effectively to the attack. Sensor systems capable of simultaneously monitoring the concentrations of multiple, related air-borne toxins have been and are continually being developed. However, there are only very few methods that are capable of utilizing sensor information in real-time for identifying the source and time of release for a contamination event. (Bagtzoglou et al., 2004)

In this thesis, we develop a Bayesian updating model that estimates the location and time of a single chemical attack using inputs from chemical sensors and Atmospheric Threat and Dispersion (ATD) models. In bridging the critical gap between raw sensor data and threat evaluation and prediction, the model will help authorities perform better hazard prediction and damage control.

There are two time scales used in the model. The *attack time scale*, denoted by the index t, represents the time horizon during which a chemical attack can be detected. This time horizon is finite and we assume that it is of length T. The *detection time scale*, denoted by the index u, represents the current time in which updates are received from the sensors and probability maps are generated. The attack time scale runs backwards relative to the current time in the detection time scale.

The model is made up of 3 modules: i) a physical model, ii) a sensor model and iii) a Bayesian updating model. The physical model serves to calculate the chemical concentration c at the location of sensor s due to an attack at location l, t time periods ago. Based on the output c of the physical model, the sensor model computes the

probability $P_{l,t}^{s}(c)$ that a sensor located at location s detects a chemical attack at location $l,$ that occurred t time periods ago. The Bayesian updating model calculates the probability map at time period $u,$ $\alpha_{l,t}^{u},$ of the posterior probability of a chemical attack at location $l,$ t time period ago after an observation at time $u.$ A high value of $\alpha_{l,t}^{u}$ at time period u indicates that there is a strong likelihood that a chemical attack occurred at location $l,$ t time periods ago.

The model is implemented and evaluated with respect to settings representing real world operations. The selected alarm criterion, whereby decision makers initiate a response, is three consecutive time periods during which the posterior probabilities $\alpha_{l,t}^{u}$ are above the alarm threshold of 0.7 for a particular attack at location $l,$ t time periods ago. The alarm criterion is a combination of a probability threshold (0.7) and a persistence measure (3 consecutive periods) to avoid responding erroneously to low posterior probabilities on the one hand, and to sudden temporary spikes in the probability map due to false positive errors, on the other hand.

The Measures of Effectiveness (MOEs) used are:
- Accurately identifying the source location; and
- Accurately identifying the time of release.

These MOEs are chosen due to their impact on operations. The source location and time of release serve as critical inputs to threat modeling and mitigation. In evaluating the effectiveness of the model through simulations, a success is declared only if both MOEs are met, that is, the model accurately identifies both location and time of the attack. Thus, *success percentage* is defined as the percentage of simulation trials that produce a success over the total number of trials performed.

Factors that affect the effectiveness of the model are the specific layout of the deployed sensors relative to the attack location, the number of false positive errors and the number of false negative errors. An experimental design is used to evaluate the effect of each factor.

Performing linear regression on the simulation results, it is found that the dominant factor is the specific layout of the deployed sensors relative to the attack location. Also, not surprisingly, we obtain that false negative errors have higher impact on the success percentage than false positive errors.

We demonstrate that given a deployment of 16 AP4C chemical point sensors, a hypothesized release of 50kg of the Sarin (nerve gas) is accurately identified with high probability for several attack locations. The model bridges the critical gap between input of raw sensor data and the operational interpretation of these data, giving authorities the capability to perform better hazard prediction and damage control.

Insights on sensor coverage are also obtained by computing, using the $P_{l,t}^{s}$ values, the probability that a certain attack location is detected by at least one sensor. This probability index allows decision makers and planners to identify both vulnerable areas and areas with no sensor coverage. For example, tradeoffs between coverage (e.g., placing sensors downwind) and timeliness (delayed warnings) could be explored.

Future research involves extending the model to (i) detect chemical attacks with different nominal attack quantity levels, (ii) detect multiple chemical attacks and (iii) incorporate different sensor types.

THIS PAGE INTENTIONALLY LEFT BLANK

ACKNOWLEDGMENTS

THIS PAGE INTENTIONALLY LEFT BLANK

I. INTRODUCTION

Knowing how to exploit the potential of technology will help us to create new solutions to deal with emerging security challenges. The increasing sophistication of IT systems now makes it possible to conduct complex analysis of massive amounts of data. Data mining, link-analysis technologies and sophisticated intelligent systems can help to provide us with early indications of threats and opportunities.

Professor S. Jayakumar,
Deputy Prime Minister, Coordinating Minister for National Security
and Minister for Law, Singapore, 27 March 2007

A. BACKGROUND

The risk of a chemical attack on the civilian population is low but real. In 1995, Aum Shinrikyo, a Japanese cult, carried out a chemical attack, using Sarin gas, on the Tokyo subway lines. The attack killed 12 and injured over 3000 people, of which some 500 were hospitalized. Dealing with such attacks in Singapore requires a total effort involving several Ministries, as well as the private sector and Singaporeans at large. (Rajah, 1995)

To minimize the damage caused by a chemical attack on the civilian population, the location and time of the attack are needed for an effective response. The location of the attack will allow first responders to quickly quench the source in accordance to decontamination procedures, preventing the spread of the chemical agent. Moreover, the time and location of the attack are critical inputs to Atmospheric Threat Dispersion (ATD) models that predict the spread of the chemical plume. Information on the spread of the chemical plume allows security and defense authorities to make decisions on sites regarding decontamination and preventing cross-contamination, and to provide advice to the civilian population via the public warning system to undertake appropriate protective measures.

In the event of a covert chemical attack, very little may be known about the source, perhaps not even its location. The best the authorities may have are reports of people becoming incapacitated, the existence of traffic pile-ups at several nearby

locations, or an isolated sensor raising an alarm. Such an undetected attack will delay actions to contain the chemical threat and provide early warning to the public. Absent early warning, the attack will inflict maximum damage leading to a high number of casualties and a large area of chemical contamination. Thus it is crucial to be able to detect the attack as soon as possible.

Sensor systems capable of simultaneously monitoring the concentrations of Chemical, Biological, Radiology, Nuclear and Explosive (CBRNE) threats are available and continually developed commercially. However, methods that are capable of utilizing the sensor information in real-time for identifying the source and time of release for a contamination event are in a research stage. Thus there are no commercial solutions available to the operational users and decision makers today. Despite the millions of dollars that are spent on chemical sensors in chemical defense, they currently only perform the role of detecting and monitoring the development of a chemical threat. Information of the time and location of the chemical attack remains largely unknown.

B. PROBLEM STATEMENT

In the aftermath of the catastrophic events of September 11, 2001 and the international anthrax and Sarin nerve gas scare, it has become clear that no reliable method currently exists to protect ordinary citizens from chemical and biological agents that are dispersed in the air. The challenge involves both the detection and identification of possible contamination sources in the shortest time possible. Therefore, a goal of paramount importance for security and response agencies is to infer in near real-time the existence of an air contaminating event, to determine its source location and time of release, and subsequently to respond effectively to the attack. Sensor systems capable of simultaneously monitoring the concentrations of multiple, related air-borne toxins have been and are continually being developed. However, methods that are capable of utilizing the sensor information in real-time for identifying the source and time of release for a contamination event do not exist. (Bagtzoglou et al., 2004)

ATD models are physical models used to predict the spread of a certain chemical attack, taking into account terrain characteristics and prevailing meteorological

conditions. These models are used to perform hazard prediction and damage assessment of the detected threat for evacuation and mitigation. In the event of a covert chemical attack, security and defense ministries cannot leverage ATD models to provide information for evacuation and mitigation strategies because the information on the location and time of the attack are critical inputs of the models.

In this thesis, we develop a model that estimates the location and time of a chemical attack using inputs from chemical sensors and ATD models. In bridging the critical gap between raw sensor data and threat evaluation and prediction, the model will help authorities perform better hazard prediction and damage control.

C.   APPROACH

In developing a model for determining the location and time of a chemical release, two main areas of uncertainty need to be addressed: the time-dependent spatial distribution of the chemical plume and the probability of detecting the chemical agent, given that the plume is in the vicinity of the sensors. The first area of uncertainty is affected by the dispersion characteristics of the source, the terrain of the area of interest, source location, the release scenario (continuous or explosion), and meteorological effects. In this thesis we are only concerned with the source characteristics (type, strength and location), with the terrain chosen to be a flat land. The second area of uncertainty is associated with the capabilities of the sensors – their sensitivity (avoiding false negative errors) and specificity (avoiding false positive errors).

The model is made up of 3 modules: i) a physical model that describes the dispersion of the chemical plume; ii) a sensor model that reflects the uncertainty associated with sensor signals; and iii) a Bayesian updating model that generates a multi-dimensional probability map representing the likelihood of a location and time of a covert chemical attack.

D.   SCOPE

This research focuses on developing a model for detecting the occurrence of a chemical attack and determining its location and time of release from sensor data. The research questions addressed are:

- Can we use a Bayesian updating model to develop a probability map of the location and time of a covert chemical attack?
- How sensitive is the probability map with respect to sensor type, location and capabilities?

E.   THESIS OVERVIEW

The thesis is organized as follows:

Chapter II reviews the various approaches used to develop algorithms for detecting the occurrence of a chemical attack, and determining its location, release rates and agent type from sensor data. The strengths and weaknesses of the approaches are briefly discussed. Chapter III describes the development of the model and its three modules: (i) a physical (atmospheric) model of plume dispersion; (ii) a sensor model that reflects the detection capabilities of the sensor; and (iii) a Bayesian updating model that generates the probability map. Chapter IV present tests results of simulation runs performed for evaluating the effectiveness of the model in a small scale scenario in order to demonstrate the effectiveness of multiple sensors. The small scale test cases also serve as a preliminary check on the model integrity and implementation. Chapter V discusses the evaluation results of the model with respect to large scale settings that depict more closely real-world operations. The experimental design and analysis of the simulation runs with respect to the Measures of Effectiveness (MOEs) are also discussed. Chapter VI draws conclusions relevant to the research questions posed. The chapter concludes by suggesting future research topics and extensions.

II. LITERATURE REVIEW

In this chapter, we discuss the various approaches used to develop algorithms for the problem of detecting the occurrence of a chemical attack and determining its location, release rates, time of release and agent type from sensor data. This problem is henceforth called "Chemical Source Isolation." The strengths and weaknesses of the approaches are also discussed.

There are three main methods for solving the Chemical Source Isolation problem: i) Backward Approach, ii) Forward Approach and iii) Bayesian probabilistic modelling. We review these methods below.

A. BACKWARD APPROACH

In the Backward approach, one reverses time to come up with estimates of the location and release rates of a chemical attack through the use of sensor data and running an ATD model backwards in time. The advantage of this approach is that it eliminates the tedious process of building a large library of threat scenarios. The disadvantages are that the model relies on simplifying assumptions that are not necessarily met in reality. Furthermore, inverse models are computational intensive and the computational burden is compounded as the model is repeatedly run with each new detection event (Fry et al., 2005).

B. FORWARD APPROACH

In the Forward approach, one guesses the location and strength of the source, then uses ATD models to estimate the location and release rates of a chemical attack. The estimates are then compared to actual sensor alarms and a series of mathematical and statistical methods are applied to iterate the initial guess. This continues until a match is achieved between the projected and actual sensor alarms. A shortcoming of this approach is that many runs of the ATD model are required. This shortcoming is overcome by

building a comprehensive pre-run library of ATD models. However scenarios not represented in the library will suffer inaccuracies due to extrapolation.

Traditional algorithms for data interpretation generally attempt to fit an ATD model to measurements of airborne pollutants. The fit is usually achieved by iteratively adjusting model input parameters until they reasonably predict the data. For real-time sensor data interpretation, this approach is too slow because it needs to execute computationally intensive ATD models, it executes the models repeatedly as new or successive sensor data become available, and it requires a considerable amount of data before the algorithm finds a unique solution or estimates the uncertainty in the calibrated parameters. Finally, the computational burdens required by the forward approach can be so great that using it for pre-event planning, such as to determine optimal monitoring locations, sampling plans, and sensor performance criteria, can be excessively cumbersome (Sohn et al., 2002).

Many of these problems can be solved using a technique called Kalman filtering. This technique is well-suited for many sensor interpretation applications and has been successfully applied, for example, to estimate the source strength of pollutant releases in multi-zone buildings. However, Kalman filtering is best used for linear systems with well conditioned input-to-output parameter covariance matrices and strong observability between the internal-state variables (e.g., the model input parameters of an ATD model) and the model outputs (e.g., concentration predictions). Many chemical kinetics and transport phenomena, such as second-order pollutant degradation, density-driven pollutant transport, aerosol coagulation, and second-order pollutant diffusion in sorption-desorption, are not linear. Furthermore, wide uncertainty bounds exist for several of the model inputs, such as, there being many possible source locations, amounts released, durations of releases, and meteorological conditions. These will invariably lead to ill-conditioned covariance matrices and poorly observable systems. Although many nonlinear models may be linearized using an extended Kalman filtering technique, the technique requires considerable tuning and adjustments because of the linear approximations (Sohn et al., 2002).

6

C. BAYESIAN PROBABLISTIC MODELS

Researchers have also tried to develop probabilistic models of both the agent's concentration in an atmospheric plume and the sensor's capability of detecting that agent in a given concentration. The probabilities will yield the likelihood of a chemical attack at a certain location and the agent type and quantity released. The advantage of this approach is that it captures the uncertainty of both the dispersion characteristic of the chemical threat and the detection characteristic of the chemical sensor, thereby providing a more realistic representation of the situation and a better solution for the chemical source isolation problem.

This approach is used by the UK's Defense Science and Technology Laboratory and is intended to form a component of the forthcoming Nuclear, Biological and Chemical Battlespace Information System Application (NBC BISA). The NBC BISA seeks to fuse data from an array of sensors to make inference about the possible source locations, times, agent types and masses of chemical release (Rapley et al., 2005).

The probabilistic atmospheric dispersion model used by the NBC BISA uses a truncated normal distribution. It does not predict the actual small scale detail of the dispersion like Gaussian puff and other ATD models. Rather, it calculates the statistical properties of the dispersing cloud. The sensor model used by the NBC BISA is developed for a generic ion mobility detector and is normally distributed with a measurement error. Also a proportionality constant that accounts for the thermal motion of the electrons in the components is used in the sensor model (Rapley et al., 2005).

D. APPROACH USED IN THIS THESIS

Taking into account the strengths and weaknesses of the different approaches available from the literature, this thesis uses a Bayesian updating model to develop a multi-dimensional probability map to identify the location and time of a chemical attack. As in the NBC BISA model, we apply Bayes's Theorem to calculate posterior probabilities; however the prior probabilities are calculated differently. The development of the model and the parameters involved are discussed in Chapter III.

THIS PAGE INTENTIONALLY LEFT BLANK

III. THE MODEL

We use a Bayesian updating model for detecting a chemical attack, determining its location l and estimating the time of attack t. The model uses data obtained from sensors deployed in the area of operations monitoring the air for a possible chemical attack.

A. MODEL DEVELOPMENT

There are two time scales used in the model. The *attack time scale*, denoted by the index t, represents the time horizon during which a chemical attack can be detected. We assume that this time horizon is of length T. The *detection time scale*, denoted by the index u, represents the current time in which updates are received from the sensors and probability maps are generated. The attack time scale runs backwards relative to the current time in the detection time scale. Both scales are illustrated in Figure 1.
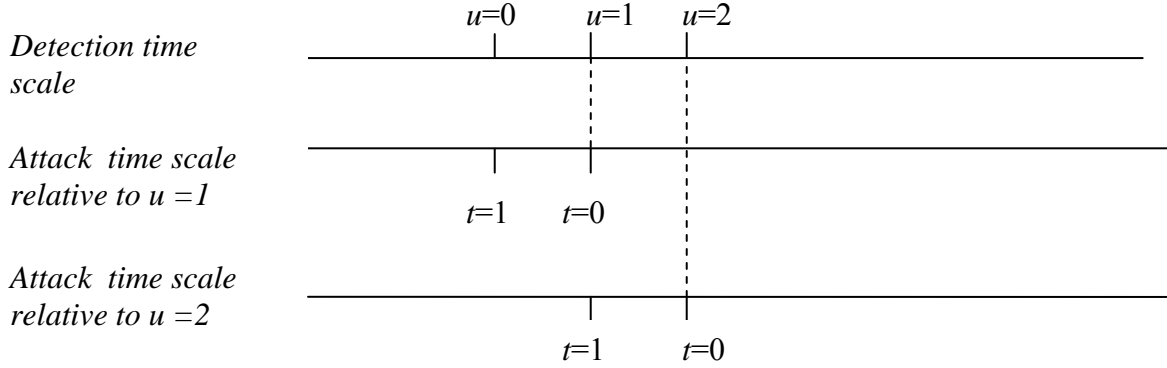
Figure 1.   Attack and detection time scales

As time progresses along the u scale, the t scale slides along with it such that the model always calculates the probability of an occurrence of a chemical attack up to T time periods before the current time u.

The model is developed based on the occurrence of two events. The first event, denoted $A_{l,t}$, is a chemical attack, characterized by its location l and time of occurrence t

9

time periods ago. The second event, denoted D_s, is a detection of a chemical attack by sensor s, out of a set of sensors S that are deployed to monitor chemical attacks.

In the model, we use the following notation.

$A_{l,t}$ –   An event that a chemical attack has occurred at location l, t time periods ago.

D_s^u –   An event that sensor s *signals* a detection at time u.

$\overline{D_s^u}$ –   Complement of D_s^u.

α_l^u = Initial (a-priori) probability of a chemical attack at location l at time period u. (Absent specific intelligence we assume that $\alpha_l^u = \alpha^0 \ \forall l,u$. Also note that these probabilities are defined on the detection time scale.)

$\widehat{\alpha}_{l,t}^u$ = Prior probability of a chemical attack at location l, t time periods ago before an observation at time period u.

$\alpha_{l,t}^u$ = Posterior probability of a chemical attack at location l, t time periods ago after observation at time period u.

$P_{l,t}^{s,u}$ = Probability that a sensor located at location s detects at time period u a chemical attack at location l that occurred t time period ago. We assume stationary detection capability, that is, $P_{l,t}^{s,u} = P_{l,t}^{s} \ \ \forall \ u$.

$1-q$ = Single-period false positive probability: the probability that a sensor signals detection given there is no attack during a time period.

T = Time horizon for detecting an attack. (We assume that there is at most one attack during any time horizon T.)

L = Number of locations in the area of operations.

The parameters α^0, $P_{l,t}^{s,u}$, L, T and $1-q$ are inputs to the model.

1.   Single Sensor Model

We start with a model only involving a single sensor monitoring a set of L locations. Thus, we suppress the index s.

The input parameter α^0 , which is the a-priori probability of a chemical attack at a certain location and time period, is determined by threat and vulnerability studies which are beyond the scope of this thesis.

Consider the first detection time period $u = 1$. The prior probabilities of an attack are the a-priori probabilities. That is,

$$\hat{\alpha}^1_{l,t} = \alpha^0 \qquad \forall \ l, t$$

To calculate the posterior probabilities $\alpha^1_{l,t}$, we use Bayes's Theorem. If the sensor signals a detection at $u = 1$, then

$$P(A_{l,t}|D^1) = \alpha^1_{l,t} = \frac{P(D^1|A_{l,t})P(A_{l,t})}{P(D^1)} = \frac{P_{l,t}\hat{\alpha}^1_{l,t}}{\sum_l \sum_t \hat{\alpha}^1_{l,t} P_{l,t} + (1-q)(1-\sum_l \sum_t \hat{\alpha}^1_{l,t})}$$

If the sensor does not signal a detection at $u = 1$, then

$$P(A_{l,t}|\overline{D}^1) = \alpha^1_{l,t} = \frac{P(\overline{D}^1|A_{l,t})P(A_{l,t})}{P(\overline{D}^1)} = \frac{(1-P_{l,t})\hat{\alpha}^1_{l,t}}{\sum_l \sum_t \hat{\alpha}^1_{l,t}(1-P_{l,t}) + q(1-\sum_l \sum_t \hat{\alpha}^1_{l,t})}$$

Hence,

$$\alpha^1_{l,t} = \begin{cases} \dfrac{P_{l,t}\hat{\alpha}^1_{l,t}}{\sum_l \sum_t \hat{\alpha}^1_{l,t} P_{l,t} + (1-q)(1-\sum_l \sum_t \hat{\alpha}^1_{l,t})} & \textit{if } D^1 \textit{ occurs, } \forall l, t \\[3ex] \dfrac{(1-P_{l,t})\hat{\alpha}^1_{l,t}}{\sum_l \sum_t \hat{\alpha}^1_{l,t}(1-P_{l,t}) + q(1-\sum_l \sum_t \hat{\alpha}^1_{l,t})} & \textit{if } \overline{D}^1 \textit{ occurs, } \forall l, t \end{cases}$$

At $u = 2$,

$$\hat{\alpha}^2_{l,t} = \begin{cases} \alpha^0 & \forall l, t = 1 \\ \alpha^1_{l,t-1} & \forall l, t = 2,\ldots,T \end{cases}$$

And the posterior probabilities are,

$$
\alpha_{l,t}^2 = \begin{cases} \dfrac{P_{l,t}\widehat{\alpha}_{l,t}^2}{\displaystyle\sum_l\sum_t \widehat{\alpha}_{l,t}^2 P_{l,t} + (1-q)(1-\sum_l\sum_t\widehat{\alpha}_{l,t}^2)} & \text{if } D^2 \text{ occurs, } \forall l,t \\[4mm] \dfrac{(1-P_{l,t})\widehat{\alpha}_{l,t}^2}{\displaystyle\sum_l\sum_t \widehat{\alpha}_{l,t}^2 (1-P_{l,t}) + q(1-\sum_l\sum_t\widehat{\alpha}_{l,t}^2)} & \text{if } \overline{D}^2 \text{ occurs, } \forall l,t \end{cases}
$$

In general,

$$
\widehat{\alpha}_{l,t}^u = \begin{cases} \alpha^0 & \forall l, t = 1 \\ \alpha_{l,t-1}^{u-1} & \forall l, t = 2,\ldots,T \end{cases} \tag{1}
$$

$$
\alpha_{l,t}^u = \begin{cases} \dfrac{P_{l,t}\widehat{\alpha}_{l,t}^u}{\displaystyle\sum_l\sum_t \widehat{\alpha}_{l,t}^u P_{l,t} + (1-q)(1-\sum_l\sum_t\widehat{\alpha}_{l,t}^u)} & \text{if } D^u \text{ occurs, } \forall l = 1,\ldots,L, t = 1,\ldots,T \\[4mm] \dfrac{(1-P_{l,t})\widehat{\alpha}_{l,t}^u}{\displaystyle\sum_l\sum_t \widehat{\alpha}_{l,t}^u (1-P_{l,t}) + q(1-\sum_l\sum_t\widehat{\alpha}_{l,t}^u)} & \text{if } \overline{D}^u \text{ occurs, } \forall l = 1,\ldots,L, t = 1,\ldots,T \end{cases} \tag{2}
$$

At each time step u the values of $\alpha_{l,t}^u$ generate a *probability map* that gives the most updated probabilities of an attack at location l, t time periods ago. At each time step, following the cue from the sensor (detection or non-detection) the probability map is updated. An alarm goes off if at a certain point u, an $\alpha_{l,t}^u$ value crosses a threshold, which triggers an action responding to the detected chemical threat.

2. Multiple Sensors Model

Now we extend the single sensor model to include updates from multiple independent sensors used to monitor a set of L locations. As for the single sensor, we use Bayes theorem to calculate $\alpha_{l,t}^1$.

If all the sensors return a detection signal at $u = 1$, then

$$P(A_{l,t} \mid D_1^1 \ldots D_s^1) = \alpha_{l,t}^1 = \frac{P(D_1^1 \ldots D_s^1 \mid A_{l,t})P(A_{l,t})}{P(D_1^1 \ldots D_s^1)}$$

$$= \frac{\widehat{\alpha}_{l,t}^1 \prod_s P_{l,t}^s}{\sum_l \sum_t \widehat{\alpha}_{l,t}^1 \prod_s P_{l,t}^s + (1-q)^s (1 - \sum_l \sum_t \widehat{\alpha}_{l,t}^1)}$$

If none of the sensors returns a detection signal at $u=1$, then

$$P(A_{l,t} \mid \overline{D}_1^1 \ldots \overline{D}_s^1) = \alpha_{l,t}^1 = \frac{P(\overline{D}_1^1 \ldots \overline{D}_s^1 \mid A_{l,t})P(A_{l,t})}{P(\overline{D}_1^1 \ldots \overline{D}_s^1)}$$

$$= \frac{\widehat{\alpha}_{l,t}^1 \prod_s (1 - P_{l,t}^s)}{\sum_l \sum_t \widehat{\alpha}_{l,t}^1 \prod_s (1 - P_{l,t}^s) + q^s (1 - \sum_l \sum_t \widehat{\alpha}_{l,t}^1)}$$

If the sensor readings are mixed, so that sensors 1 to n record a detection, and sensors $n+1$ to S do not record a detection at $u=1$, then

$$P(A_{l,t} \mid D_1^1 \ldots D_n^1, \overline{D}_{n+1}^1 \ldots \overline{D}_s^1) = \alpha_{l,t}^1 = \frac{P(D_1^1 \ldots D_n^1, \overline{D}_{n+1}^1 \ldots \overline{D}_s^1 \mid A_{l,t})P(A_{l,t})}{P(D_1^1 \ldots D_n^1, \overline{D}_{n+1}^1 \ldots \overline{D}_s^1)}$$

$$= \frac{\widehat{\alpha}_{l,t}^1 \prod_{s=1}^n P_{l,t}^s \prod_{s=n+1}^S (1 - P_{l,t}^s)}{\sum_l \sum_t \widehat{\alpha}_{l,t}^1 \prod_{s=1}^n P_{l,t}^s \prod_{s=n+1}^S (1 - P_{l,t}^s) + q^{s-n}(1-q)^n (1 - \sum_l \sum_t \widehat{\alpha}_{l,t}^1)}$$

In general, $\widehat{\alpha}_{l,t}^u$, the prior probability at time step u for an attack at location l, t time periods ago is shown below

$$\widehat{\alpha}_{l,t}^u = \begin{cases} \alpha^0 & \forall l, t = 1 \\ \alpha_{l,t-1}^{u-1} & \forall l, t = 2, \ldots, T \end{cases} \qquad (3)$$

If at time u, sensors $1 \ldots n$ produce detection cues while sensor $n+1 \ldots S$ did not, then the posterior probability is defined as follows

$$\alpha_{l,t}^{u} = \frac{\widehat{\alpha}_{l,t}^{u} \prod_{s=1}^{n} P_{l,t}^{s} \prod_{s=n+1}^{S} (1-P_{l,t}^{s})}{\sum_{l}\sum_{t}\widehat{\alpha}_{l,t}^{u} \prod_{s=1}^{n} P_{l,t}^{s} \prod_{s=n+1}^{S} (1-P_{l,t}^{s}) + q^{s-n}(1-q)^{n}(1-\sum_{l}\sum_{t}\widehat{\alpha}_{l,t}^{u})} \qquad (4)$$

Equations 3 and 4 are computed for each time step u, based on the sensor cues in that time step and the prior probabilities. The resulting values constitute an $L \times T$ probability map at time period u, where the $(l,t)^{u}$ entry , the probability at time step u of a chemical attack at location l, t time periods ago is $\alpha_{l,t}^{u}$.

B.   ESTIMATING THE VALUES OF $P_{l,t}^{s}$

The probability that a sensor located at location s detects a chemical attack at location l that occurred t time periods ago, represented by $P_{l,t}^{s}$, is an important parameter in the model. The estimation of the $P_{l,t}^{s}$ values entails the use of a physical model and a sensor model.

Section 1 describes the physical model that is used to calculate the chemical concentration at the sensor location from a chemical attack at location l that occurred t time periods ago. Section 2 describes the sensor model that derives the probability of detection given the chemical concentration calculated by the physical model in section 1.

1.   Physical Model

The probability density function (PDF) of the chemical concentration in an atmospheric plume is very hard to determine. Measurements of the frequency distribution of fluctuating plume concentrations have revealed that the PDF is generally strongly skewed to the right with an upper tail that is heavier than that of the Gaussian form. A large number of mathematical forms have been used to model the concentration PDF such as the lognormal distribution, the exponential distribution, the truncated normal distribution, the beta-Jacobi distribution, and a linear combination of exponential and generalized Pareto PDFs. However, despite this enormous effort, there is still no general

agreement on the parametric PDF model that provides the best fit to plume concentration data over a wide range of experimental conditions (Chan et al., 1997).

Hence, due to the difficulties mentioned above, a deterministic physical model is used instead to calculate the expected temporal and spatial concentration of a chemical plume resulting from a chemical attack.

The physical model consists of two main components: (i) the source emission model and (ii) the dispersion model. The source emission model serves to calculate the initial concentration at the chemical attack location, while the dispersion model calculates the spread of the chemical agent, taking into account weather and terrain characteristics. The inputs and outputs of the various components of the two models and their relationships are depicted in Figure 2.

Release Type:
instantaneous, continuous,
etc

Identity of chemical
agent

Time of release

Source Emission Models

Release rate or release amount

Terrain characteristics

Meteorological
Data

Atmospheric Threat
Dispersion Model

Spread and concentration of
chemical contaminant
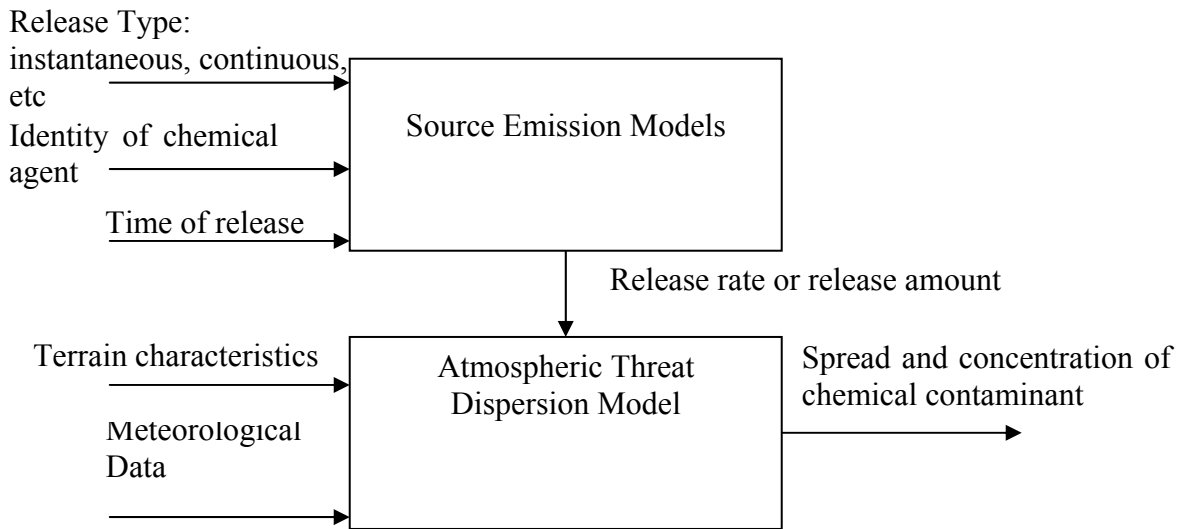
Figure 2.   Components of the physical model

For this study the Atmospheric Threat Dispersion Model are the Gaussian Puff model for attacks that encompass an instantaneous release, and the steady state Gaussian Plume model for continuous releases. Although both Gaussian Models are reviewed, only the Gaussian Puff model is used in the study. The source emission models depend on the

15

chemical agent being modeled and are typically classified. In this study, we bypass the source emission models and feed a release amount directly to the ATD model.

a.   Gaussian Puff Model

The Gaussian Puff model describes the temporal and spatial concentration of material from a single release of a fixed amount of material. Figure 3 shows the development of a Gaussian Puff (Crowl et al., 2002).
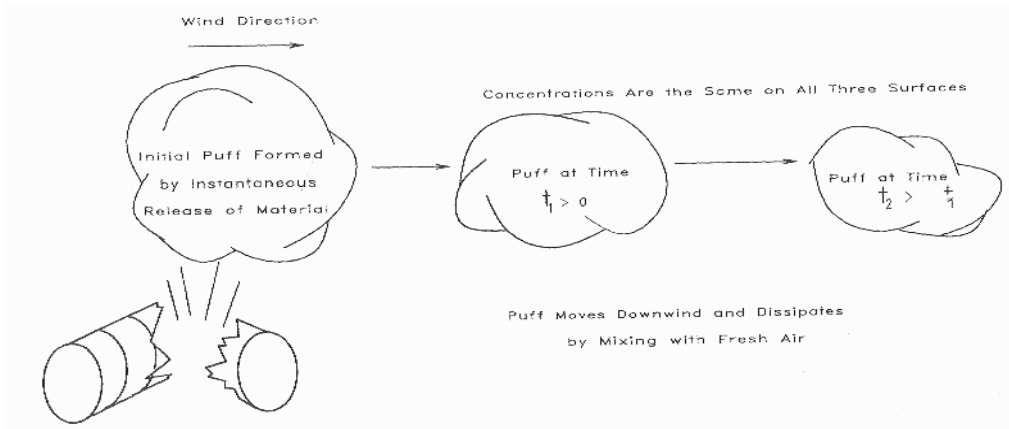
Figure 3.   Gaussian Puff development over time [From: Crowl et al., 2002]

The assumption is that the chemical attack is expected to be executed at ground level ($z=0$) and the sensors are also placed on the ground, hence the Gaussian Puff model equations can be simplified as follows (Crowl et al., 2002).

$$C(x,y,0,t) = \frac{Q_m^*}{\sqrt{2}\pi^{3/2}\sigma_x\sigma_y\sigma_z}\exp\left\{-\frac{1}{2}\left[\left(\frac{x-wt}{\sigma_x}\right)^2 + \frac{y^2}{\sigma_y^2}\right]\right\} \qquad (5)$$

where : C is the concentration in mg/m^3

x is the distance away from the source in the x-coordinate in meters;

y is the distance away from the source in the y-coordinate in meters;

Q_m^* is the amount of chemical released in mg/m^3;

w is the wind speed in the direction of the x-coordinate in meters/second

16

t is the time, in seconds, since the chemical release; and

$\sigma_x, \sigma_y, \sigma_z$, are the Pasquill Gifford (PG) dispersion coefficients for puff dispersion.

Equation 5 can also be used to calculate the temporal concentration of material from a single release of a fixed amount of material even when the prevailing wind direction is not in the direction of the *x*-coordinate of the area cells. This is achieved via a transformation of the coordinate systems.

The PG dispersion coefficients are functions of the atmospheric conditions and the distance downwind from the release point. The atmospheric conditions are classified according to six different stability classes shown in Table 1. The stability class depends on wind speed and quantity of sunlight. During the day, increased wind speed results in greater atmospheric stability whereas at night the reverse is true. This difference is due to a change in vertical temperature profiles from day to night (Crowl et al., 2002).

Table 1.   PG stability classes [From: Crowl et al., 2002]

Surface wind speed (m/s)	Day-time Insolation			Night-time conditions	
	Strong	Moderate	Slight	Thin overcast	Cloudy
<2	A	A-B	B	F	F
2-3	A-B	B	C	E	F
3-4	B	B-C	C	D	E
4-6	C	C-D	D	D	D
>6	C	D	D	D	D

The equations for PG dispersion Coefficients for Puff Dispersion with *x* as the distance away from the source in the *x*-coordinate in meters are as shown in Table 2 (Crowl et al., 2002).

Table 2.   Recommended functions for PG dispersion Coefficients [From: Crowl et al., 2002]

PG stability class	σ_x, σ_y (meters)	σ_z (meters)
A	$0.18x^{0.92}$	$0.60x^{0.75}$
B	$0.14x^{0.92}$	$0.53x^{0.73}$
C	$0.10x^{0.92}$	$0.34x^{0.71}$
D	$0.06x^{0.92}$	$0.15x^{0.70}$
E	$0.04x^{0.92}$	$0.10x^{0.65}$
F	$0.02x^{0.89}$	$0.05x^{0.61}$

Equation 5, together with Tables 1 and 2 facilitate the calculation of the concentration of the chemical at every location in the area of operations.

b.   *Gaussian Plume Model*

A Gaussian Plume model represents the plume diffusion in a continuous release for a range of atmospheric conditions. The technique applies the standard deviations of the Gaussian distribution in two directions to represent the characteristics of the plume downwind of its origin. The plume's shape, and hence the standard deviations, varies according to the specific meteorological conditions (Liu, 1997).

A number of assumptions are typically used for Gaussian modeling of a plume. First, the analysis assumes a steady state system (i.e., a source continuously emits at a constant strength, the wind speed, direction, and diffusion characteristics of the plume remain steady, and no chemical transformations take place in the plume). Second, diffusion in the x direction is ignored, although transport in this direction is accounted for by wind speed. Third, the plume is reflected up at the ground rather than being deposited, according to the rules of conservation of matter (i.e., none of the pollutant is removed from the plume as it moves downwind). Fourth, the model applies to an ideal aerosol or an inert gas. Particles greater than 20 mm in diameter tend to settle out of the atmosphere at an appreciable rate (Liu, 1997).

For the concentrations at ground level, z can be set equal to zero and if the emission source is located at ground level with no effective plume rise, the steady state Gaussian plume equation is as follows (Liu, 1997) :

$$C(x, y, 0) = \frac{Q_m}{\pi \sigma_y \sigma_z w} \exp\left[-\frac{1}{2}\left(\frac{y}{\sigma_y}\right)^2\right] \qquad (6)$$

where : C is the concentration in mg/m^3;

x is the distance away from the source in the x-coordinate in meters;

y is the distance away from the source in the y-coordinate in meters;

Q_m is the amount of chemical released in mg/m^{3}s;

w is the wind speed in the direction of the x-coordinate in meters/second;

σ_y, σ_z, are PG dispersion coefficients for plume dispersion.

The recommended PG dispersion coefficients for plume dispersion are shown in Table 3, where x is the distance away from the source in the x-coordinate in meters Crowl et al., 2002).

Table 3. Recommended PG plume dispersion coefficients [From: Crowl et al., 2002]

PG stability class	σ_y (meters)	σ_z (meters)
A	$0.22x(1+ 0.0001x)^{-1/2}$	$0.20x$
B	$0.16x(1+ 0.0001x)^{-1/2}$	$0.12x$
C	$0.11x(1+ 0.0001x)^{-1/2}$	$0.08x(1+ 0.0002x)^{-1/2}$
D	$0.08x(1+ 0.0001x)^{-1/2}$	$0.06x(1+ 0.0015x)^{-1/2}$
E	$0.06x(1+ 0.0001x)^{-1/2}$	$0.03x(1+ 0.0003x)^{-1}$
F	$0.04x(1+ 0.0001x)^{-1/2}$	$0.016x(1+ 0.0003x)^{-1}$

Equation 6, together with the stability class for the attack scenario and its corresponding PG dispersion coefficients for varying distances from the chemical source, lets us calculate the concentration of the chemical at every location in the area of operations.

2.   Sensor Model

The Gaussian puff and plume models described in section 1 provide techniques for calculating the chemical concentration at a certain point relative to the release point.

To calculate the values of $P_{l,t}^s$, we need to develop a model that captures the detection performance characteristics of a sensor. Specifically, the sensor model calculates the probability that a sensor will detect a chemical release at a given concentration.

In order to develop a probabilistic model of the sensor's capability to detect a chemical threat, the modeler must have a good grasp of the detection technology used, as well as have access to detection data obtained from laboratory trials. For example, ion mobility-based sensors have an upper alarm threshold, beyond which they cannot indicate the presence of a higher concentration due to a limiting ionizing capability of the sensor. Sensor model parameters are usually classified information as they reveal the sensor's detection effectiveness and hence strength and vulnerabilities of the defender.

Next, we develop two different sensor models: a cookie cutter model and a continuous model. For a given agent, a sensor model determines the probability $P^s(c)$ of sensor s detecting the agent at concentration c. If, following a release at location l, t time periods ago, the concentration of the agent at the location of sensor s is $c_{l,t}^s$, then $P_{l,t}^s = P^s(c_{l,t}^s)$. The values of $c_{l,t}^s$ are obtained from the physical model.

a. Cookie Cutter Model

According to the cookie cutter model, the value of $P^s(c)$ is given by

$$P^s(c) = \begin{cases} 1 & \text{if } c \geq dt \\ 1-q & \text{otherwise} \end{cases} \qquad (7)$$

The detection threshold dt is obtained from the technical specifications of the sensor being modeled. As before, $1-q$ is the false positive probability. In this thesis the sensor modeled is the AP4C chemical warfare agent detector manufactured by Proengin (Proengin, 2009). The values of dt for the AP4C sensor, with respect to three different classes of chemical agents, are given in Table 4.

Table 4.   Detection thresholds for the AP4C sensor [From: Proengin, 2009]

	Agent Type		
	Nerve	Blister	Blood
Detection Threshold (mg/m^3)	0.01	1.5	10

Chemical agents are typically classified into nerve, blister or blood agents, in accordance to the way that they affect the human body. Nerve agents are a class of organophosphates that disrupt the mechanism by which nerves transfer messages to organs. Poisoning by a nerve agent leads to convulsions and eventual death by asphyxiation as control is lost over respiratory muscles. Blister agents consist of either nitrogen-based, or sulphur-based mustards, and Lewisites (organoarsenic compounds). They cause severe chemical burns, resulting in large, painful water blisters on the bodies of those affected. Blood agents are a class of chemicals containing cyanide or arsenic. They cause death through respiratory failure by blocking the blood's ability to deliver oxygen to body tissues.

The cookie cutter sensor model is a simplistic model which gives a rough representation of the sensor's capabilities. However this model can be used as a reasonable approximation if detailed information of the detection performance of the sensor is not available. Most of the time, the only available information of the sensor's detection capability is its detection threshold which is used in the cookie cutter model. Further in-house laboratory trials are required to assess the sensor's detection capabilities across various concentration and environmental ranges.

b.   *Continuous Model*

In a continuous sensor model $P^s(c)$ is a continuous function of c. For the AP4C chemical sensor the continuous function is approximated by six ranges, or alarm thresholds, called *bars*. A bar is an indicator alarm on the AP4C detector that indicates the concentration of the agent detected. Table 5 presents these alarm thresholds for the three types of agents—Nerve, Blister and Blood.

Table 5.　　　　Alarm thresholds in mg/m^3 of the AP4C sensor [From: Proengin, 2009]

Alarm Thresholds	Agent Type		
	Nerve	Blister	Blood
1 bar	0.01	1.5	10
2 bar	0.125	2	30
3 bar	0.5	4	50
4 bar	2	10	100
5 bar	7.5	25	200
5 bar flashing	30	50	500

The detection technology of the AP4C sensor is flame spectrophotometry. The chemical agent is detected by analyzing the light spectrum created by burning the gas. Quantification is achieved by measuring the amplitude of the relevant peaks. The sensor's response is linear below the saturation point where the detector burning capacity is reached, as reflected by the 5 bar flashing threshold.

Hence, for the AP4C sensor, $P^s(c)$ is equal to 1 if the chemical concentration c is equal to or exceeds the alarm threshold of 5 bars blinking. $P^s(c)$ decreases by 0.1 across the lower alarm thresholds until the detection threshold of one bar is reached, after which $P^s(c)$ equals $1-q$, the false positive probability. This relationship is summarized below.

$$P^s(c) = \begin{cases} 1 & \textit{if } c \geq \textit{alarm threshold of } 5 \textit{ bar blinking} \\ 0.9 & \textit{if } c \geq \textit{alarm threshold of } 5 \textit{ bars and } < 5 \textit{ bars blinking} \\ 0.8 & \textit{if } c \geq \textit{alarm threshold of } 4 \textit{ bars and } < 5 \textit{ bars} \\ 0.7 & \textit{if } c \geq \textit{alarm threshold of } 3 \textit{ bars and } < 4 \textit{ bars} \\ 0.6 & \textit{if } c \geq \textit{alarm threshold of } 2 \textit{ bars and } < 3 \textit{ bars} \\ 0.5 & \textit{if } c \geq \textit{alarm threshold of } 1 \textit{ bar and } < 2 \textit{ bars} \\ 1-q & \textit{otherwise} \end{cases}$$

The continuous sensor model gives a better resolution to the probability of detection then the cookie cutter sensor. However a comprehensive understanding of the sensor's principles of operation as well as detailed laboratory trial results are needed to obtain this more refined formulation.

3. Summary of the Detection Model

The detection model is made up of 3 modules: i) a physical model; ii) a sensor model; and iii) a Bayesian updating model . The physical model serves to calculate the chemical concentration c at the location of sensor s due to an attack at location l, t time periods ago. Based on the output c of the physical model, the sensor model computes the probabilities, $P^s(C)$. The combination of the physical and sensor models produce the $P^s_{l,t}$ values. The Bayesian updating model calculates the probability map at time period u, $\alpha^u_{l,t}$. High value of $\alpha^u_{l,t}$ indicates that there is a strong likelihood that a chemical attack has occurred at location l, t time periods ago.

The three modules are illustrated in Figure 4.

THE MODEL

Physical model:
- Gaussian Puff for instantaneous releases
- Gaussian Plume for continuous releases

c, chemical concentration due to an attack at location l, t time periods ago arriving at the location of sensor s

Sensor model:
- Cookie cutter sensor model
- Continuous sensor model

$P_{l,t}^{s}$, the probability that a sensor located at location s detects a chemical attack at location l, that occurred t time period ago

Bayesian updating model:
- Single sensor model
- Multiple sensors model

Figure 4.   Overview of the model

IV. SMALL SCALE TEST CASES: RESULTS AND DISCUSSION

In this chapter, we perform small scale simulation tests using MATLAB for evaluating the effectiveness of the model developed in Chapter III. We compare the single sensor and multiple-sensors models and illustrate the advantage of having a larger number of sensors in achieving better estimates of the attack location and time. The small scale test cases also serve as preliminary checks on the model integrity and implementation.

The Measures of Effectiveness (MOEs) used are:

- Accurately identifying the source location; and
- Accurately identifying the time of release.

These MOEs are chosen due to their impact on operations. The source location and time of release are critical inputs for threat management and control and therefore their accuracy is paramount for making important tactical decisions.

The small scale scenario comprises an area of 300m x 300m divided into nine cells of 100m x 100m each. The time period is one minute and the chemical attack occurs at cell 4 at $u = 4$.

A. SINGLE-SENSOR

The single sensor is placed in cell 5 (see Figure 5). The sensor is operational at $u = 0$ (0800h). During the simulation run, which ends 10 time periods later at 0810h, the sensor only returns a single alarm at $u = 5$. Figure 5 illustrates the setup for the single sensor case.
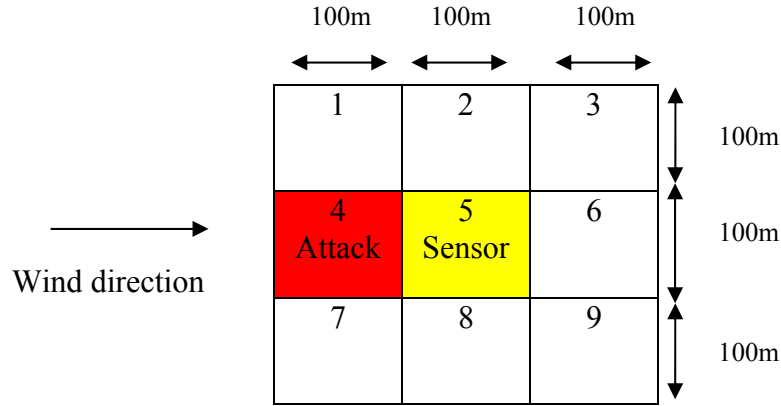
Figure 5. Test setup of the small scale case study for a single sensor

The input parameters for this model are summarized in Table 6.

The attack location is area cell 4, the nerve agent used in the attack is Sarin and the amount of agent released is 50kg. The time of attack is simulated to occur at $u = 4$. We assume α_l^0 ,probability of a chemical attack at location l in a given time period to be 0.001.

Table 6. Model input parameters for the small-scale test case scenarios

(I) Physical model(Gaussian Puff)	
Type of Chemical Warfare Agent	Nerve Agent
Quantity released (kg/m^3)	50
Wind direction (°)	90
Wind speed (m/s)	2
Pasquill-Gifford stability class	A
(II) Sensor model	
c, the chemical concentration arriving at sensor s is obtained from the physical model	
Cookie cutter	$P_{l,t}^s(c) = \begin{cases} 1 & if\ c \geq 0.01 mg/m^3 \\ 1-q & otherwise \end{cases}$

Continuous	$$P_{l,t}^{s}(c) = \begin{cases} 1 & \text{if } c \geq 30 \text{ mg}/m^3 \\ 0.9 & \text{if } c \geq 7.5 \text{ mg}/m^3 \text{ and } < 30 \text{ mg}/m^3 \\ 0.8 & \text{if } c \geq 2 \text{ mg}/m^3 \text{ and } < 7.5 \text{ mg}/m^3 \\ 0.7 & \text{if } c \geq 0.5 \text{ mg}/m^3 \text{ and } < 2 \text{ mg}/m^3 \\ 0.6 & \text{if } c \geq 0.125 \text{ mg}/m^3 \text{ and } < 0.5 \text{ mg}/m^3 \\ 0.5 & \text{if } c \geq 0.01 \text{ mg}/m^3 = \text{Detection threshold} \\ 1-q & \text{otherwise} \end{cases}$$	
(III) Bayesian updating model		
α_l^0, probability of a chemical attack at location l in a given time period	0.001	
$1-q$, false positive probability	0.2	
$P_{l,t}^{s}$, Probability that a sensor located at location s detects at time u a chemical attack at location l, t time periods ago.	Obtained from sensor model	

1. Results from the Physical Model

The results from the Gaussian puff model are listed in Table 7, where *X* represents the distance away from the source in the *x*-axis in meters, and *Y* represents the distance away from the source in the *y*-axis in meters.

Table 7. Chemical concentration according to the Gaussian Puff model for the small-scale test scenario

X(meters)	Y(meters)	Concentration in mg/m³						
		0 min	1 min	2 min	3 min	4 min	5 min	6 min
0	0	1053503	0.00	0.00	0.00	0.00	0.00	0.00
0	100	0.00	0.00	0.00	0.00	0.00	0.00	0.00
0	200	0.00	0.00	0.00	0.00	0.00	0.00	0.00
100	0	0.00	213.42	0.00	0.00	0.00	0.00	0.00
100	100	0.00	0.00	0.00	0.00	0.00	0.00	0.00
100	200	0.00	0.00	0.00	0.00	0.00	0.00	0.00
200	0	0.00	0.40	30.47	0.00	0.00	0.00	0.00
200	100	0.00	0.00	0.00	0.00	0.00	0.00	0.00
200	200	0.00	0.00	0.00	0.00	0.00	0.00	0.00

2. Results from the Sensor Model

Using c, the chemical concentration arriving at sensor s obtained from the output of the Gaussian puff model, both the cookie cutter and continuous sensor model yield the following values of $P_{l,t}^5$, where $P_{l,t}^5$ is the probability that the sensor placed at location 5 currently detects a chemical attack at location l, that occurred t time period ago. The values of $P_{l,t}^5$ are shown in Table 8.

Table 8. $P_{l,t}^5$ values for the small-scale test scenario

	Attack time scale, t time periods since the occurrence of the chemical attack									
Location(l)	0	1	2	3	4	5	6	7	8	9
1	0.2	0.2	0.2	0.2	0.2	0.2	0.2	0.2	0.2	0.2
2	0.2	0.2	0.2	0.2	0.2	0.2	0.2	0.2	0.2	0.2
3	0.2	0.2	0.2	0.2	0.2	0.2	0.2	0.2	0.2	0.2
4	0.2	1	0.2	0.2	0.2	0.2	0.2	0.2	0.2	0.2
5	1	0.2	0.2	0.2	0.2	0.2	0.2	0.2	0.2	0.2
6	0.2	0.2	0.2	0.2	0.2	0.2	0.2	0.2	0.2	0.2
7	0.2	0.2	0.2	0.2	0.2	0.2	0.2	0.2	0.2	0.2
8	0.2	0.2	0.2	0.2	0.2	0.2	0.2	0.2	0.2	0.2
9	0.2	0.2	0.2	0.2	0.2	0.2	0.2	0.2	0.2	0.2

3. Results from the Bayesian Updating Model

At $u = 0$, we have no updates from the sensor located at cell 5, hence, α_l^0, the probability of a chemical attack at location l in a given time period, is determined by threat and vulnerability studies of the defender. For this test case, we assume that it is uniformly distributed over the area cells with a value of 0.001. The probability map for α_l^0 is shown in Figure 6.
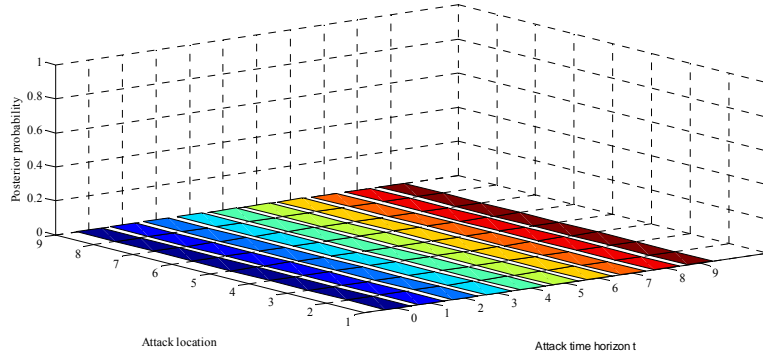
Figure 6.   Probability map at $u = 0$ for the small scale case study for a single sensor

At $u = 1$, the sensor records no detection, hence $\alpha_{l,t}^1$ decreases for the cells at which a chemical attack at $t = 0$ to 9 time periods ago are expected to give off a sensor alarm. The cells affected are 4 and 5. The probability map for $\alpha_{l,t}^1$ is shown in Figure 7.
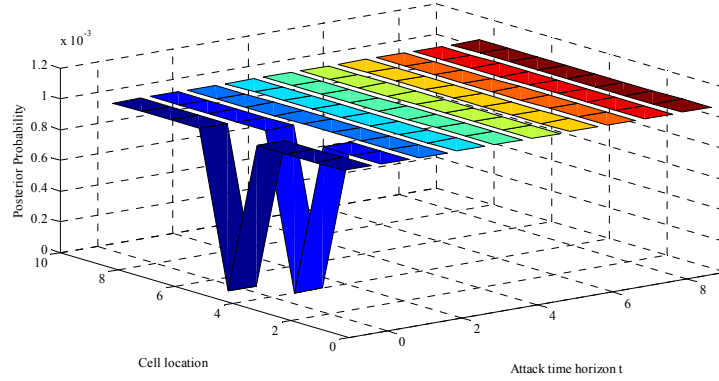
Figure 7.   Probability map at $u = 1$ for the small scale case study for a single sensor

The sensor continues with no detections up to $u = 4$. Hence $\alpha_{l,t}^4$ decreases for the cells at which a chemical attack at $t = 0$ to 9 time periods are expected to give off a sensor alarm. The cells affected are 4 and 5. The probability map at $u = 4$ is as shown in Figure 8.
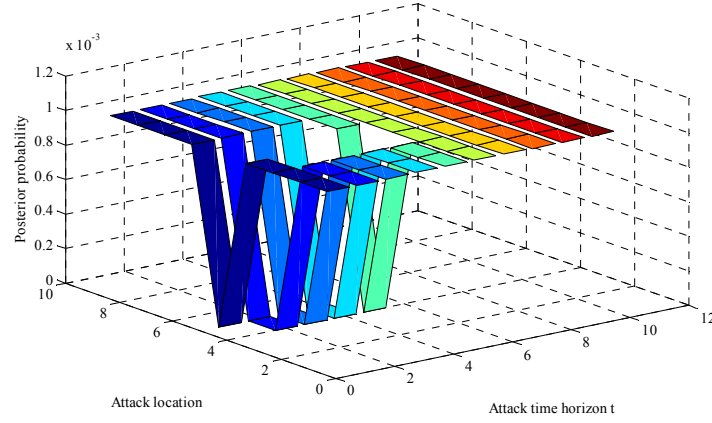
Figure 8. Probability map at $u = 4$ for the small scale case study for a single sensor

At $u = 5$, the sensor updates with a detection alarm, hence $\alpha_{l,t}^5$ increases for the cells at which a chemical attack at $t = 0$ to 9 time periods ago are expected to give off a sensor alarm. From Figure 9, we can see peaks for releases at (i) location 5 at $t = 0$, (ii) location 4 at $t = 1$.
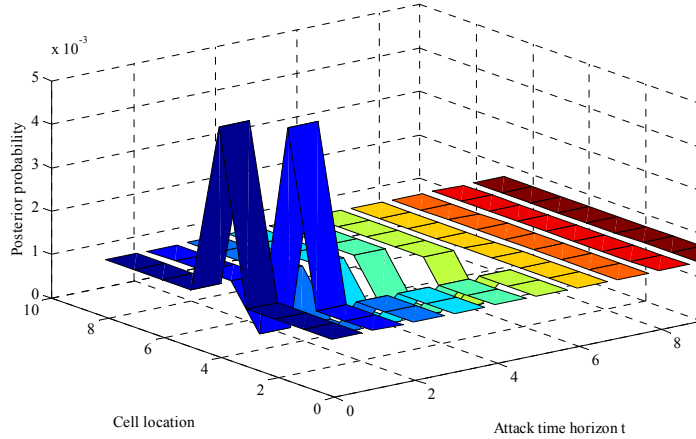
Figure 9. Probability map at $u = 5$ for the small scale case study for a single sensor

From the Gaussian puff model, the chemical plume generated from the chemical attack at location 4 at $u = 4$ passes over the sensor placed at location 5 at $u = 5$. Hence no more correct detection updates can be received from the sensor from time $u = 6$ onwards.

30

The peaks observed are preserved and continue to slide across the attack time horizon, as shown in Figure 10, which shows the probability map for $u = 6$.
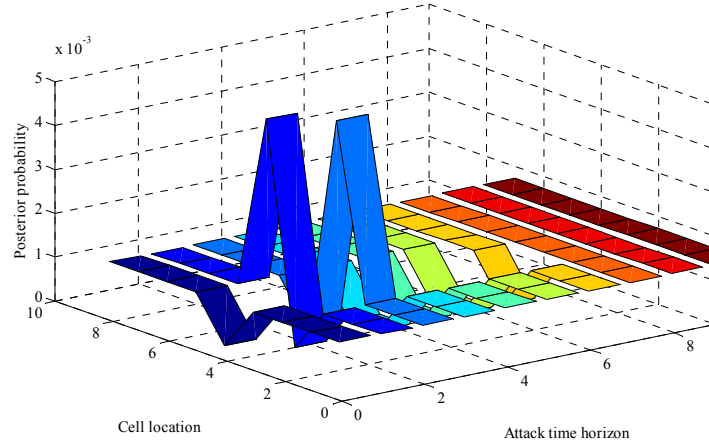
Figure 10.   Probability map at $u = 6$ for the small scale case study for a single sensor

The peaks observed are preserved and continues to slide across the attack time horizon with each update till the end of the simulation at $u = 10$. From the contour plot in Figure 11, it can be seen that the model produces two estimates of the location and time of the chemical attack. They are (i) cell location 5 at $u = 5$ ($t = 5$) with a posterior probability of 0.00501 and (ii) cell location 4 at $u = 4$ which is the true attack, with a posterior probability of 0.00502.
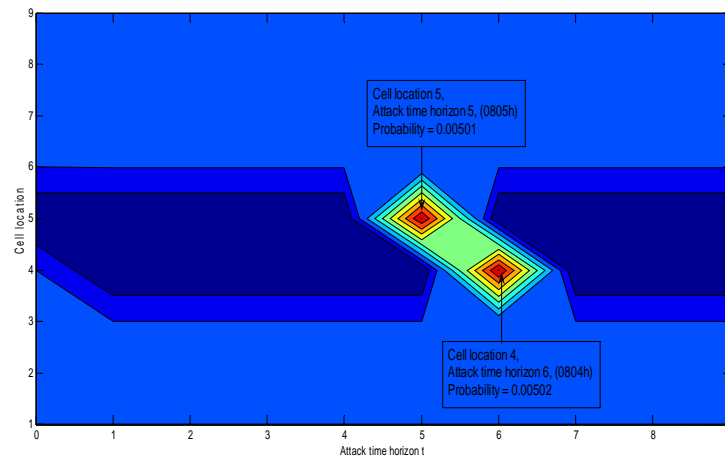
Figure 11.   Probability map at $u = 10$ for the small scale case study for a single sensor

31

Notice that both estimates – the erroneous one in i and the correct one in ii – are identified with negligible probabilities. These inconclusive results are due to the relatively high false positive probability (0.2) and the poor coverage by only one sensor.

Next we extend the single sensor model to a multiple-sensors model, which is a more accurate abstraction of reality.

B.   MULTIPLE SENSORS SMALL SCALE TEST SCENARIO

Suppose that in addition to the sensor in cell 5, sensors are also placed in cells 4 and 6. During the simulation run, which ends 10 time periods later, the sensor placed at cell 4 returns a single alarm at $u = 4$, the sensor placed at cell 5 returns a single alarm at $u = 5$ and the sensor placed at cell 6 returns a single alarm at $u = 6$. Figure 12 illustrates this setup.
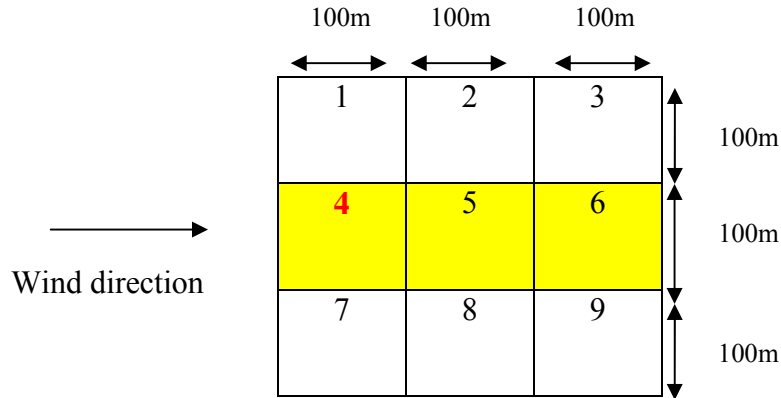
Figure 12.   Test setup of the small scale case study with multiple sensors

1.   Results from the Physical Model

The results from the Gaussian puff model for the multiple sensors small scale scenario are exactly the same as that of the single sensor case test since they share the same chemical attack scenario.

2. Results from the Sensor Model

Using c, the chemical concentration arriving at sensor s obtained from the output of the Gaussian puff model, both the cookie cutter and continuous sensor model yield the following values of $P_{l,t}^s$, where s = 4, 5 and 6. This is because the dispersion of the chemical plume over the area of the small scale test scenario does not exhibit large deviations in concentrations.

Table 9.   Results from the sensor model for sensor 4

$P_{l,t}^4$	Attack time scale, t time steps since the occurrence of the chemical attack									
Location	0	1	2	3	4	5	6	7	8	9
1	0.2	0.2	0.2	0.2	0.2	0.2	0.2	0.2	0.2	0.2
2	0.2	0.2	0.2	0.2	0.2	0.2	0.2	0.2	0.2	0.2
3	0.2	0.2	0.2	0.2	0.2	0.2	0.2	0.2	0.2	0.2
4	1	0.2	0.2	0.2	0.2	0.2	0.2	0.2	0.2	0.2
5	0.2	0.2	0.2	0.2	0.2	0.2	0.2	0.2	0.2	0.2
6	0.2	0.2	0.2	0.2	0.2	0.2	0.2	0.2	0.2	0.2
7	0.2	0.2	0.2	0.2	0.2	0.2	0.2	0.2	0.2	0.2
8	0.2	0.2	0.2	0.2	0.2	0.2	0.2	0.2	0.2	0.2
9	0.2	0.2	0.2	0.2	0.2	0.2	0.2	0.2	0.2	0.2

Table 10.   Results from the sensor model for sensor 5 (the same as for the single sensor case)

$P_{l,t}^5$	Attack time scale, t time steps since the occurrence of the chemical attack									
Location	0	1	2	3	4	5	6	7	8	9
1	0.2	0.2	0.2	0.2	0.2	0.2	0.2	0.2	0.2	0.2
2	0.2	0.2	0.2	0.2	0.2	0.2	0.2	0.2	0.2	0.2
3	0.2	0.2	0.2	0.2	0.2	0.2	0.2	0.2	0.2	0.2
4	0.2	1	0.2	0.2	0.2	0.2	0.2	0.2	0.2	0.2
5	1	0.2	0.2	0.2	0.2	0.2	0.2	0.2	0.2	0.2
6	0.2	0.2	0.2	0.2	0.2	0.2	0.2	0.2	0.2	0.2
7	0.2	0.2	0.2	0.2	0.2	0.2	0.2	0.2	0.2	0.2
8	0.2	0.2	0.2	0.2	0.2	0.2	0.2	0.2	0.2	0.2
9	0.2	0.2	0.2	0.2	0.2	0.2	0.2	0.2	0.2	0.2

Table 11.   Results from the sensor model for sensor 6

$P_{l,t}^6$	Attack time scale, t time steps since the occurrence of the chemical attack									
Location	0	1	2	3	4	5	6	7	8	9
1	0.2	0.2	0.2	0.2	0.2	0.2	0.2	0.2	0.2	0.2
2	0.2	0.2	0.2	0.2	0.2	0.2	0.2	0.2	0.2	0.2
3	0.2	0.2	0.2	0.2	0.2	0.2	0.2	0.2	0.2	0.2
4	0.2	0.2	1	0.2	0.2	0.2	0.2	0.2	0.2	0.2
5	0.2	1	0.2	0.2	0.2	0.2	0.2	0.2	0.2	0.2
6	1	0.2	0.2	0.2	0.2	0.2	0.2	0.2	0.2	0.2
7	0.2	0.2	0.2	0.2	0.2	0.2	0.2	0.2	0.2	0.2
8	0.2	0.2	0.2	0.2	0.2	0.2	0.2	0.2	0.2	0.2
9	0.2	0.2	0.2	0.2	0.2	0.2	0.2	0.2	0.2	0.2

3.   Results from the Bayesian Updating Model

At $u = 0$ (0800h), all three sensors do not report, hence α^0, the probability of a chemical attack at any location in a given time period is determined by threat and vulnerability studies. As before, we assume that $\alpha^0 = 0.001$. The probability map at $u = 0$ is shown in Figure 13.
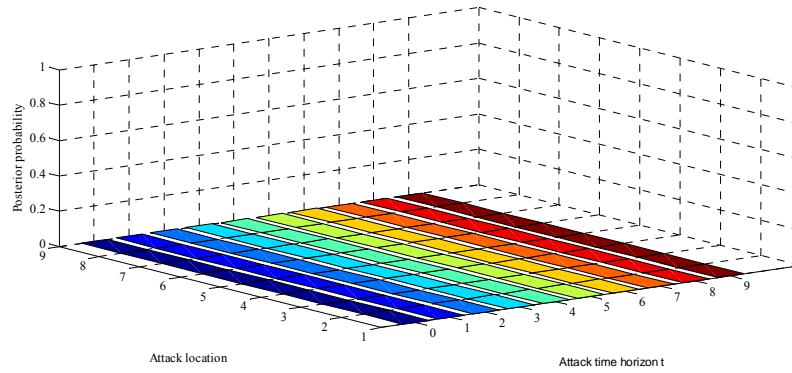
Figure 13.   Probability map at $u = 0$ for the small scale case study with multiple sensors

At $u = 1$, all 3 sensors still do not report, hence $\alpha_{l,t}^1$ decreases for the cells at which a chemical attack at $t = 0$ to 9 time periods ago relative to $u = 1$, is expected to give off a sensor alarm. The cells affected are 4, 5 and 6. The probability map at $u = 1$ is as shown in Figure 14.
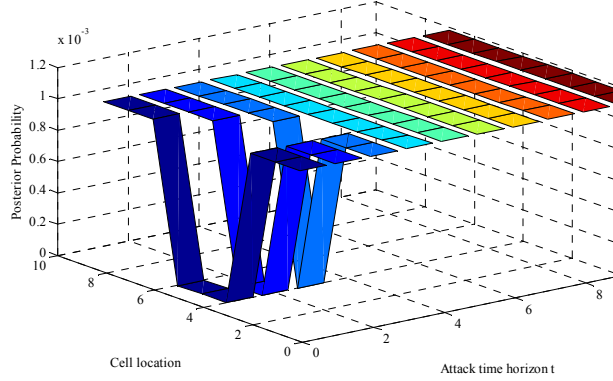
Figure 14.   Probability map at $u = 1$ for the small scale case study with multiple sensors

The 3 sensors continue not to respond up to $u = 3$ (0803h). Hence the values of $\alpha_{l,t}^3$ decrease for the cells at which a chemical attack at $t = 0$ to 9 time periods ago relative to $u = 3$, is expected to give off a sensor alarm. The cells affected are 4, 5 and 6. The probability map at $u = 3$ is as shown in Figure 15.
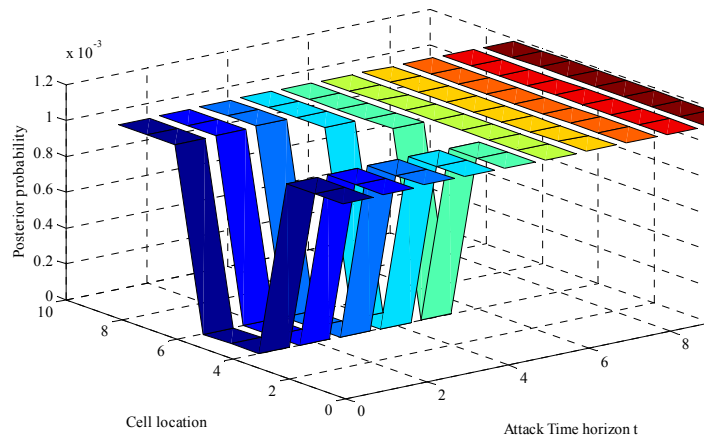
Figure 15.   Probability map at $u = 3$ for the small scale case study with multiple sensors

At $u = 4$, the sensor placed at cell 4 reports a detection, hence the value of $\alpha_{l,t}^4$ increases for the cells at which a chemical attack at $t = 0$ to 9 time periods ago relative to u, is expected to give off a sensor alarm. The sensors in cells 5 and 6 do not signal detection. From Figure 16, we can see a peak for a release at location 4 at $t = 0$.
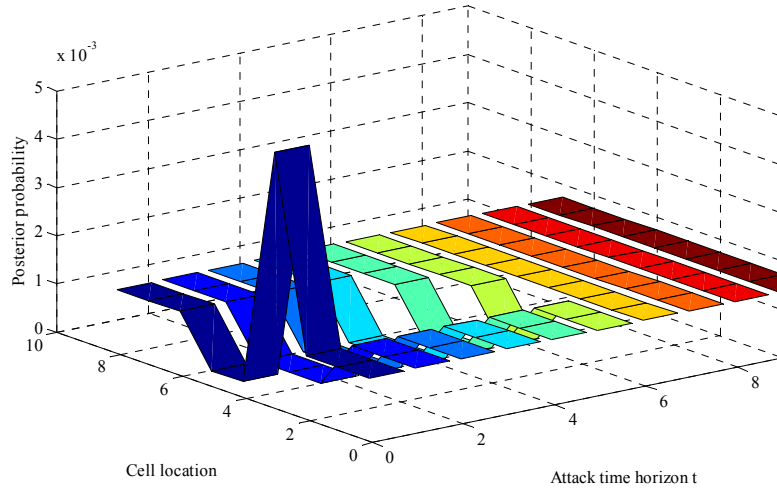
Figure 16.   Probability map at $u = 4$ for the small scale case study with multiple sensors

At $u = 5$, the sensor placed at cell 5 reports a detection while the sensors in 4 and 6 do not report a detection. The value of $\alpha_{l,t}^5$ increases for the cells at which a chemical attack at $t = 0$ to 9 time periods ago relative to u, is expected to give off a sensor alarm. From Figure 17, we can see a new peak for a release at location 5 at $t = 0$ and an increase in intensity of the previous peak for a release at $l = 4$, $t = 1$.
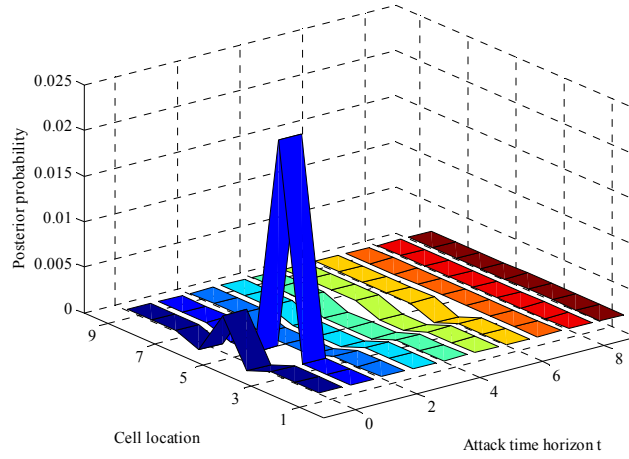
Figure 17.   Probability map at $u = 5$ for the small scale case study with multiple sensors

At $u = 6$, the sensor placed at cell 6 reports a detection while the sensors at cells 4 and 5 do not report a detection. The value of $\alpha_{l,t}^6$ increases for the cells at which a chemical attack at $t = 0$ to 9 time periods ago relative to u, is expected to give off a sensor alarm. From Figure 18, we can see a new peak for a release at location 6 at $t = 0$ and an increase in intensity of the previous peaks at location 5 at $t = 1$ and at location 4 at $t = 2$.
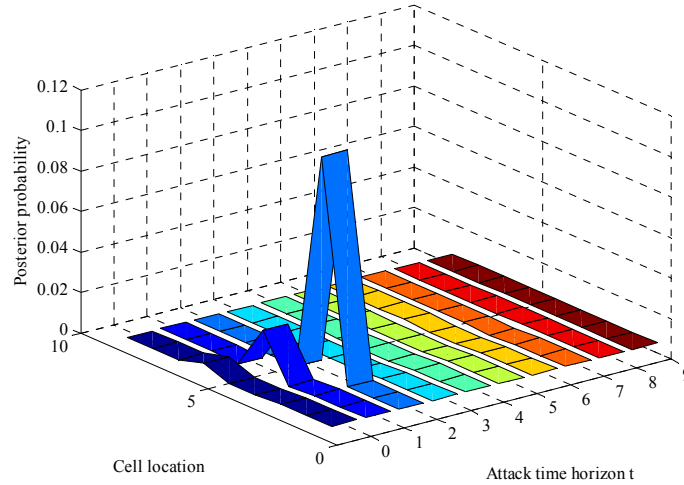
Figure 18.   Probability map at $u = 6$ for the small scale case study with multiple sensors

From the Gaussian puff model, the chemical plume generated from the chemical attack at location 4 at $u = 4$ passes over all the sensors placed in the area of operation at $u = 7$. Hence no more detection reports can be received from the sensors. The peaks observed are preserved and continue to slide across the attack time horizon as shown in Figure 19, which shows the probability map for $u = 7$.
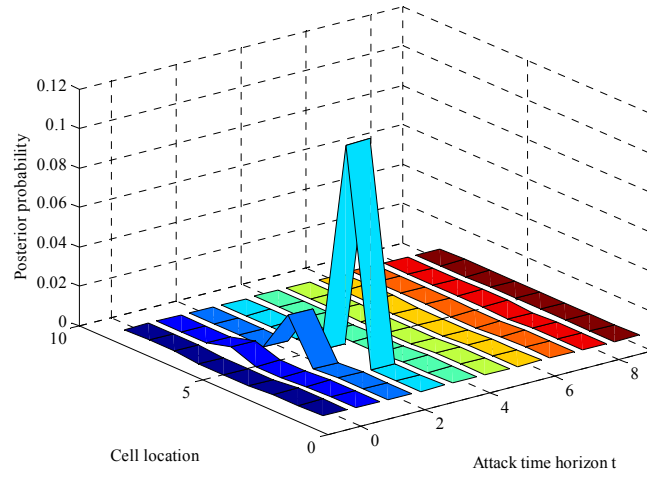
Figure 19.   Probability map at $u = 7$ for the small scale case study with multiple sensors

From the contour plot at $u = 10$, in Figure 20, it can be seen that the model produces a single estimate of the location and time of the chemical attack.
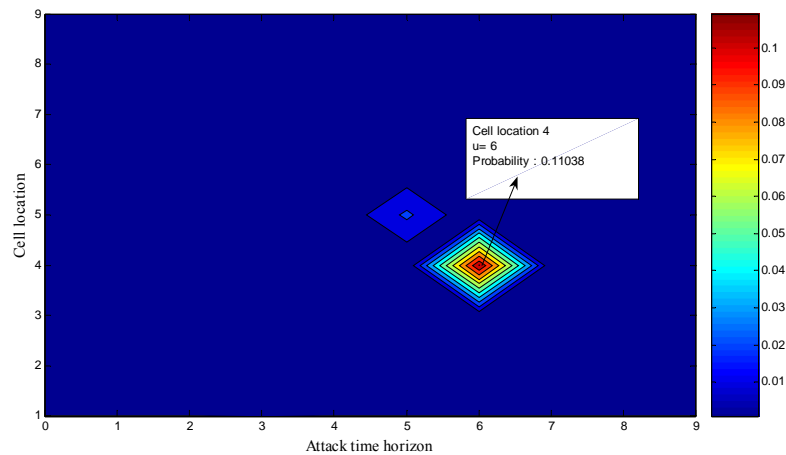
Figure 20.   Probability map at $u = 10$ for the small scale case study with multiple sensors

38

From the series of probability maps above, the peaks observed from the onset of the first alarm continue to slide across the attack horizon with each update until the end of the simulation. The chemical attack characteristic can be identified to be at location 4 at $u = 4$ with a probability of occurrence of 0.11.

The actual time of release and attack location in this simulation is $l = 4$ and $u = 4$, which is the estimate given by the model. The posterior probability obtained for an attack at $u = 4$ at $l = 4$ is 0.11 is too low to sound an alarm that triggers a response. This probability value, while larger than the value obtained for the single sensor case, is still low because of relatively high false positive probability and insufficient coverage.

C.   COMPARISON STUDY BETWEEN SINGLE-SENSOR AND MULTIPLE-SENSORS MODEL

With all scenario parameters kept constant with the exception of the number of sensors used, it is evident that with multiple sensors, the model is better able to estimate both the location and time of attack. Table12 summarizes the results obtained from both models for the same threat scenario.

Table 12.   Results of comparison study between single and multiple sensors model

	Attack Location (l)	Time of attack (t)	Probability of attack at location l and time t
Actual	4	0804	-
Single Sensor	4	0804	0.00501
	5	0805	0.00502
Multiple Sensor	4	0804	0.11

For the same attack scenario, the multiple-sensors model provides more accurate estimates of the location and time of the attack (probability of 0.11). The single sensor model, on the other hand, returns multiple estimates with low probabilities. Hence it is concluded that a multiple sensors model provides better estimates of a chemical attack.

The simple test cases serve as a preliminary check on the model integrity and implementation. The multiple-sensors model was found to able to estimate accurately both the time and location of the attack. With this encouragement, the multiple-sensors model will next be implemented with respect to large scale settings that better depict real-world operations.

V.   MODEL EVALUATION

In this chapter, we evaluate the model with respect to settings that more closely depict real-world scenarios. Preliminary simulation runs are first performed to (i) establish the noise floor of the model and (ii) select an alarm threshold for the probability map provided that will trigger a response to the chemical attack detected. The noise floor of the model is the baseline value of the posterior probabilities in the probability maps that is attributed to the presence of false positive signals. Based on the preliminary simulation runs, an experimental test matrix is developed to evaluate the model and determine the contribution of the lead factors.

In evaluating the model, a false positive error is defined as a signal from a sensor that is exposed to a chemical concentration below its detection threshold. A false negative error is defined as the absence of a signal from a sensor that is exposed to a chemical concentration which is above the detection threshold of the sensor.

Section A describes the basic scenario that is used for the evaluation. Section B discusses the results of the preliminary simulation runs. Section C details the test matrix used for evaluating the model. Section D discusses the evaluation results of the model. Section E discusses the insights obtained on sensor coverage and deployment.

A.   BASIC SCENARIO

The area of operations is a 1km $\times$ 1km square divided into a grid of 100 location cells (henceforth called cells) each of size 100m $\times$ 100m. A total of 16 sensors are deployed in the area of operations. The placement of the sensors is fixed throughout and follows common operational tactics. The prevailing wind speed and direction are 1.67m/s and east, respectively.

It is assumed that on average there are 10 false positive signals during a one-hour period. Hence $1-q$, the probability of a false positive cue from any of the 16 sensors deployed in a one-minute time period is set to be 10/(60 x 16) =0.0104. The quantity of

chemical agent which is assumed to be Sarin to be released, is set to a nominal attack quantity of 50kg and we assume that the attack occurs at u = 5.

Figure 21 depicts the area of operations with the 16 sensors located in the shaded cells.

N ↑
→ E

1.67m/s

1	2	3	4	5	6	7	8	9	10
1 1	1 2	1 3	1 4	1 5	1 6	1 7	1 8	1 9	2 0
2 1	2 2	2 3	2 4	2 5	2 6	2 7	2 8	2 9	3 0
3 1	3 2	3 3	3 4	3 5	3 6	3 7	3 8	3 9	4 0
4 1	4 2	4 3	4 4	4 5	4 6	4 7	4 8	4 9	5 0
5 1	5 2	5 3	5 4	5 5	5 6	5 7	5 8	5 9	6 0
6 1	6 2	6 3	6 4	6 5	6 6	6 7	6 8	6 9	7 0
7 1	7 2	7 3	7 4	7 5	7 6	7 7	7 8	7 9	8 0
8 1	8 2	8 3	8 4	8 5	8 6	8 7	8 8	8 9	9 0
9 1	9 2	9 3	9 4	9 5	9 6	9 7	9 8	9 9	100
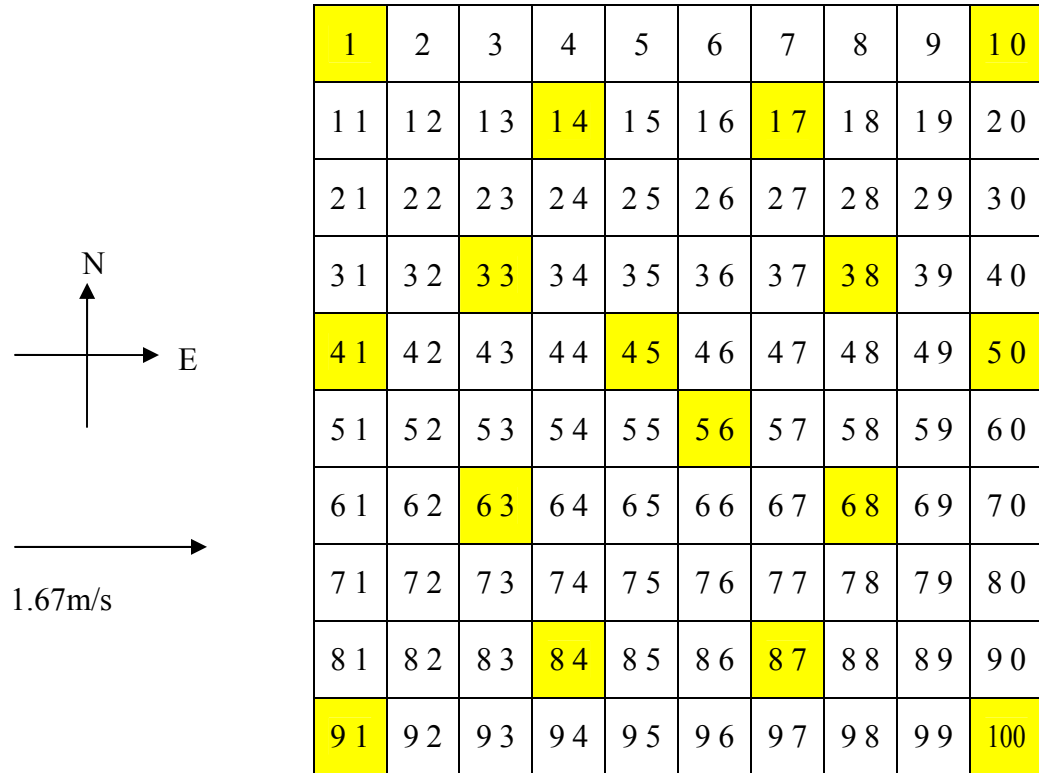
Figure 21.   Illustration of the area of operations

B.   PRELIMINARY TRIALS

Four attack locations are randomly selected amongst the 100 locations possible. In addition, a simulation test case with no attack is also performed. Each of the five preliminary simulation test cases is replicated five times. The simulation tests cases are summarized in Table 13.

Table 13.　　Test cases and their attack location for the preliminary trials

Test Case Number	Attack location
1	No attack
2	45
3	48
4	51
5	85

The simulation details of the test cases are summarized in Table 14.

Table 14.　　Simulation details of the preliminary trials

Simulation Details	
Fixed parameters	
Area of operations	1km × 1km
Grid representation	10 by 10 cells
Cell resolution	100m
Meteorological Data	
wind speed	1.67
wind direction	East
stability class	A
Sensor Data	
Number of sensors deployed	16
Locations of sensors	Cell 1, 10,14,17,33,38,41,45,50,56,63,68,84,87,91,100
Chemical attack data	
Chemical agent used	Sarin
Release type	Instantaneous
Quantity released	50kg
Time of attack	$u = 5$
Parameters varied	
Sensor signal return	Simulated to return 1 with a probability of detection $P_{l,t}^s$, 0 with probability $1 - P_{l,t}^s$, where $P_{l,t}^s$ is determined by the physical and sensor models.

The inputs parameters of the model are summarized in Table 15.

Table 15.	Input parameters of the model

(I) Physical model(Gaussian Puff)	
Chemical Warfare Agent	Sarin
Quantity released (kg/m^3)	50
Wind direction (°)	90
Wind speed (m/s)	1.666666667
Pasquill-Gifford stability class	A

(II) Sensor model	
c, the chemical concentration arriving at sensor s is obtained from the physical model	

Continuous	$$P_{l,t}^s(c) = \begin{cases} 1 & \textit{if } c \geq 30 \ mg/m^3 \\ 0.9 & \textit{if } c \geq 7.5 \ mg/m^3 \textit{ and } < 30 \ mg/m^3 \\ 0.8 & \textit{if } c \geq 2 \ mg/m^3 \textit{ and } < 7.5 \ mg/m^3 \\ 0.7 & \textit{if } c \geq 0.5 \ mg/m^3 \textit{ and } < 2 \ mg/m^3 \\ 0.6 & \textit{if } c \geq 0.125 \ mg/m^3 \textit{ and } < 0.5 \ mg/m^3 \\ 0.5 & \textit{if } c \geq 0.01 \ mg/m^3 = \text{Detection threshold} \\ 1-q & \textit{otherwise} \end{cases}$$

(III) Bayesian updating model	
L, number of attack locations	100
T, time horizon of an attack in the area of operation	15
α^0, *a priori* probability of a chemical attack at a certain location in a given time period	0.001
1-q , false positive probability	0.0104
$P_{l,t}^s$, probability that a sensor located at location s detects at time u a chemical attack at location l, that has occurred t time periods ago.	Obtained from sensor model

## 1.	Results from the Physical Model

The results from the Gaussian puff model give the temporal concentration of material from the release of 50kg of the nerve agent Sarin at $u = 0$. Figure 22 depicts the dispersion of the nerve agent along the x and y directions from the chemical release source, at 1 minute intervals. The x-axis and y-axis show the distance in meters from the chemical source in the x and y direction, respectively. The right hand side scale shows the concentration of the chemical plume in mg/m^3.
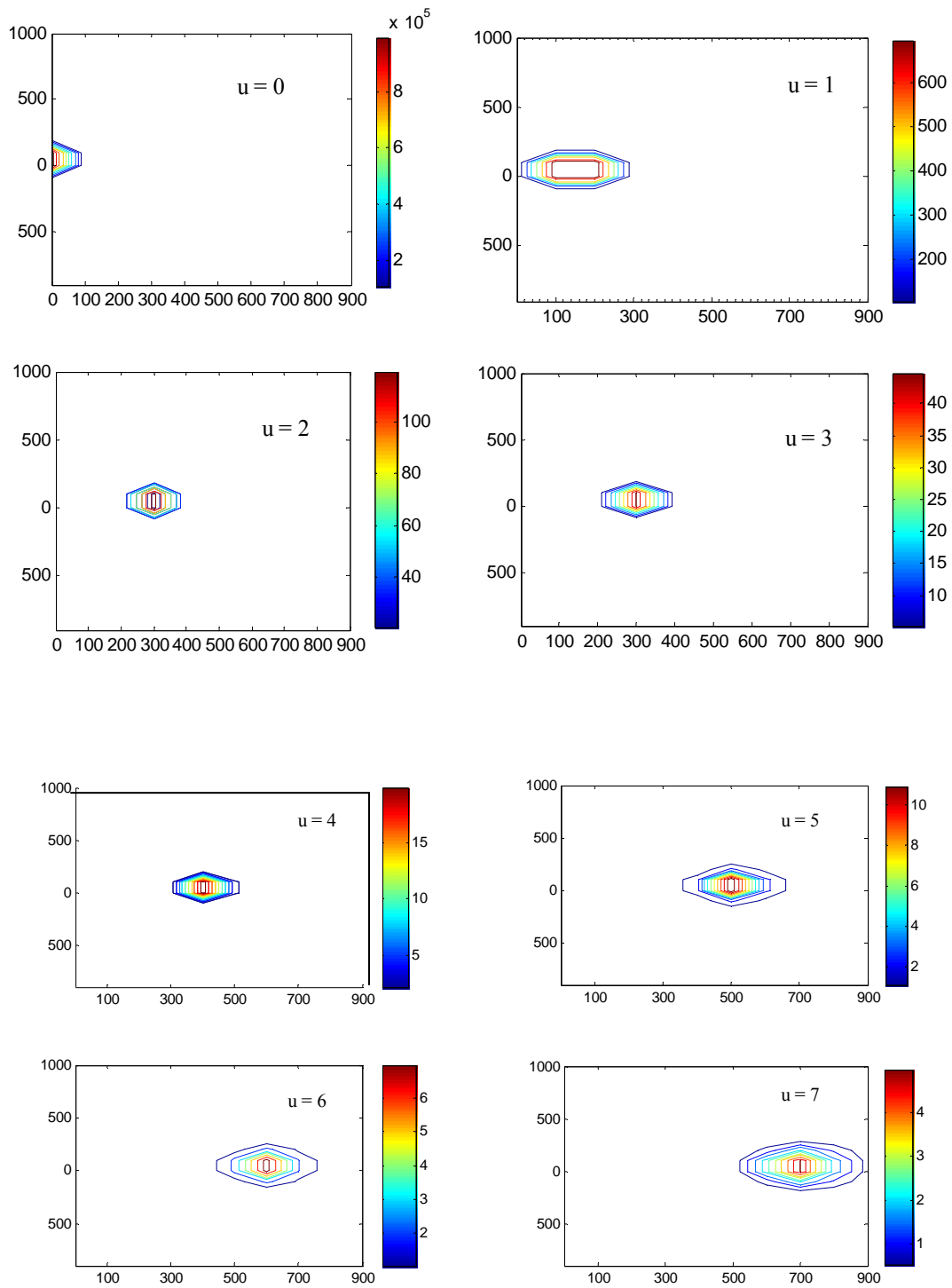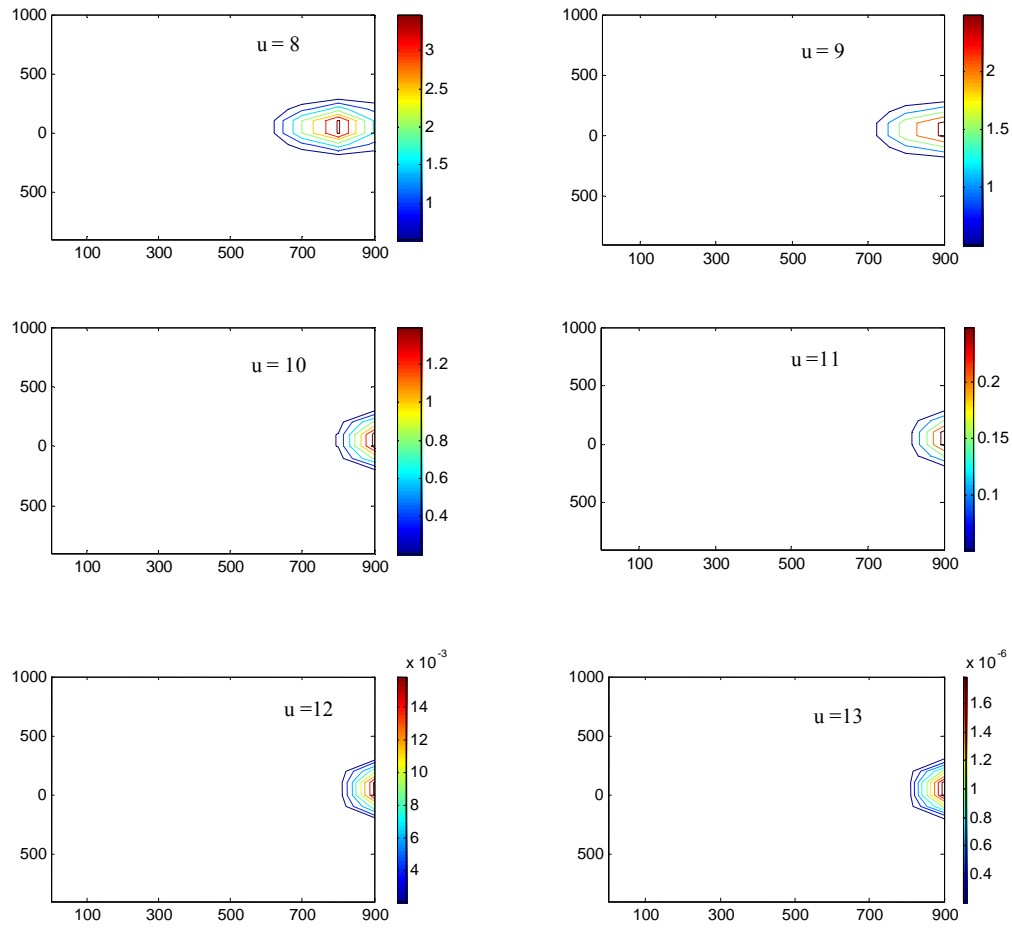
Figure 22.   Series of time plots that show concentration profiles of the chemical puff over distances from the source in the *x* and *y* direction

From the series of time plots in Figure 22, it can be seen that in 13 minutes, the chemical puff has passed over 1km, only leaving traces of low concentrations, 1×10^{-6} mg/m^3 , at a distance of 1km from the source location. Hence in our area of operations of size 1km by 1km, the chemical puff generated from any release location would pass over in at most 13 minutes, leaving trace concentrations that are below the detection threshold of the sensors. Thus, the time horizon *T* is bounded by 13 minutes.

2. Results of the Sensor Model

The results of the sensor model for the inputs given in Table 15 are shown in the Appendix.

3. Simulation Results for Test Case 1, No Chemical Attack

A no-attack test case aims to establish the noise floor of the system of sensors. This enables decision makers to set a lower bound on the alarm threshold for an action to be taken. Table 16 summarizes the number of false positive signals return for each simulation run.

Table 16.   Number of false positive signals in each of the simulation runs

Simulation run number	Number of false positive signals
1	1
2	0
3	7
4	5
5	3

Figure 23 shows the plot of $g(u) = \max_{l,t} \alpha_{l,t}^u$, the highest values per time period in the probability map during the detection time horizon, for each of the five simulation runs.
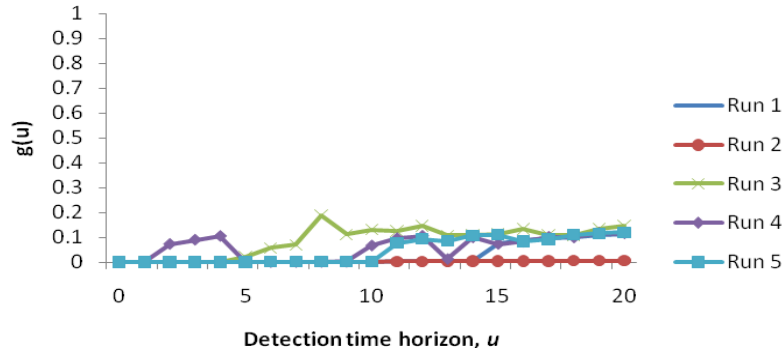
Figure 23.   Highest probability values, $g(u) = \max_{l,t} \alpha_{l,t}^u$, within the probability map across the detection time horizon.

47

From Figure 23, it can be seen that, as expected, the noise floor increases with the number of false positive errors. Based on the 5 simulation runs performed we set the lower bound on the alarm threshold at 0.2. In setting an alarm threshold for an action to be taken; a posterior probability of 0.7 is selected, which is reasonable for an estimated noise floor of 0.2.

4. Simulation Results for Test Case 2, Attack at Location 45

For an attack at cell 45, the Expected Number of Correct Signals (ENCS) is 5.27 from 3 different sensors. The parameter ENCS is associated with a given cell l, and is defined as the expected number of signals from the deployed sensors given a chemical attack at location l. The ENCS is a measure of the sensor coverage; the higher the value of ENCS for a certain cell, the better the sensor coverage of that cell. The ENCS is dependent on the specific layout of the deployed sensors relative to the attack location. It is important to take notice of the ENCS as it is a factor that affects the performance of the model. The statistics of the five simulation runs are summarized in Table 17.

Table 17.　　　Simulated sensor signals and model outputs for preliminary test case 2

	Run 1	Run 2	Run 3	Run 4	Run 5
Simulated signal returns					
Number signals from sensor deployed	7	7	7	6	13
False positive errors	0	1	1	0	8
False negative errors	0	1	1	1	1
Correct signals	7	6	6	6	5
Model outputs					
Estimate of attack location	Cell 45	Cell 45	Cell 45	Cell 45	Cell 45
Estimate of time of attack	$u = 5$	$u = 5$	$u = 5$	$u = 5$	$u = 5$
Location error (meters)	0	0	0	0	0
Time of release error (mins)	0	0	0	0	0
Time at which alarm threshold of 0.7 is crossed	$u = 8$	$u = 8$	$u = 8$	$u = 9$	$u = 8$
Highest posterior for the correct location and time, $Max_u \alpha_{45,u-5}^u$	0.997	0.997	0.986	0.994	1
Time at which the highest value of the correct posterior is	$u = 12$	$u = 10$	$u = 12$	$u = 12$	$u = 9$

observed, $ArgMax_u \alpha^u_{45,u-5}$					
Presence of incorrect posteriors > alarm threshold of 0.7	No	No	No	No	No
Presence of incorrect posteriors > noise floor of 0.2	No	No	No	No	Yes
Is $\alpha^u_{45,u-5} \geq \alpha^u_{l,t} \ \forall \ l, t, u$?	Yes	Yes	Yes	Yes	Yes

From Table 17, it can be seen that despite the presence of false positive and false negative errors the model accurately estimates the location and time of the attack within 4 minutes of the occurrence of the attack. It is observed from run #4 that false negative errors can lead to a delay in crossing the alarm threshold ($u = 9$ as opposed to $u = 8$). It is observed from run #5 that false positive and false negative errors can result in the presence of false estimates, where a false estimate is a posterior of an attack that is above the noise floor in a wrong location and/or at a time.

We present here only the results of run #1. This run represents an ideal scenario in which there is no occurrence of any false positive or false negative errors. The respective times of the signals (indicated by 1) and the corresponding sensors that produced them are shown in Table 18

Table 18.   Signals from the respective sensors for run #1 of test case 1

Detection time horizon(u)	Location of sensor															
	1	10	14	17	33	38	41	45	50	56	63	68	84	87	91	100
0	0	0	0	0	0	0	0	0	0	0	0	0	0	0	0	0
1	0	0	0	0	0	0	0	0	0	0	0	0	0	0	0	0
2	0	0	0	0	0	0	0	0	0	0	0	0	0	0	0	0
3	0	0	0	0	0	0	0	0	0	0	0	0	0	0	0	0
4	0	0	0	0	0	0	0	0	0	0	0	0	0	0	0	0
5	0	0	0	0	0	0	0	1	0	0	0	0	0	0	0	0
6	0	0	0	0	0	0	0	0	0	0	0	0	0	0	0	0
7	0	0	0	0	0	0	0	0	0	0	0	0	0	0	0	0
8	0	0	0	0	0	1	0	0	1	0	0	0	0	0	0	0
9	0	0	0	0	0	0	0	0	1	0	0	0	0	0	0	0

10	0	0	0	0	0	0	0	0	1	0	0	0	0	0	0	0
11	0	0	0	0	0	0	0	0	1	0	0	0	0	0	0	0
12	0	0	0	0	0	0	0	0	1	0	0	0	0	0	0	0
13	0	0	0	0	0	0	0	0	0	0	0	0	0	0	0	0
14	0	0	0	0	0	0	0	0	0	0	0	0	0	0	0	0
15	0	0	0	0	0	0	0	0	0	0	0	0	0	0	0	0
16	0	0	0	0	0	0	0	0	0	0	0	0	0	0	0	0
17	0	0	0	0	0	0	0	0	0	0	0	0	0	0	0	0
18	0	0	0	0	0	0	0	0	0	0	0	0	0	0	0	0
19	0	0	0	0	0	0	0	0	0	0	0	0	0	0	0	0
20	0	0	0	0	0	0	0	0	0	0	0	0	0	0	0	0

The series of probability maps for simulation run #1 is shown in Figure 24.

Figure 24 compares the values of $\max_{l,t} \alpha_{l,t}^{u}$ with $\alpha_{45,u-5}^{u}$ for $u \geq 5$.
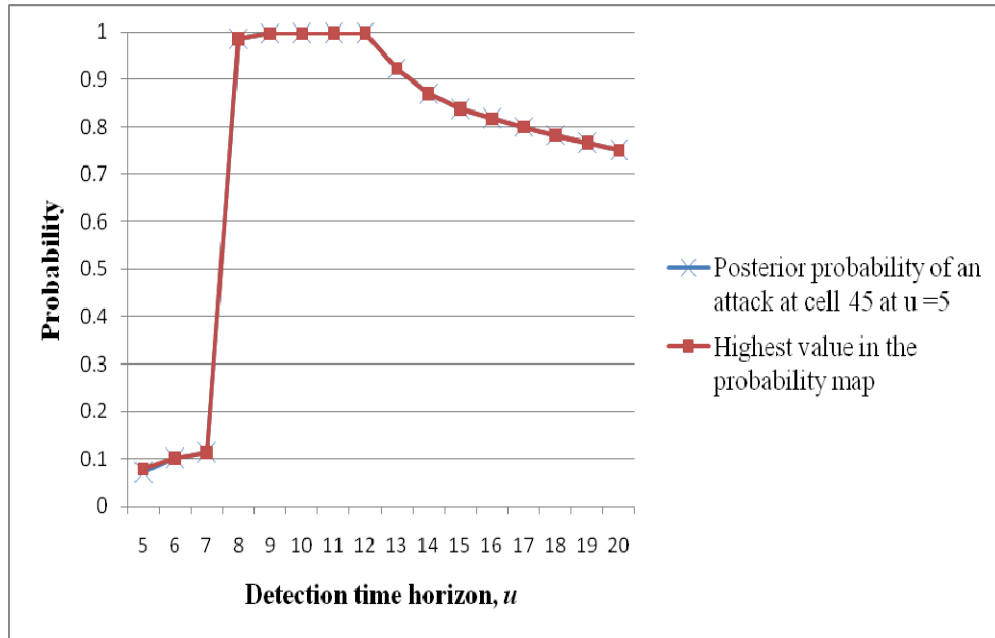
Figure 24.   Comparison between the values of $\max_{l,t} \alpha_{l,t}^{u}$ and $\alpha_{45,u-5}^{u}$ for $u = $ 5

From Figure 24 it is observed that $\alpha_{45,u-5}^{u}$ has the highest value within all the probability maps across the detection time horizon. The model returns a single estimate of the attack location and time – cell 45 at $u = 5$. In addition, $\alpha_{45,u-5}^{u}$ crosses the alarm threshold of 0.7 at $u = 8$. Hence the model is able to estimate accurately the attack location and time within 3 minutes of the attack.

5. Simulation Results for Test Case 3, Attack at Location 48

For an attack at cell 48, the ENCS is 2, from a single sensor at cell 50. The statistics of the five simulation runs are summarized in Table 19.

Table 19.   Simulated sensor signals and model outputs for pre-screening test case 3

	Run 1	Run 2	Run 3	Run 4	Run 5
Simulated signal returns					
Number signals from sensor deployed	4	10	4	3	6
False positive errors	1	7	1	0	3
False negative errors	0	0	0	0	0
Correct signals	3	3	3	3	3
Model outputs					
Estimate of attack location	NA	NA	NA	NA	Cell 44
Estimate of time of attack	NA	NA	NA	NA	$u = 13$
Location error (meters)	NA	NA	NA	NA	100
Time of release error (mins)	NA	NA	NA	NA	8
Time at which alarm threshold of 0.7 is crossed	NA	NA	NA	NA	$u = 15$
Highest posterior for the correct location and time, $Max_u \alpha_{48,u-5}^{u}$	0.446	0.431	0.446	0.494	0.446
Time at which the highest value of the correct posterior is observed, $ArgMax_u \alpha_{48,u-5}^{u}$	$u = 8$	$u = 8$	$u = 8$	$u = 20$	$u = 8$
Presence of incorrect posteriors > alarm threshold of 0.7	No	No	No	No	Yes
Presence of incorrect posteriors > noise floor of 0.2	Yes	Yes	Yes	Yes	Yes
Is $\alpha_{48,u-5}^{u} \geq \alpha_{l,t}^{u}$ $\forall$ l, t, u?	No	No	No	No	No

a. *Results and Discussions for Simulation Runs 1, 2 3, and 4*

For simulation runs 1, 2, 3, and 4, the model is able to estimate accurately the time and location of the attack, but fails to trigger an alarm as the likelihood observed is lower than the alarm threshold of 0.7. This is due to the presence of a false estimate of an attack at cell 47 that presumably occurred at time at $u = 4$.

For discussion purposes, we present the results for simulation run #4 where there are no false positive and false negative errors in the simulated return signals. Figure 25 compares the posterior probabilities of the correct event, $\alpha_{48,u-5}^{u}$ with the posterior probabilities of the false event, $\alpha_{47,u-4}^{u}$ and $\max_{l,t} \alpha_{l,t}^{u}$ for $u \geq 5$ for run #4 of the simulation for test case 3.
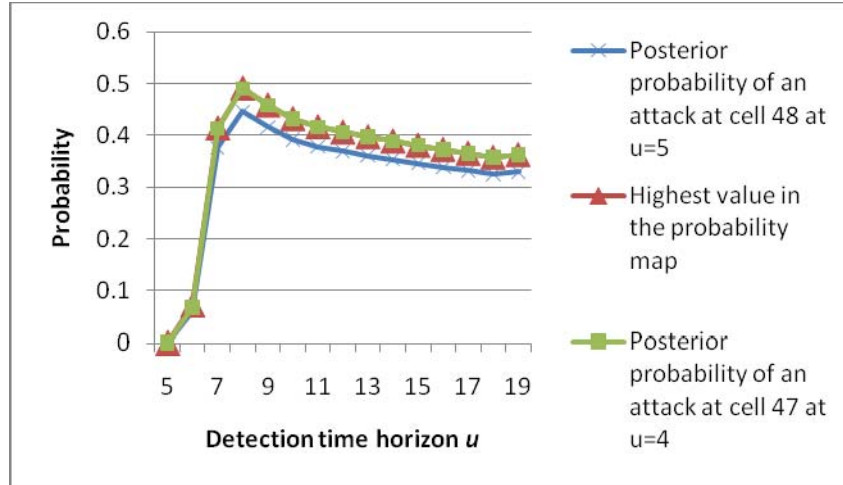
Figure 25. Comparison between the values of $\max_{l,t} \alpha_{l,t}^{u}$, $\alpha_{47,u-4}^{u}$ and $\alpha_{48,u-5}^{u}$ for $u = 5$ for run #4 of the simulation for test case 3

It can be seen the value of $\alpha_{47,u-4}^{u}$ is slightly higher than the value of $\alpha_{48,u-5}^{u}$ and is equal to the value of $\max_{l,t} \alpha_{l,t}^{u}$ over the detection time horizon. It is important to note that in run #4 there are no false positive and false negative errors in the simulated return signals. Hence the model is unable to differentiate between an attack at

cell 48 at $u = 5$ and an attack at cell 47 at $u = 4$ with just 3 signal returns from the single sensor at cell 50. This can be explained by the $P_{l,t}^{50}$ values for these attacks in Table 20.

Table 20. $P_{l,t}^{50}$ values for sensor 50 for attacks at location cell 47 and cell 48

$P_{l,t}^{50}$	Attack time scale, t time steps since the occurrence of the chemical attack						
Location	0	1	2	3	4	5	6
47	0.01	0.01	0.70	1.00	0.70	0.01	0.01
48	0.01	0.50	1.00	0.50	0.01	0.01	0.01

As seen from Table 20, when 3 consecutive alarms are received from sensor 50 at $u = 6$ till $u = 8$, the Bayesian updating model will increase $\alpha_{47,u-4}^{u}$ and $\alpha_{48,u-5}^{u}$. Hence given only signal returns from a single sensor, the model is unable to differentiate between the two attacks. The consolation is that in such an event, the probability map will show only 2 competing estimates with a spatial difference of 100m and a temporal difference of 1 minute. Figure 26 shows the contour plot of the probability map at $u = 8$, for simulation run 4.
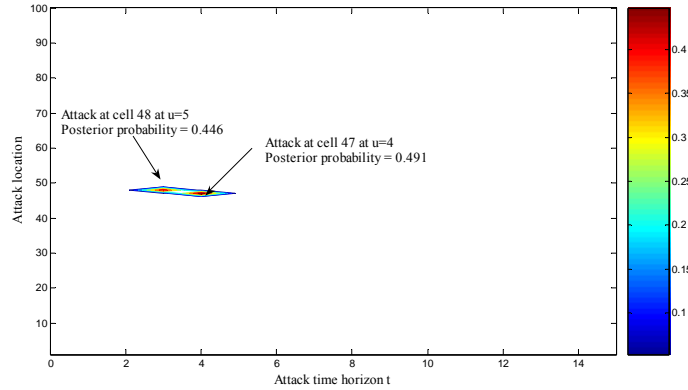
Figure 26.   Contour plot of the probability map at $u = 8$ for simulation run 4 of test case 3

It is important to note that the competition between the two attack events lowers their posterior probability as the model is conditioned on the event of at most a single attack. Hence the alarm threshold of 0.7 cannot be met. Competing events cannot

53

be resolved by the model when limited information is available to differentiate between them. To resolve competing events, updates of the events are needed from sensors located at different locations. To overcome this, one possible approach is to sum the posterior probabilities of attack events that have attack locations adjacent to each other with respect to the prevailing wind direction and whose times of attacks are one minute apart. This will allow the collective estimate to meet the alarm criterion, giving two estimates with a spatial difference of 100m and a temporal difference of 1 minute. However in this thesis, this approach is not implemented.

b. Results and Discussions for Simulation Run 5

For simulation run #5, a total of six correct signals are received from the 16 sensors in the field. Three false positives are encountered in this simulation run. The respective times of the signals (indicated by 1) and the corresponding sensors that produced them are shown in Table 21.

Table 21.   Simulated signal returns for run #5 of pre-screening test case 3

Detection time horizon(*u*)	Location of sensor															
	1	10	14	17	33	38	41	45	50	56	63	68	84	87	91	100
0	0	0	0	0	0	0	0	0	0	0	0	0	0	0	0	0
1	0	0	0	0	0	0	0	0	0	0	0	0	0	0	0	0
2	0	0	0	0	0	0	0	0	0	0	0	0	0	0	0	0
3	0	0	0	0	0	0	0	0	0	0	0	0	0	0	0	0
4	0	0	0	0	0	0	0	0	0	0	0	0	0	0	0	0
5	0	0	0	0	0	0	0	0	0	0	0	0	0	0	0	0
6	0	0	0	0	0	0	0	0	1	0	0	0	0	0	0	0
7	0	0	0	0	0	0	0	0	1	0	0	0	0	0	0	0
8	0	0	0	0	0	0	0	0	1	0	0	0	0	0	0	0
9	0	0	0	0	0	0	0	0	0	0	0	0	0	0	0	0
10	0	0	0	0	0	0	0	0	0	0	0	0	0	0	0	0
11	0	0	0	0	0	0	0	0	0	0	0	0	0	0	0	0
12	0	0	0	0	0	0	0	0	0	0	0	0	0	0	0	0
13	0	0	0	0	0	0	0	0	0	0	0	0	0	0	0	0

14	0	0	0	0	0	0	0	1	0	0	0	0	0	0	0	0
15	0	0	0	0	0	0	0	0	0	1	0	0	0	0	0	0
16	0	0	0	0	0	0	0	0	0	0	0	0	0	0	0	0
17	0	0	0	0	0	0	0	0	0	0	0	0	0	0	0	0
18	0	0	0	0	0	0	0	0	0	0	0	0	1	0	0	0
19	0	0	0	0	0	0	0	0	0	0	0	0	0	0	0	0
20	0	0	0	0	0	0	0	0	0	0	0	0	0	0	0	0

For simulation run #5, the alarm threshold is crossed for an attack at location cell 44 at $u = 13$, that is $\alpha_{44,2}^{15} \geq 0.7$. However the likelihood of this attack drops drastically in the next update to a value of 0.27. Figure 27 plots the values of $\alpha_{44,u-13}^{u}$, $\alpha_{47,u-4}^{u}$, $\alpha_{48,u-5}^{u}$, and $\max_{l,t} \alpha_{l,t}^{u}$ for $u \geq 5$.
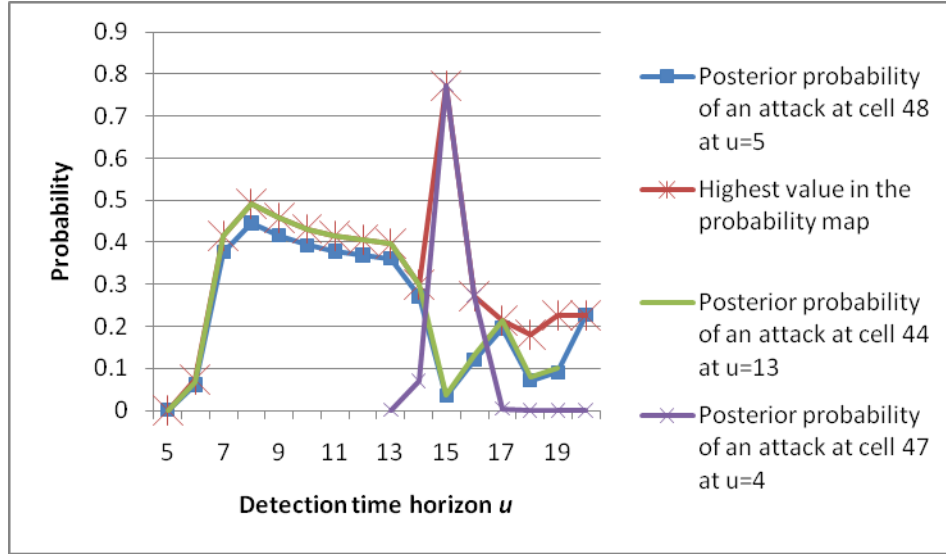
Figure 27. Values of $\alpha_{44,u-13}^{u}$, $\alpha_{47,u-4}^{u}$, $\alpha_{48,u-5}^{u}$, and $\max_{l,t} \alpha_{l,t}^{u}$ for $u \geq 5$.

From Figure 27, it can be seen that similar to simulation runs 1, 2, 3, and 4 the model is unable to resolve the competing events of an attack at cell 47 at $u = 4$ and an attack at cell 48 at $u = 5$. However the posterior probabilities of these two events start to drop due to a third competing event, an attack at cell 44 at $u = 13$. The third competing

event is due to a false signal from the sensor at cell 45 at $u = 14$ followed by a false signal from the sensor at cell 56 at $u = 15$. This is evident from the $P_{44,t}^{s}$ values of sensor 45 and sensor 56 in Table 22.

Table 22. $P_{44,t}^{s}$ values for sensor 45 and 56 for attacks at location cell 44

$P_{l,t}^{45}$	Attack time scale, t time steps since the occurrence of the chemical attack						
Location	0	1	2	3	4	5	6
44	0.01	1	0.01	0.01	0.01	0.01	0.01
$P_{l,t}^{56}$	Attack time scale, t time steps since the occurrence of the chemical attack						
Location	0	1	2	3	4	5	6
44	0.01	0.01	0.5	0.01	0.01	0.01	0.01

However in the absence of further signal returns that support the occurrence of the third event, its posterior probability drops drastically in the next update at $u = 16$ to a value of 0.27. Hence the third event produces a peak that crosses the alarm threshold only at $u = 15$. The peak is not persistent and fades away as shown in Figure 28.
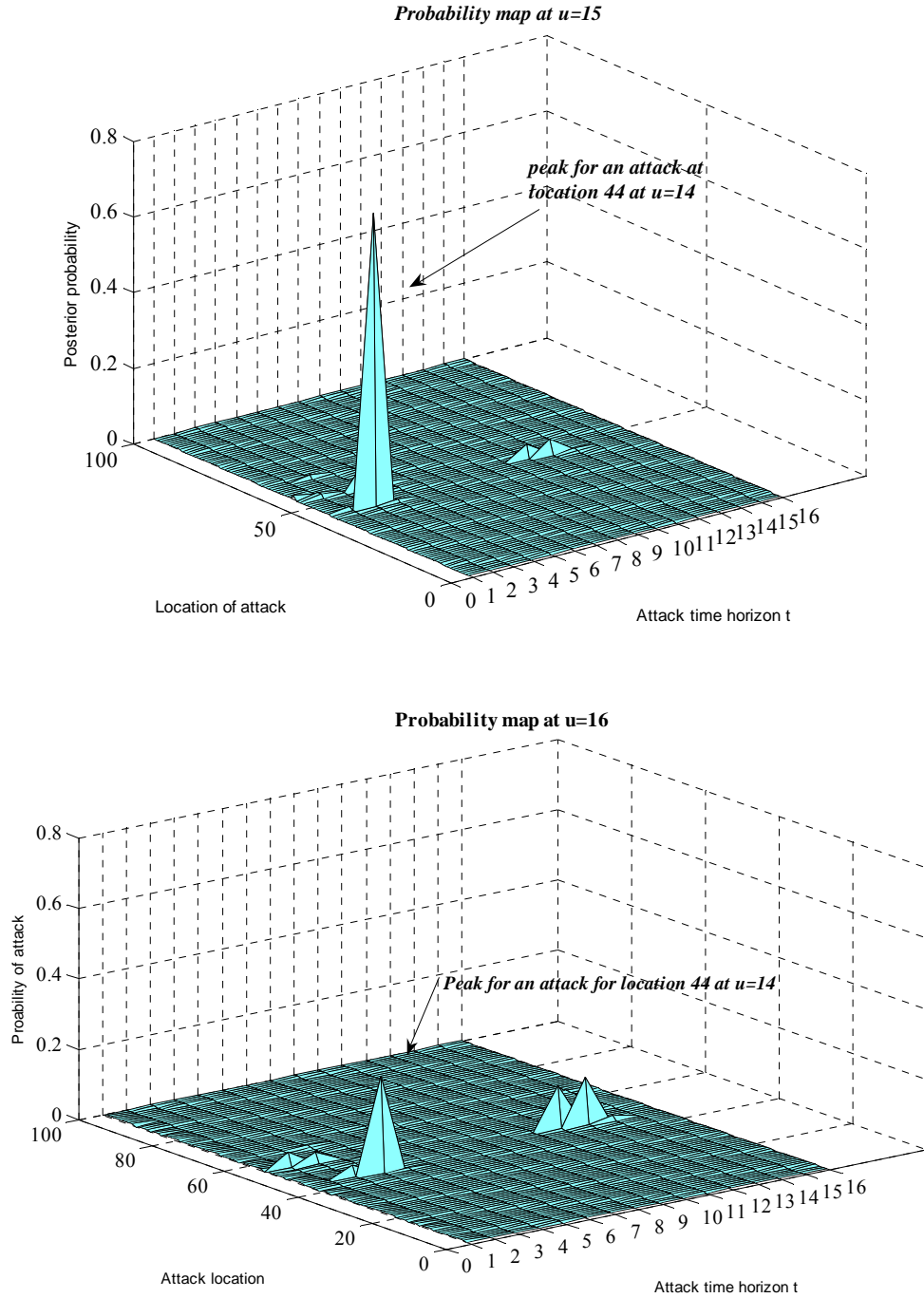
Figure 28. Probability maps for simulation run #5 at *u* = 15 and *u* = 16

In simulation run #5, the number of false positive and false negative signals is lower than that of run #2 which did not produce a false estimate. Yet a false estimate is made with a strong possibility of 0.77. Hence the accuracy the model is

affected not only by the number of false positives but also significantly by the time and place of their occurrence. If the false positives collectively form a pattern that mimics the possible occurrence of a chemical attack, the model will provide an estimate of the false attack. We suspect such an occurrence is rare as false positives are random in nature. Still this can be overcome with a more stringent requirement such as the need for consecutive posterior probabilities that cross the alarm threshold before an alarm is set off.

6. Simulation Results for Test Case 4, Attack at Location 51

For an attack at cell 51, the ENCS is 18, from five different sensors. The statistics of the five simulation runs are summarized in Table 23.

Table 23.   Simulated sensor signals and model outputs for pre-screening test case 4

	Run 1	Run 2	Run 3	Run 4	Run 5
Simulated signal returns					
Number signals from sensor deployed	21	21	20	22	24
False positive errors	1	1	2	3	5
False negative errors	1	1	3	2	2
Correct signals	20	20	18	19	19
Model outputs					
Estimate of attack location	Cell 51	Cell 51	Cell 51	Cell 51	Cell 51
Estimate of time of attack	$u = 5$	$u = 5$	$u = 5$	$u = 5$	$u = 5$
Location error (meters)	0	0	0	0	0
Time of release error (mins)	0	0	0	0	0
Time at which alarm threshold of 0.7 is crossed	$u = 9$	$u = 11$	$u = 10$	$u = 10$	$u = 10$
Highest posterior for the correct location and time, $Max_u \alpha_{51,u-5}^u$	1	1	0.998	0.999	1
Time at which the highest value of the correct posterior is observed, $ArgMax_u \alpha_{51,u-5}^u$	$u = 12$	$u = 12$	$u = 13$	$u = 14$	$u = 13$
Presence of incorrect posteriors > alarm threshold of 0.7	No	No	Yes	No	No
Presence of incorrect posteriors > noise floor of 0.2	Yes	Yes	Yes	Yes	Yes
Is $\alpha_{51,u-5}^u \geq \alpha_{l,t}^u \ \forall \ l, t, u$?	No	No	No	No	No

58

The model is able to estimate the time and location of the attack accurately for all five runs despite the presence of false positive and false negative errors. For discussion purposes we present the results for simulation run #1 and run #3.

a. *Results and Discussions for Simulation Run 1*

For simulation run #1, a total of 21 signals are received. One false positive error and one false negative error are encountered in this simulation run. The respective times of the signals and the corresponding sensors that produced them are shown in Table 24.

Table 24.　　Simulated signal returns for run 1 of pre-screening test case 4

Detection time horizon(u)	Location of sensor															
	1	10	14	17	33	38	41	45	50	56	63	68	84	87	91	100
0	0	0	0	0	0	0	0	0	0	0	0	0	0	0	0	0
1	0	0	0	0	0	0	0	0	0	0	0	0	0	0	0	0
2	0	0	0	0	0	0	0	0	0	0	0	0	0	0	0	0
3	0	0	0	0	0	0	0	0	0	0	0	0	0	0	0	0
4	0	0	0	0	0	0	0	0	0	0	0	0	0	0	0	0
5	0	0	0	0	0	0	0	0	0	0	0	0	0	0	0	0
6	0	0	0	0	0	0	0	0	0	0	0	0	0	0	0	0
7	0	0	0	0	0	0	0	0	0	0	0	0	0	0	0	0
8	0	0	0	0	0	0	0	1	0	1	0	0	0	0	0	0
9	0	0	0	0	0	0	0	1	0	1	0	0	0	0	0	0
10	0	0	0	0	0	0	0	1	0	1	0	1	0	0	0	0
11	0	0	0	0	0	1	0	0	0	1	0	1	0	0	0	0
12	0	0	0	0	0	1	0	0	1	1	0	1	0	0	0	0
13	0	0	0	0	0	0	0	0	1	0	0	1	0	0	0	0
14	0	0	0	0	0	0	0	0	1	0	0	1	0	0	0	0
15	0	0	0	0	0	0	0	0	1	0	0	0	0	0	0	1
16	0	0	0	0	0	0	0	0	1	0	0	0	0	0	0	0
17	0	0	0	0	0	0	0	0	0	0	0	0	0	0	0	0
18	0	0	0	0	0	0	0	0	0	0	0	0	0	0	0	0
19	0	0	0	0	0	0	0	0	0	0	0	0	0	0	0	0
20	0	0	0	0	0	0	0	0	0	0	0	0	0	0	0	0

For run #1, the probability map at $u = 8$, shows two probable events of an attack: cell 53 at $u = 6$ with $\alpha_{53,2}^8 = 0.39$, and cell 52 at $u = 5$ with $\alpha_{52,3}^8 = 0.43$. Figure 29 depicts the probability map at $u = 8$.
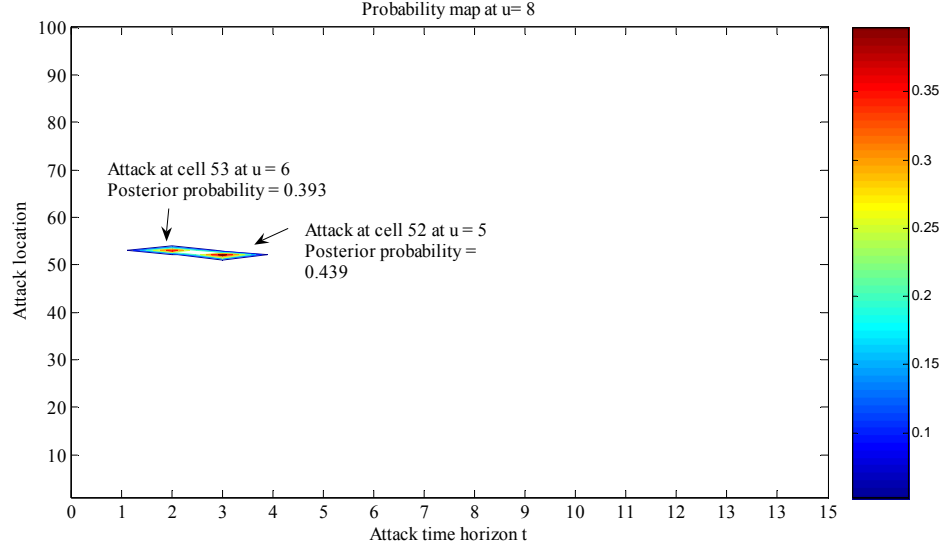
Figure 29.   Probability map at $u = 8$, for simulation run #1 of test case 4

However at $u = 9$, the posterior probabilities of both events, an attack at cell 53 at $u = 6$ and cell 52 at $u = 5$, drop drastically. The model returns only a single estimate, an attack at cell 51 at $u = 5$ with a posterior probability of 0.72 which crosses the alarm threshold. For the rest of the simulation, the posterior probability of this correct estimate continues to increase and remain the dominant peak within the probability maps. Figure 30 depicts the probability map at $u = 9$.
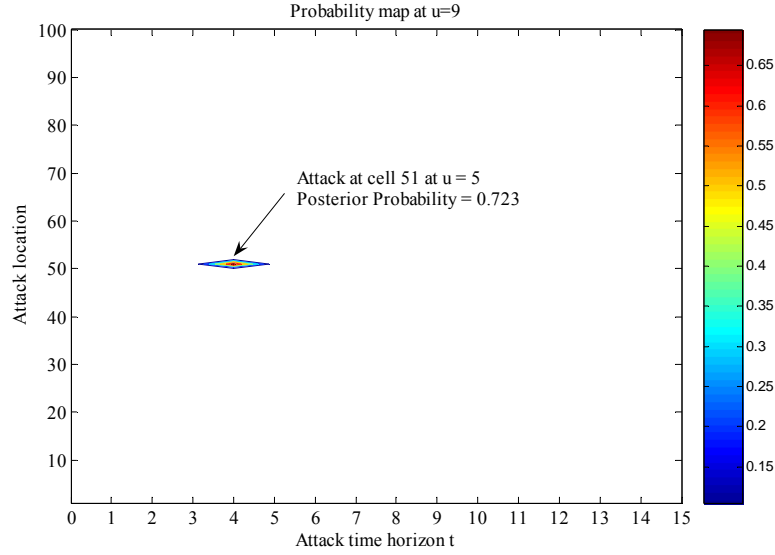
Figure 30.   Probability map at $u = 9$ for simulation run #1 of test case 4

Figure 31 plots the values of $\alpha^u_{53,u-6}$, $\alpha^u_{52,u-5}$, $\alpha^u_{51,u-5}$ and $\max_{l,t} \alpha^u_{l,t}$ for u $\geq$ 5. It can be seen that the posterior probabilities of an attack at cell 53 at $u = 6$ and cell 52 $u = 5$ are dominant in the probability map only at the $u = 8$ update. Thereafter their probabilities drop below the noise floor of the model. The correct estimate of an attack at cell 51 at $u = 5$ remains the dominant estimate during the entire simulation run.
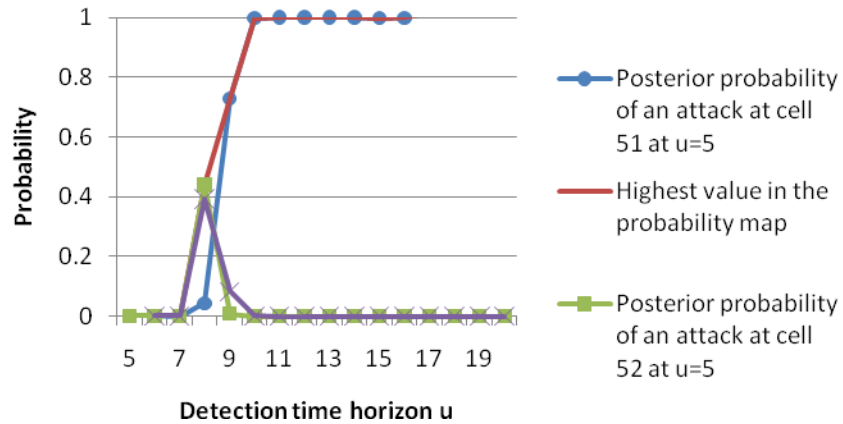
Figure 31.   Plot of the values of $\alpha^u_{53,u-6}$, $\alpha^u_{52,u-5}$, $\alpha^u_{51,u-5}$ and $\max_{l,t} \alpha^u_{l,t}$ for $u \geq 5$

To understand the transient spikes in the values of $\alpha^u_{53,u-6}$ and $\alpha^u_{52,u-5}$, we observe from Table 25 that at $u = 8$, $P^{45}_{51,3}$, $P^{45}_{52,3}$, and $P^{45}_{53,2}$ have large values and similarly $P^{56}_{51,3}$, $P^{56}_{52,3}$ and $P^{56}_{53,2}$. Hence the signals given by the sensors located at 45 and 56 at $u = 8$ generate high posterior probabilities for an attack in these three locations.

Table 25.   Expected pattern of sensor responses for an attack at (i) cell 51 at $u = 5$ (ii) cell 52 at $u = 5$ and (iii) cell 53 at $u = 6$

Detection time horizon u	Attack at cell 51 at $u = 5$				
	Sensor				
	38	45	50	56	68
5	0.01	0.01	0.01	0.01	0.01
6	0.01	0.01	0.01	0.01	0.01
7	0.01	0.01	0.01	0.01	0.01
8	0.01	0.6	0.01	0.5	0.01
9	0.01	0.7	0.01	0.8	0.01
10	0.01	0.6	0.01	0.9	0.5
11	0.5	0.01	0.01	0.8	0.7
12	0.6	0.01	0.6	0.5	0.8
13	0.5	0.01	0.7	0.01	0.7
14	0.01	0.01	0.7	0.01	0.5
15	0.01	0.01	0.7	0.01	0.01
16	0.01	0.01	0.6	0.01	0.01
	Attack at cell 52 at $u = 5$				
5	0.01	0.01	0.01	0.01	0.01
6	0.01	0.01	0.01	0.01	0.01
7	0.01	0.01	0.01	0.01	0.01
8	0.01	0.7	0.01	0.7	0.01
9	0.01	0.01	0.01	0.9	0.5
10	0.5	0.01	0.01	0.7	0.7
11	0.5	0.01	0.5	0.01	0.8
12	0.5	0.01	0.7	0.01	0.7
13	0.01	0.01	0.7	0.01	0.5
14	0.01	0.01	0.7	0.01	0.01
15	0.01	0.01	0.5	0.01	0.01
16	0.01	0.01	0.01	0.01	0.01

Detection time horizon u	Attack at cell 53 at $u = 6$				
5	0.01	0.01	0.01	0.01	0.01
6	0.01	0.01	0.01	0.01	0.01
7	0.01	0.01	0.01	0.01	0.01
8	0.01	0.5	0.01	0.7	0.01
9	0.01	0.01	0.01	1	0.01
10	0.01	0.01	0.01	0.7	0.6
11	0.5	0.01	0.5	0.01	0.8
12	0.01	0.01	0.7	0.01	0.6
13	0.01	0.01	0.8	0.01	0.01
14	0.01	0.01	0.7	0.01	0.01
15	0.01	0.01	0.5	0.01	0.01
16	0.01	0.01	0.01	0.01	0.01

At $u = 9$, once again simultaneous signals from the sensors in cell 45 and 56 are received, which increase the posterior probability of an attack at cell 51 at $u = 5$, but reduce the posterior probabilities of an attack at cells 53 and 52 since $P_{52,4}^{45} = P_{53,3}^{45} = 0.01$. In addition no signal is received from the sensor at cell 68 for which $P_{52,4}^{68} = 0.5$. The posterior probability of the correct estimate, $\alpha_{51,u-5}^{u}$ continues to increase as the simulated signals match the expected response pattern of this attack with respect to the timing of the signals received as well as the sensors responsible for the signals.

b.   Results and Discussions for Simulation Run 3

For simulation run 3, a total of 20 signals are received. Two false positive errors and two false negative errors are encountered in this simulation run. The respective times of the signals and the corresponding sensors that produced them are shown in Table 26.

Table 26.   Simulated signal returns for run #3 of pre-screening test case 4

Detection time horizon(u)	Location of sensor															
	1	10	14	17	33	38	41	45	50	56	63	68	84	87	91	100
0	0	0	0	0	0	0	0	0	0	0	0	0	0	0	0	0
1	0	0	0	0	0	0	0	0	0	0	0	0	0	0	0	0
2	0	0	0	0	0	0	0	0	0	0	0	0	0	0	0	0
3	0	0	0	0	0	0	0	0	0	0	0	0	0	0	0	0
4	0	0	0	0	0	0	0	0	0	0	0	0	0	0	0	0
5	0	0	0	0	0	0	0	0	0	0	0	0	0	0	0	0
6	0	0	0	0	0	0	0	0	0	0	0	0	0	0	0	0
7	0	0	0	0	0	0	0	0	0	0	0	0	0	0	0	0
8	0	0	0	0	0	0	0	1	1	0	0	0	0	0	0	0
9	0	0	0	0	0	0	0	1	0	1	0	0	0	0	0	0
10	0	0	0	0	0	0	0	1	0	1	0	1	0	0	0	0
11	0	0	0	0	0	1	0	0	0	0	0	1	0	0	0	0
12	0	0	0	0	0	1	0	0	1	1	0	1	0	0	0	0
13	0	0	0	1	0	1	0	0	1	0	0	1	0	0	0	0
14	0	0	0	0	0	0	0	0	0	0	0	1	0	0	0	0
15	0	0	0	0	0	0	0	0	1	0	0	0	0	0	0	0
16	0	0	0	0	0	0	0	0	1	0	0	0	0	0	0	0
17	0	0	0	0	0	0	0	0	0	0	0	0	0	0	0	0
18	0	0	0	0	0	0	0	0	0	0	0	0	0	0	0	0
19	0	0	0	0	0	0	0	0	0	0	0	0	0	0	0	0
20	0	0	0	0	0	0	0	0	0	0	0	0	0	0	0	0

For run #3, the probability map at $u = 9$ reveals an attack at location 43 at $u = 6$ with the value of $\alpha_{43,3}^{9} = 0.86$ which crosses the alarm threshold. Figure 32 depicts the probability map at $u = 9$.
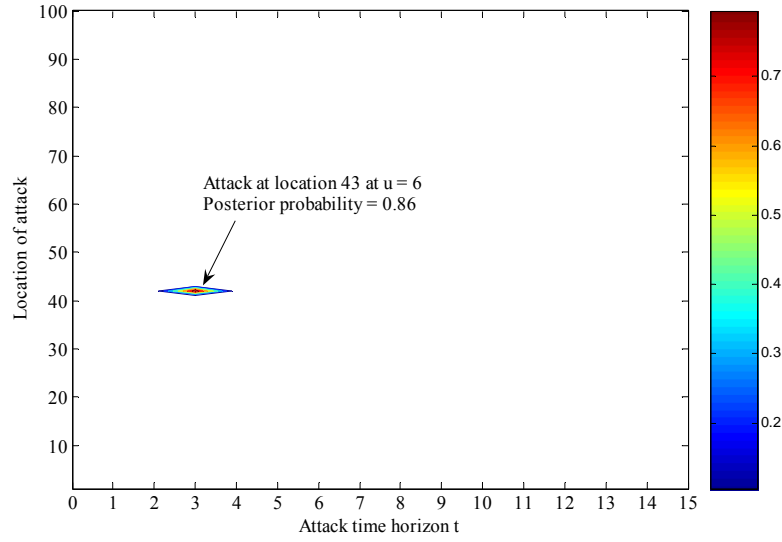
Figure 32.   Probability map at $u = 9$ for simulation run #3 of test case 4

However at $u = 10$, the value of $\alpha_{43,4}^{10}$ drops drastically to 0.09. The model returns only a single estimate, an attack at cell 51 at $u = 5$ with $\alpha_{51,5}^{10} = 0.88$ which crosses the alarm threshold. For the rest of the simulation, the posterior probability of this correct estimate continues to increase and remain the dominant peak within the probability maps. Figure 33 depicts the probability map at $u = 10$.
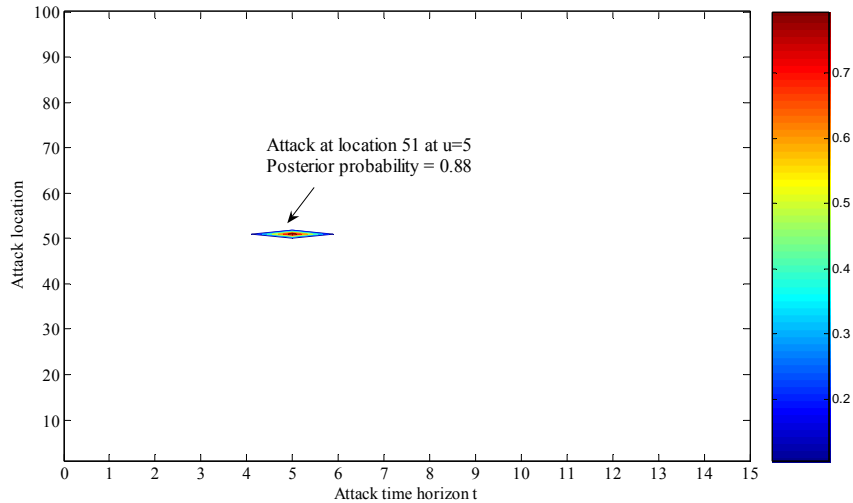
Figure 33.   Probability map at $u = 10$, for simulation run #3 of test case 4

It can be seen that the posterior probability of an attack at cell 43 at $u = 6$ crosses the threshold only for the update at $u = 10$ and fades away thereafter. The posterior probability of an attack at cell 51 at $u = 5$ remains the dominant estimate for the rest of the detection time horizon.
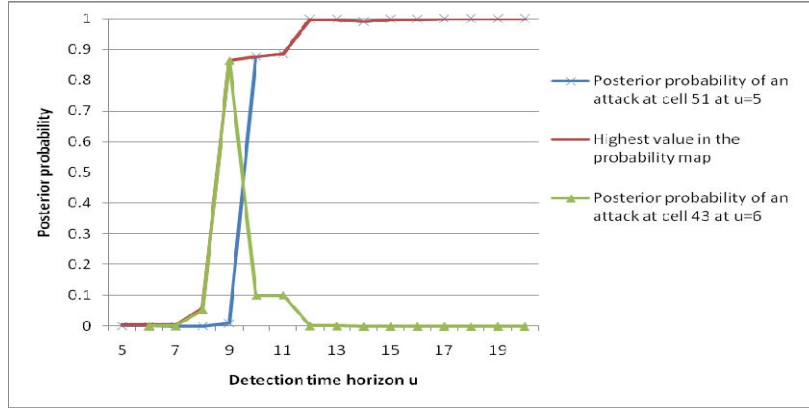
Figure 34.   Plot of the values of $\alpha_{43,u-6}^{u}$, $\alpha_{51,u-5}^{u}$ and $\max_{l,t} \alpha_{l,t}^{u}$ for $u \geq 5$

Figure 34 plots the values of $\alpha_{43,u-6}^{u}$, $\alpha_{51,u-5}^{u}$ and $\max_{l,t} \alpha_{l,t}^{u}$ for $u \geq 5$. It can be seen from Figure 35 that the value of $\alpha_{43,3}^{9}$ rises above the alarm threshold to 0.86 at $u = 9$ due to a false positive error from sensor 50 and a false negative error from sensor 56. At $u = 10$, simultaneous alarms are received from the sensors placed at cell 45, 56 and 68. This increases the value of $\alpha_{51,u-5}^{u}$ but decreases the value of $\alpha_{43,u-6}^{u}$ since at $u = 10$, $P_{43,4}^{45} = P_{43,4}^{56} = P_{43,4}^{68} = 0.01$. The posterior probability of the correct estimate, $\alpha_{51,u-5}^{u}$ continues to increase as the simulated signals match the expected response pattern of this attack with respect to timing of the signals received as well as the sensors responsible for the signals.

Hence false negatives in conjunction with false positives can result in a wrong estimate that is very far in physical proximity from the true attack location. To overcome this, an additional requirement to trigger an alarm will be at least three consecutive observations that are above the alarm threshold. This added more stringent

66

requirement for persistency should weed out transient spikes due to false negatives and false positive signals adding greater confidence and reliability in triggering an alarm.

7. Simulation Results for Test Case 5, Attack at Location 85

For an attack at cell 85, the ENCS is 2 from two different sensors. The statistics of the five simulation runs are summarized in Table 27.

Table 27.   Simulated sensor signals and model outputs for pre-screening test case 4

	Run 1	Run 2	Run 3	Run 4	Run 5
Simulated signal returns					
Number signals from sensor deployed	6	13	6	8	12
False positive errors	0	7	1	3	6
False negative errors	0	0	1	1	0
Correct signals	6	6	4	5	6
Model outputs					
Estimate of attack location	Cell 85	Cell 85	Cell 85	Cell 85	Cell 85
Estimate of time of attack	$u = 5$	$u = 5$	$u = 5$	$u = 5$	$u = 5$
Location error (meters)	0	0	0	0	0
Time of release error (mins)	0	0	0	0	0
Time at which alarm threshold of 0.7 is crossed	$u = 8$	$u = 8$	$u = 8$	$u = 8$	$u = 8$
Highest posterior for the correct location and time, $Max_u \alpha_{85,u-5}^u$	1	1	1	1	1
Time at which the highest value of the correct posterior is observed, $ArgMax_u \alpha_{85,u-5}^u$	$u = 12$	$u = 13$	$u = 13$	$u = 9$	$u = 12$
Presence of incorrect posteriors > alarm threshold of 0.7	No	No	No	No	No
Presence of incorrect posteriors > noise floor of 0.2	Yes	Yes	Yes	Yes	Yes
Is $\alpha_{85,u-5}^u \geq \alpha_{l,t}^u \ \forall \ l, t, u$?	No	No	No	No	No

For all five simulation runs, the model is able to estimate accurately the attack location and time to be cell 85 at $u = 5$. We present only the results for simulation run #1. Figure 35 plots the values of $\alpha_{85,u-5}^u$ and $\max_{l,t} \alpha_{l,t}^u$ for $u \geq 5$.
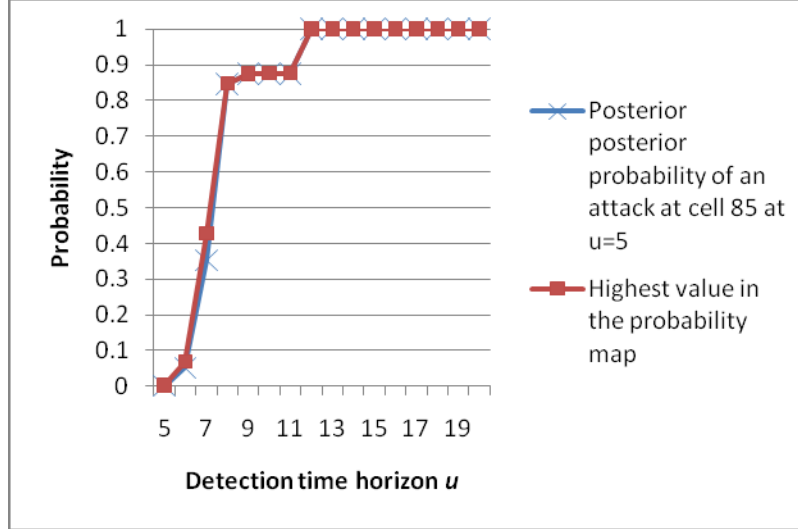
Figure 35.   Plot of the values of $\alpha_{85,u-5}^u$ and $\max_{l,t} \alpha_{l,t}^u$ for $u \geq 5$

From Figure 35, it can be seen that the posterior probability of an attack at cell 85 at $u = 5$ crosses the alarm threshold at the update at $u = 8$ and remains the sole dominant estimate for the entire simulation run.

8.   Insights Gained from the Preliminary Simulation Trials

The preliminary trials helped to determine the alarm criterion for responding to an attack. The alarm criterion is at least three consecutive instances of posterior probabilities that are above the alarm threshold of 0.7. The alarm threshold is set at 0.7 to avoid responding to competing cues representing possible attack events early in the update process. The requirement for three consecutive observations eliminates false estimates caused by sudden spikes in the probability maps due to false positive errors and/or false negative errors that are encountered in the operational environment.

The preliminary trials also revealed that the model requires signals from sensors located in at least two different locations to resolve between competing cues representing

possible attack events that are spatially and temporally close. This adds another constraint on top of other operational requirements in the deployment of sensors such as early warning and detection coverage of the area of operations.

Factors that affect the model's capability to accurately estimate the location and time of an attack are (i) the Expected Number of Correct Signals (ENCS) (ii) the number of false positive errors and (iii) the number of false negative errors.

Implementing the alarm criterion stated, Table 28 summarizes the model performance statistic for the preliminary trials. If we exclude the runs for an attack at location 48 where the model is unable to resolve between 2 competing events, the percentage success will be 100% instead.

Table 28.   Overall statistics of the preliminary trials

Total number of runs	20
Average number of false positives	2.55
Average number of false negatives	0.7
Average number of correct signals	8.65
Number of runs with correct estimates	15
Percentage success	75
Average time taken to sound an alarm (mins)	6

C.   TEST DESIGN MATRIX

Screening experiments are used to estimate the magnitude and direction of factor effects; that is how much does the response variable change when each factor is changed (Montgomery, 2009).

Factors that affect the model's capability to accurately estimate the location and time of an attack given a (i) sensor deployment plan, (ii) set of meteorological conditions and (iii) chemical attack quantity are

(i)   Expected Number of Correct Signals (ENCS)

(ii)   Number of false positive errors

(iii)   Number of false negative errors

The relationship between the factors identified and the model input parameters are summarized in Table 29.

Table 29.   Relationship between the factors and model input parameters

Factors	Model Input parameters
1) ENCS	Location of attack
2) Number of false positive errors	$1-q$, false positive probability
3) Number of false negative errors	Sensitivity of the sensor being modeled

To evaluate the model we categorize the three factors. With respect to the ENCS, the attack locations are divided into 3 categories, each corresponding to low, medium and high values of ENCS, as shown in Table 30. In the evaluation trials, an attack location is randomly selected from each of the three categories. We require however that each attack location is covered by at least two sensors. This is to ensure that the model is able to resolve between competing cues representing possible attack events that are close to each other spatially and temporally.

Table 30.   Categories of ENCS

	ENCS categories		
	Low	Medium	High
ENCS	less than 6	6 to 10	More than 10
Number of locations within category	38	18	13

We consider two categories for the error rates: high and low. A low false positive rate is 10 errors in an hour from all 16 sensors, which implies $1-q = 0.0104$. A high false positive rate is 30 errors in an hour from all 16 sensors, which implies $1-q = 0.03125$. For the false negative errors we consider the following two sensor models:

Model I, which represents the current detection capabilities, is

$$P^{I}(c) = \begin{cases} 1 & \text{if } c \geq 30 \; mg/m^3 \\ 0.9 & \text{if } c \geq 7.5 \; mg/m^3 \text{ and } < 30 \; mg/m^3 \\ 0.8 & \text{if } c \geq 2 \; mg/m^3 \text{ and } < 7.5 \; mg/m^3 \\ 0.7 & \text{if } c \geq 0.5 \; mg/m^3 \text{ and } < 2 \; mg/m^3 \\ 0.6 & \text{if } c \geq 0.125 \; mg/m^3 \text{ and } < 0.5 \; mg/m^3 \\ 0.5 & \text{if } c \geq 0.01 \; mg/m^3 = \text{Detection threshold} \\ 1-q & \text{otherwise} \end{cases}$$

Model II, which represents an improved sensor is:

$$P^{II}(c) = \begin{cases} 1.0 & \text{if } c \geq 2 \; mg/m^3 \\ 0.9 & \text{if } c \geq 0.5 \; mg/m^3 \text{ and } < 2 \; mg/m^3 \\ 0.8 & \text{if } c \geq 0.125 \; mg/m^3 \text{ and } < 0.5 \; mg/m^3 \\ 0.7 & \text{if } c \geq 0.01 \; mg/m^3 \text{ and } < 0.125 \; mg/m^3 \\ 1-q & \text{otherwise} \end{cases}$$

The chemical attack involves 50kg of Sarin, which is a nerve agent. The alarm criterion is at least three consecutive time periods in which the posterior probability of a certain entry in the probability map is above the alarm threshold 0.7. We recognize that other alarm criteria such as two consecutive observations that are above the alarm threshold of 0.8 may also be applicable. In evaluating the model, the emphasis is not on determining an optimal alarm criterion, as this is dependent on the risk attitude and objectives of the decision maker. Recall that the MOEs used in evaluating the model are:

a)   Accurately identifying the attack location

b)   Accurately identifying the time of attack

We design a screening experiment with input factors (ENCS, false positive errors, and false negative errors). The experimental design matrix, which is a full factorial in the three factors defined, consists of 300 simulation trials. There are 12 test cases, with 25 replications per test case. This matrix is shown in Table 31. A test case (or single experiment) is defined by the levels of ENCS (three categories) and the levels of false positive and false negative errors (two categories each). A full factorial will allow us to screen for all main effects and two factor interactions in the variables of interest.

71

Table 31.   Experimental design matrix

	High ENCS		Medium ENCS		Low ENCS	
	High false positives	Low false positives	High false positives	Low false positives	High false positives	Low false positives
High false negatives	25	25	25	25	25	25
Low false negatives	25	25	25	25	25	25

D.   EVALUATION AND DISCUSSION

In this section we present the results of the simulation runs for the 12 test cases, develop a linear regression model for identifying the effects of the factors on the MOEs and discuss the results obtained.

1.   Evaluation of Test Results

It is observed that in most instances the alarm criterion successfully ignores false estimates caused by sudden spikes in the probability maps due to false positive errors and false negative signals. False estimates that satisfy the alarm criterion deviate substantially from the actual location and time of the attack. As the accuracy of both the time and location of the attack is critical, a success is only declared if both MOEs are satisfied.

We define success percentage as

$$= \frac{Number\ of\ trials\ that\ estimated\ the\ time\ and\ location\ of\ attack\ accurately}{Total\ number\ of\ trials\ within\ the\ test\ category} \times 100$$

and use this measure for evaluating the results of the simulations. Note that *success percentage* is only defined on the range 0 to 100. As a result of this, it would be ideal to fit the response with a logistic model. However, in this section, we are concerned with identifying the important factors and determining the magnitude and direction of their effect on the response, *success percentage*, rather than create a fitted model to use a predictor.

Myers et al., (2002) point out that a factorial design can be used to effectively identify significant factors through a linear fit, even if the response is logistic. The linear

model should not however be used for making adequate predictions. After the significant factors are identified, follow on experiments could be preformed and used for fitting a logistic model.

The *success percentage* values for the 12 test cases are presented in Table 32.

Table 32.   Success percentage for the 12 test cases

	High ENCS		Medium ENCS		Low ENCS	
	High false positives	Low false positives	High false positives	Low false positives	High false positives	Low false positives
High false negatives	68	88	52	72	24	44
Low false negatives	92	96	84	88	52	80

From Table 32, it is observed that the *success percentage* increases with high levels of ENCS, decreases with high levels of false positive errors and high levels of false negative errors. In the presence of low false positive errors and low false negative errors, the success percentage is $\geq 80\%$. Next, we develop a linear regression model to assess the effect of each one of the three factors on the success percentage.

2.   Linear Regression Model

In a screening experiment, a linear regression model is often used to identify the significant factors from an experiment. We use a linear regression model to investigate the effect of the factors on the success percentage. The full model is:

$$Y = \beta_0 + \beta_1 x_1 + \beta_2 x_2 + \beta_3 x_3 + \beta_{12} x_1 x_2 + \beta_{13} x_1 x_3 + \beta_{23} x_2 x_3 + \varepsilon,$$

where

Y :   represents the *success percentage;*

x_1 :   represents false positive rates, $-1 \leq x_1 \leq 1$ in coded units, with $x_1 = 1$ indicating high false positives rates and $x_1 = -1$ low false positives rates;

x_2 :   represents false negative rates, $-1 \leq x_2 \leq 1$ in coded units, with $x_2 = 1$ indicating high false positives rates and $x_2 = -1$ low false positives rates;

73

x_3 : represents ENCS, $-1 \le x_3 \le 1$ in coded units, with $x_3 = 1$ indicating high

ENCS, $x_3 = 0$ medium ENCS and $x_3 = -1$ low ENCS; and

ε : represents noise, taken to be independent identically distributed Normal random variates.

The results of the linear regression, fitted using Minitab, indicate that only the main effects (ENCS, false positive errors, false negative errors) are significant and no two factor interactions are statistically significant. The estimated linear model in coded units takes the form

$$\hat{Y} = 70 - 8x_1 - 12x_2 + 18x_3 \qquad (8)$$

The corresponding statistics of the linear model are shown in Table 33 and the normal probability plot of the residuals is shown in Figure 36.

Table 33.   Statistics of the linear model

Estimator	value	Standard error	t-statistic	p-value
β_0	70.000	2.198	31.84	0.000
β_1	-8.000	2.198	-3.64	0.007
β_2	-12.000	2.198	-5.46	0.001
β_3	18.000	2.693	6.69	0.000
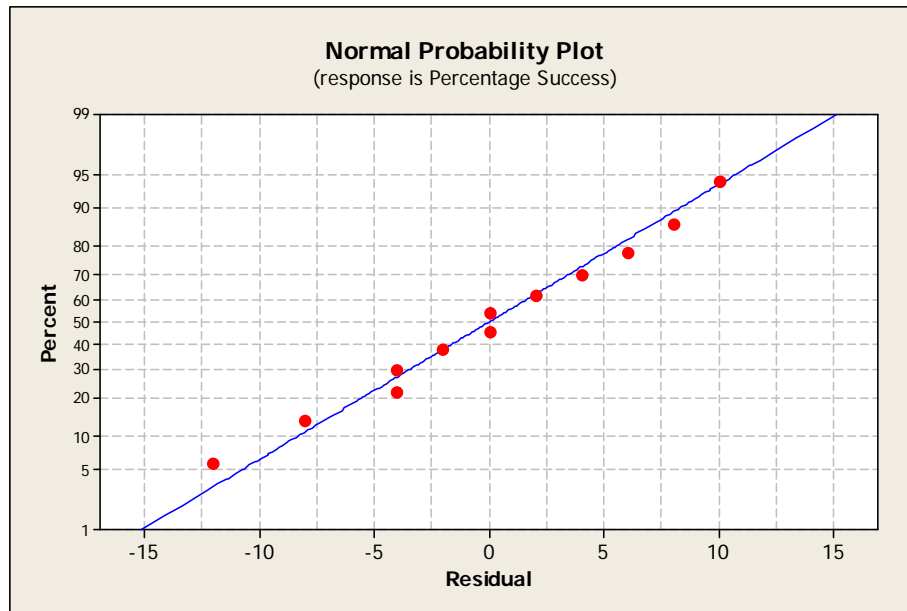
Figure 36.   Normal probability plot of percentage *success* against residuals

As seen from Table 33, the p-value of each the regressors is less than 0.05. The R^2 value of the linear model is 91.6% and the R^2 adjusted is 88.5%. The linear model provides an adequate fit to the data for its intended purpose of identifying significant factors and demonstrating the magnitude and direction those effects.

Other adequacy checks such as the plot of residuals against the fitted value and residual vs. run order indicate a possible slight violation of the constant variance assumption. As a result a transformation was applied to the response in order to stabilize the variance. This transformation resulted in no changes in conclusions about the main factor effects and their magnitude or direction.

3.   Discussion

Clearly, the best test-case situation is when the value of ENCS is high and the rates of false positive and false negative errors are low. The worst-test case situation is when the value of ENCS is low and the rates of false positive and false negative errors are high. For the best-test case situation, *success percentage* is 96%. For the worst-test case situation, *success percentage* is only 24%.

From the linear regression model, it is found that with all other factors held at their nominal levels the *success percentage* (i) increases by 18% when the ENCS is increased from low levels of ENCS to high levels of ENCS, (ii) decreases by 8% when false positive rate is tripled from 0.0104 to 0.03125 and (iii) decreases by 12% when the false negative rate is doubled from 0.0045 to 0.009. From the regression equation in (8), we observe that the dominant factor is the ENCS with the highest coefficient value of 18. As a result, in sensor placement, considerations should be made to increase the ENCS for sensors in the area of operations. We also observe that the false negative errors have a higher impact on the *success percentage* than the false positive errors.

Note that placing all of the factors at their high levels results in a greater than 100 percent success rate based on the fitted modeling in equation (8). This result is clearly impossible. While the fitted linear model was able to provide insight as to the main effects and their relative importance, follow on experiments and the use of a fitted logistic model would be needed to make more precise predictions.

E.   INSIGHTS ON SENSOR COVERAGE

The $P_{l,t}^{s}$ values derived from the output of the physical and sensor model give the probability that a sensor located at location *s* will detect a chemical attack at location *l, t* time periods ago. These values also give the coverage of a given sensor deployment plan..

Figure 37 shows the coverage of the sensor deployment plan used in the large scale setting for a 50kg nerve agent attack with a wind speed of 1.67m/s blowing to the east. The lightly shaded area cells contain sensors while the darkly shaded area cells indicate attack locations not covered by the set of deployed sensors.
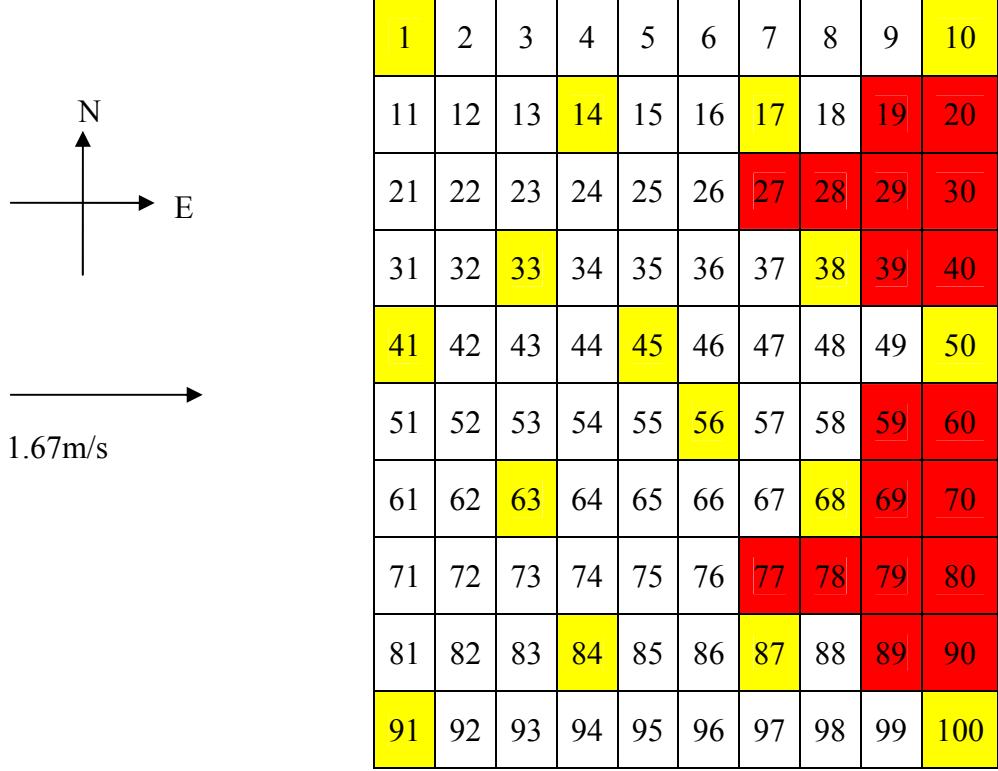
Figure 37. Sensor coverage for a 50kg nerve agent attack

From Figure 37, it can be seen that an attack originating in any of the 18 darkly shaded area cells will not be detected by any of the sensors in the current deployment plan, given the meteorological conditions. A plume originating in these cells will drift eastward without encountering any sensors.

We take it a step further to give a coverage index to each area cell. This index, β_l, is the probability that an attack in cell l is correctly detected by at least one sensor. Assuming stationary detection capability of the sensors and independence between sensor signals, β_l is calculated as follows:

$$\beta_l = 1 - \prod_{t,s}(1 - P_{l,t}^s) \qquad (9)$$

The value of β_l increases with the ENCS since the product term in Equation 9 is dependent on the ENCS. Hence area cells that have a high value of ENCS also have a high value of β_l.

Figure 38 shows the values of the coverage index of the sensor deployment plan used in the large scale setting for a 50kg nerve agent attack with a wind speed of 1.67m/s in the eastern direction. The lightly shaded area cells contain sensors.

From Figure 38, the coverage index informs decision makers and planners on the probability of detecting a chemical attack relative to a sensor deployment plan. With the coverage index, vulnerable locations (locations with low probability of detection) as well as locations with no coverage are identified.

Chemical sensors placed downwind of the area of operations give better coverage at the expense of delayed warning. This is a tradeoff that decision makers have to make in sensor placement. The detection of a chemical attack depends on the location, quantity and type of chemical agent used as well as the prevailing meteorological conditions relative to the sensor deployment plan and the detection performance of the sensors. The $P_{l,t}^{s}$ values offer an important tool to provide decision makers information on the coverage of a sensor deployment plan. The coverage index allows decision makers and planners to identify both vulnerable areas and areas with no sensor coverage. This allows gaps to be identified and improvements to be made by adding sensors or redeploying forward sensors downwind at the expense of late warning.

1	2	3	4	5	6	7	8	9	10
1	0.99	0.99	0.99	0.99	0.99	1	1	1	1
11	12	13	14	15	16	17	18	19	20
1	1	1	1	1	1	1	0.5	0	0
21	22	23	24	25	26	27	28	29	30
1	1	0.99	0.99	0.96	0.5	0	0	0	0
31	32	33	34	35	36	37	38	39	40
1	1	1	0.99	1	1	1	1	0	0
41	42	43	44	45	46	47	48	49	50
1	1	1	1	1	0.99	1	1	1	1
51	52	53	54	55	56	57	58	59	60
1	1	1	1	1	1	0.7	0.5	0	0
61	62	63	64	65	66	67	68	69	70
1	1	1	0.99	1	1	1	1	0	0
71	72	73	74	75	76	77	78	79	80
1	1	0.99	0.99	0.92	0.5	0	0	0	0
81	82	83	84	85	86	87	88	89	90
1	1	1	1	1	1	1	0.5	0	0
91	92	93	94	95	96	97	98	99	100
1	0.99	0.99	0.99	0.99	0.99	1	1	1	1

Figure 38.   Values of the coverage index for a 50kg nerve agent attack by cell location

THIS PAGE INTENTIONALLY LEFT BLANK

VI. SUMMARY AND CONCLUSIONS

A Bayesian updating model is used to detect a chemical attack, determine its location l and estimate the time of the attack t. The model uses data obtained from sensors deployed in the area of operations monitoring the air for a possible chemical attack. The detection model is made up of 3 modules: (i) a physical model; (ii) a sensor model; and (iii) a Bayesian updating model.

The physical model serves to calculate the chemical concentration c at the location of sensor s due to an attack at location l, t time periods ago. Based on the output c of the physical model, the sensor model computes the probabilities, $P_{l,t}^{s}$. The Bayesian updating model calculates the probability map at time period u, $\alpha_{l,t}^{u}$, of the posterior probability of a chemical attack at location l, t time period ago after the observations obtained by the sensors at time u. High value of $\alpha_{l,t}^{u}$ at time period u, indicates that there is a strong likelihood that a chemical attack has occurred at location l, t time periods ago.

The model is evaluated with respect to settings representing real-world operations. The selected alarm criterion by which decision makers initiate a response is at least three consecutive instances of posterior probabilities of an attack at location l, t time periods ago that is above the alarm threshold of 0.7. The alarm threshold is set at 0.7 to avoid responding to competing cues representing possible attack events early in the update process. The requirement for three consecutive observations eliminates false estimates caused by sudden spikes in the probability maps due to false positive errors and/or false negative errors that are encountered in the operational environment.

Factors that affect the model's capability to accurately estimate the location and time of an attack are (i) the specific layout of the deployed sensors relative to the attack location; (ii) the number of false positive errors; and (iii) the number of false negative errors.

From the linear regression model, it is found that, of the factors studied, the dominant factor is the ENCS, which depends on the specific layout of the deployed

81

sensors relative to the attack location. As a result, in sensor placement, considerations should be made to increase the ENCS for sensors in the area of operations. In the battle between sensitivity and specificity of the sensors deployed, it is more worthwhile to invest in sensitivity. This is because false negative rates are found to affect the model performance to a greater extent.

In conclusion, we have demonstrated that the model developed is able, in many cases, to accurately identify the location and time of a chemical attack with a nominal attack quantity of 50kg using inputs from chemical sensors and ATD models. The model bridges a critical gap between raw sensor data and threat evaluation and prediction models, giving authorities the capability to perform better hazard detection and damage control.

Insights on sensor coverage were also obtained. By using the $P_{l,t}^s$ values of all the point sensors deployed, the coverage of the sensors for a given chemical attack quantity and set of meteorological conditions can be ascertained. The $P_{l,t}^s$ values offer an important tool to provide decision makers information on the coverage of a sensor deployment plan. A coverage index indicating the probability of detecting a chemical attack relative to a sensor deployment plan was also developed. The coverage index allows decision makers and planners to identify both vulnerable areas and areas with no sensor coverage. This allows coverage gaps to be identified and improvements to be made by the addition of sensors or redeploying forward sensors downwind at the expense of early warning.

Future research involves extending the model to (i) detect chemical attacks with different nominal attack quantity levels, (ii) detect multiple chemical attacks and (iii) incorporate different sensor types. The insights obtained on sensor coverage through the use of the $P_{l,t}^s$ values in the model motivate further research in the area of sensor deployment and optimization.

APPENDIX

A. $P_{l,t}^s$ VALUES OF ALL 16 SENSORS FOR A NERVE AGENT ATTACK

Table 34. $P_{l,t}^1$ values for sensor in cell 1

$P_{l,t}^1$	Attack time scale, t time steps since the occurrence of the chemical attack															
Location	0	1	2	3	4	5	6	7	8	9	10	11	12	13	14	15
1	1.00	0.01	0.01	0.01	0.01	0.01	0.01	0.01	0.01	0.01	0.01	0.01	0.01	0.01	0.01	0.01
2	0.01	0.01	0.01	0.01	0.01	0.01	0.01	0.01	0.01	0.01	0.01	0.01	0.01	0.01	0.01	0.01
⋮	⋮	⋮	⋮	⋮	⋮	⋮	⋮	⋮	⋮	⋮	⋮	⋮	⋮	⋮	⋮	⋮
⋮	⋮	⋮	⋮	⋮	⋮	⋮	⋮	⋮	⋮	⋮	⋮	⋮	⋮	⋮	⋮	⋮
100	0.01	0.01	0.01	0.01	0.01	0.01	0.01	0.01	0.01	0.01	0.01	0.01	0.01	0.01	0.01	0.01

Table 35. $P_{l,t}^{10}$ values for sensor in cell 10

$P_{l,t}^{10}$	Attack time scale, t time steps since the occurrence of the chemical attack															
Location	0	1	2	3	4	5	6	7	8	9	10	11	12	13	14	15
1	0.01	0.01	0.01	0.01	0.01	0.01	0.50	0.60	0.70	0.80	0.70	0.60	0.50	0.01	0.01	0.01
2	0.01	0.01	0.01	0.01	0.01	0.01	0.60	0.70	0.80	0.70	0.60	0.01	0.01	0.01	0.01	0.01
3	0.01	0.01	0.01	0.01	0.01	0.60	0.80	0.80	0.80	0.60	0.01	0.01	0.01	0.01	0.01	0.01
4	0.01	0.01	0.01	0.01	0.50	0.80	0.80	0.80	0.50	0.01	0.01	0.01	0.01	0.01	0.01	0.01
5	0.01	0.01	0.01	0.50	0.80	0.90	0.80	0.50	0.01	0.01	0.01	0.01	0.01	0.01	0.01	0.01
6	0.01	0.01	0.01	0.70	0.90	0.70	0.01	0.01	0.01	0.01	0.01	0.01	0.01	0.01	0.01	0.01
7	0.01	0.01	0.70	1.00	0.70	0.01	0.01	0.01	0.01	0.01	0.01	0.01	0.01	0.01	0.01	0.01
8	0.01	0.50	1.00	0.50	0.01	0.01	0.01	0.01	0.01	0.01	0.01	0.01	0.01	0.01	0.01	0.01
9	0.01	1.00	0.01	0.01	0.01	0.01	0.01	0.01	0.01	0.01	0.01	0.01	0.01	0.01	0.01	0.01
10	1.00	0.01	0.01	0.01	0.01	0.01	0.01	0.01	0.01	0.01	0.01	0.01	0.01	0.01	0.01	0.01
11	0.01	0.01	0.01	0.01	0.01	0.01	0.01	0.60	0.70	0.70	0.70	0.60	0.01	0.01	0.01	0.01
12	0.01	0.01	0.01	0.01	0.01	0.01	0.50	0.70	0.70	0.70	0.50	0.01	0.01	0.01	0.01	0.01
13	0.01	0.01	0.01	0.01	0.01	0.50	0.70	0.80	0.70	0.50	0.01	0.01	0.01	0.01	0.01	0.01
14	0.01	0.01	0.01	0.01	0.50	0.70	0.80	0.70	0.50	0.01	0.01	0.01	0.01	0.01	0.01	0.01
15	0.01	0.01	0.01	0.01	0.60	0.80	0.60	0.01	0.01	0.01	0.01	0.01	0.01	0.01	0.01	0.01
16	0.01	0.01	0.01	0.60	0.70	0.60	0.01	0.01	0.01	0.01	0.01	0.01	0.01	0.01	0.01	0.01
17	0.01	0.01	0.01	0.70	0.01	0.01	0.01	0.01	0.01	0.01	0.01	0.01	0.01	0.01	0.01	0.01
18	0.01	0.01	0.50	0.01	0.01	0.01	0.01	0.01	0.01	0.01	0.01	0.01	0.01	0.01	0.01	0.01

19	0.01	0.01	0.01	0.01	0.01	0.01	0.01	0.01	0.01	0.01	0.01	0.01	0.01	0.01	0.01	0.01
20	0.01	0.01	0.01	0.01	0.01	0.01	0.01	0.01	0.01	0.01	0.01	0.01	0.01	0.01	0.01	0.01
21	0.01	0.01	0.01	0.01	0.01	0.01	0.01	0.50	0.60	0.60	0.60	0.50	0.01	0.01	0.01	0.01
22	0.01	0.01	0.01	0.01	0.01	0.01	0.50	0.50	0.60	0.50	0.50	0.01	0.01	0.01	0.01	0.01
23	0.01	0.01	0.01	0.01	0.01	0.01	0.50	0.60	0.50	0.01	0.01	0.01	0.01	0.01	0.01	0.01
24	0.01	0.01	0.01	0.01	0.01	0.50	0.50	0.50	0.01	0.01	0.01	0.01	0.01	0.01	0.01	0.01
25	0.01	0.01	0.01	0.01	0.01	0.50	0.01	0.01	0.01	0.01	0.01	0.01	0.01	0.01	0.01	0.01
26	0.01	0.01	0.01	0.01	0.01	0.01	0.01	0.01	0.01	0.01	0.01	0.01	0.01	0.01	0.01	0.01
⋮	⋮	⋮	⋮	⋮	⋮	⋮	⋮	⋮	⋮	⋮	⋮	⋮	⋮	⋮	⋮	⋮
⋮	⋮	⋮	⋮	⋮	⋮	⋮	⋮	⋮	⋮	⋮	⋮	⋮	⋮	⋮	⋮	⋮
99	0.01	0.01	0.01	0.01	0.01	0.01	0.01	0.01	0.01	0.01	0.01	0.01	0.01	0.01	0.01	0.01
100	0.01	0.01	0.01	0.01	0.01	0.01	0.01	0.01	0.01	0.01	0.01	0.01	0.01	0.01	0.01	0.01

Table 36. $P_{l,t}^{14}$ values for sensor in cell 14

$P_{l,t}^{14}$	Attack time scale, t time steps since the occurrence of the chemical attack															
Location	0	1	2	3	4	5	6	7	8	9	10	11	12	13	14	15
1	0.01	0.01	0.01	0.70	0.01	0.01	0.01	0.01	0.01	0.01	0.01	0.01	0.01	0.01	0.01	0.01
2	0.01	0.01	0.50	0.01	0.01	0.01	0.01	0.01	0.01	0.01	0.01	0.01	0.01	0.01	0.01	0.01
3	0.01	0.01	0.01	0.01	0.01	0.01	0.01	0.01	0.01	0.01	0.01	0.01	0.01	0.01	0.01	0.01
⋮	⋮	⋮	⋮	⋮	⋮	⋮	⋮	⋮	⋮	⋮	⋮	⋮	⋮	⋮	⋮	⋮
⋮	⋮	⋮	⋮	⋮	⋮	⋮	⋮	⋮	⋮	⋮	⋮	⋮	⋮	⋮	⋮	⋮
11	0.01	0.01	0.70	1.00	0.70	0.01	0.01	0.01	0.01	0.01	0.01	0.01	0.01	0.01	0.01	0.01
12	0.01	0.50	1.00	0.50	0.01	0.01	0.01	0.01	0.01	0.01	0.01	0.01	0.01	0.01	0.01	0.01
13	0.01	1.00	0.01	0.01	0.01	0.01	0.01	0.01	0.01	0.01	0.01	0.01	0.01	0.01	0.01	0.01
14	1.00	0.01	0.01	0.01	0.01	0.01	0.01	0.01	0.01	0.01	0.01	0.01	0.01	0.01	0.01	0.01
15	0.01	0.01	0.01	0.01	0.01	0.01	0.01	0.01	0.01	0.01	0.01	0.01	0.01	0.01	0.01	0.01
⋮	⋮	⋮	⋮	⋮	⋮	⋮	⋮	⋮	⋮	⋮	⋮	⋮	⋮	⋮	⋮	⋮
⋮	⋮	⋮	⋮	⋮	⋮	⋮	⋮	⋮	⋮	⋮	⋮	⋮	⋮	⋮	⋮	⋮
21	0.01	0.01	0.01	0.70	0.01	0.01	0.01	0.01	0.01	0.01	0.01	0.01	0.01	0.01	0.01	0.01
22	0.01	0.01	0.50	0.01	0.01	0.01	0.01	0.01	0.01	0.01	0.01	0.01	0.01	0.01	0.01	0.01
23	0.01	0.01	0.01	0.01	0.01	0.01	0.01	0.01	0.01	0.01	0.01	0.01	0.01	0.01	0.01	0.01
⋮	⋮	⋮	⋮	⋮	⋮	⋮	⋮	⋮	⋮	⋮	⋮	⋮	⋮	⋮	⋮	⋮
⋮	⋮	⋮	⋮	⋮	⋮	⋮	⋮	⋮	⋮	⋮	⋮	⋮	⋮	⋮	⋮	⋮
100	0.01	0.01	0.01	0.01	0.01	0.01	0.01	0.01	0.01	0.01	0.01	0.01	0.01	0.01	0.01	0.01

Table 37. $P_{l,t}^{17}$ values for sensor in cell 17

$P_{l,t}^{17}$	Attack time scale, t time steps since the occurrence of the chemical attack															
Location	0	1	2	3	4	5	6	7	8	9	10	11	12	13	14	15
1	0.01	0.01	0.01	0.01	0.50	0.70	0.80	0.70	0.50	0.01	0.01	0.01	0.01	0.01	0.01	0.01
2	0.01	0.01	0.01	0.01	0.60	0.80	0.60	0.01	0.01	0.01	0.01	0.01	0.01	0.01	0.01	0.01
3	0.01	0.01	0.01	0.60	0.70	0.60	0.01	0.01	0.01	0.01	0.01	0.01	0.01	0.01	0.01	0.01
4	0.01	0.01	0.01	0.70	0.01	0.01	0.01	0.01	0.01	0.01	0.01	0.01	0.01	0.01	0.01	0.01
5	0.01	0.01	0.50	0.01	0.01	0.01	0.01	0.01	0.01	0.01	0.01	0.01	0.01	0.01	0.01	0.01
6	0.01	0.01	0.01	0.01	0.01	0.01	0.01	0.01	0.01	0.01	0.01	0.01	0.01	0.01	0.01	0.01
7	0.01	0.01	0.01	0.01	0.01	0.01	0.01	0.01	0.01	0.01	0.01	0.01	0.01	0.01	0.01	0.01
8	0.01	0.01	0.01	0.01	0.01	0.01	0.01	0.01	0.01	0.01	0.01	0.01	0.01	0.01	0.01	0.01
9	0.01	0.01	0.01	0.01	0.01	0.01	0.01	0.01	0.01	0.01	0.01	0.01	0.01	0.01	0.01	0.01
10	0.01	0.01	0.01	0.01	0.01	0.01	0.01	0.01	0.01	0.01	0.01	0.01	0.01	0.01	0.01	0.01
11	0.01	0.01	0.01	0.01	0.50	0.80	0.80	0.80	0.50	0.01	0.01	0.01	0.01	0.01	0.01	0.01
12	0.01	0.01	0.01	0.50	0.80	0.90	0.80	0.50	0.01	0.01	0.01	0.01	0.01	0.01	0.01	0.01
13	0.01	0.01	0.01	0.70	0.90	0.70	0.01	0.01	0.01	0.01	0.01	0.01	0.01	0.01	0.01	0.01
14	0.01	0.01	0.70	1.00	0.70	0.01	0.01	0.01	0.01	0.01	0.01	0.01	0.01	0.01	0.01	0.01
15	0.01	0.50	1.00	0.50	0.01	0.01	0.01	0.01	0.01	0.01	0.01	0.01	0.01	0.01	0.01	0.01
16	0.01	1.00	0.01	0.01	0.01	0.01	0.01	0.01	0.01	0.01	0.01	0.01	0.01	0.01	0.01	0.01
17	1.00	0.01	0.01	0.01	0.01	0.01	0.01	0.01	0.01	0.01	0.01	0.01	0.01	0.01	0.01	0.01
18	0.01	0.01	0.01	0.01	0.01	0.01	0.01	0.01	0.01	0.01	0.01	0.01	0.01	0.01	0.01	0.01
19	0.01	0.01	0.01	0.01	0.01	0.01	0.01	0.01	0.01	0.01	0.01	0.01	0.01	0.01	0.01	0.01
20	0.01	0.01	0.01	0.01	0.01	0.01	0.01	0.01	0.01	0.01	0.01	0.01	0.01	0.01	0.01	0.01
21	0.01	0.01	0.01	0.01	0.50	0.70	0.80	0.70	0.50	0.01	0.01	0.01	0.01	0.01	0.01	0.01
22	0.01	0.01	0.01	0.01	0.60	0.80	0.60	0.01	0.01	0.01	0.01	0.01	0.01	0.01	0.01	0.01
23	0.01	0.01	0.01	0.60	0.70	0.60	0.01	0.01	0.01	0.01	0.01	0.01	0.01	0.01	0.01	0.01
24	0.01	0.01	0.01	0.70	0.01	0.01	0.01	0.01	0.01	0.01	0.01	0.01	0.01	0.01	0.01	0.01
25	0.01	0.01	0.50	0.01	0.01	0.01	0.01	0.01	0.01	0.01	0.01	0.01	0.01	0.01	0.01	0.01
26	0.01	0.01	0.01	0.01	0.01	0.01	0.01	0.01	0.01	0.01	0.01	0.01	0.01	0.01	0.01	0.01
⋮	⋮	⋮	⋮	⋮	⋮	⋮	⋮	⋮	⋮	⋮	⋮	⋮	⋮	⋮	⋮	⋮
31	0.01	0.01	0.01	0.01	0.01	0.50	0.50	0.50	0.01	0.01	0.01	0.01	0.01	0.01	0.01	0.01
32	0.01	0.01	0.01	0.01	0.01	0.50	0.01	0.01	0.01	0.01	0.01	0.01	0.01	0.01	0.01	0.01
33	0.01	0.01	0.01	0.01	0.01	0.01	0.01	0.01	0.01	0.01	0.01	0.01	0.01	0.01	0.01	0.01
⋮	⋮	⋮	⋮	⋮	⋮	⋮	⋮	⋮	⋮	⋮	⋮	⋮	⋮	⋮	⋮	⋮
⋮	⋮	⋮	⋮	⋮	⋮	⋮	⋮	⋮	⋮	⋮	⋮	⋮	⋮	⋮	⋮	⋮
100	0.01	0.01	0.01	0.01	0.01	0.01	0.01	0.01	0.01	0.01	0.01	0.01	0.01	0.01	0.01	0.01

Table 38. $P_{l,t}^{33}$ values for sensor in cell 33

$P_{l,t}^{33}$	Attack time scale, t time steps since the occurrence of the chemical attack															
Location	0	1	2	3	4	5	6	7	8	9	10	11	12	13	14	15
1	0.01	0.01	0.01	0.01	0.01	0.01	0.01	0.01	0.01	0.01	0.01	0.01	0.01	0.01	0.01	0.01
2	0.01	0.01	0.01	0.01	0.01	0.01	0.01	0.01	0.01	0.01	0.01	0.01	0.01	0.01	0.01	0.01
⋮	⋮	⋮	⋮	⋮	⋮	⋮	⋮	⋮	⋮	⋮	⋮	⋮	⋮	⋮	⋮	⋮
⋮	⋮	⋮	⋮	⋮	⋮	⋮	⋮	⋮	⋮	⋮	⋮	⋮	⋮	⋮	⋮	⋮
21	0.01	0.01	0.50	0.01	0.01	0.01	0.01	0.01	0.01	0.01	0.01	0.01	0.01	0.01	0.01	0.01
22	0.01	0.01	0.01	0.01	0.01	0.01	0.01	0.01	0.01	0.01	0.01	0.01	0.01	0.01	0.01	0.01
23	0.01	0.01	0.01	0.01	0.01	0.01	0.01	0.01	0.01	0.01	0.01	0.01	0.01	0.01	0.01	0.01
24	0.01	0.01	0.01	0.01	0.01	0.01	0.01	0.01	0.01	0.01	0.01	0.01	0.01	0.01	0.01	0.01
25	0.01	0.01	0.01	0.01	0.01	0.01	0.01	0.01	0.01	0.01	0.01	0.01	0.01	0.01	0.01	0.01
26	0.01	0.01	0.01	0.01	0.01	0.01	0.01	0.01	0.01	0.01	0.01	0.01	0.01	0.01	0.01	0.01
27	0.01	0.01	0.01	0.01	0.01	0.01	0.01	0.01	0.01	0.01	0.01	0.01	0.01	0.01	0.01	0.01
28	0.01	0.01	0.01	0.01	0.01	0.01	0.01	0.01	0.01	0.01	0.01	0.01	0.01	0.01	0.01	0.01
29	0.01	0.01	0.01	0.01	0.01	0.01	0.01	0.01	0.01	0.01	0.01	0.01	0.01	0.01	0.01	0.01
30	0.01	0.01	0.01	0.01	0.01	0.01	0.01	0.01	0.01	0.01	0.01	0.01	0.01	0.01	0.01	0.01
31	0.01	0.50	1.00	0.50	0.01	0.01	0.01	0.01	0.01	0.01	0.01	0.01	0.01	0.01	0.01	0.01
32	0.01	1.00	0.01	0.01	0.01	0.01	0.01	0.01	0.01	0.01	0.01	0.01	0.01	0.01	0.01	0.01
33	1.00	0.01	0.01	0.01	0.01	0.01	0.01	0.01	0.01	0.01	0.01	0.01	0.01	0.01	0.01	0.01
34	0.01	0.01	0.01	0.01	0.01	0.01	0.01	0.01	0.01	0.01	0.01	0.01	0.01	0.01	0.01	0.01
35	0.01	0.01	0.01	0.01	0.01	0.01	0.01	0.01	0.01	0.01	0.01	0.01	0.01	0.01	0.01	0.01
36	0.01	0.01	0.01	0.01	0.01	0.01	0.01	0.01	0.01	0.01	0.01	0.01	0.01	0.01	0.01	0.01
37	0.01	0.01	0.01	0.01	0.01	0.01	0.01	0.01	0.01	0.01	0.01	0.01	0.01	0.01	0.01	0.01
38	0.01	0.01	0.01	0.01	0.01	0.01	0.01	0.01	0.01	0.01	0.01	0.01	0.01	0.01	0.01	0.01
39	0.01	0.01	0.01	0.01	0.01	0.01	0.01	0.01	0.01	0.01	0.01	0.01	0.01	0.01	0.01	0.01
40	0.01	0.01	0.01	0.01	0.01	0.01	0.01	0.01	0.01	0.01	0.01	0.01	0.01	0.01	0.01	0.01
41	0.01	0.01	0.50	0.01	0.01	0.01	0.01	0.01	0.01	0.01	0.01	0.01	0.01	0.01	0.01	0.01
42	0.01	0.01	0.01	0.01	0.01	0.01	0.01	0.01	0.01	0.01	0.01	0.01	0.01	0.01	0.01	0.01
43	0.01	0.01	0.01	0.01	0.01	0.01	0.01	0.01	0.01	0.01	0.01	0.01	0.01	0.01	0.01	0.01
⋮	⋮	⋮	⋮	⋮	⋮	⋮	⋮	⋮	⋮	⋮	⋮	⋮	⋮	⋮	⋮	⋮
⋮	⋮	⋮	⋮	⋮	⋮	⋮	⋮	⋮	⋮	⋮	⋮	⋮	⋮	⋮	⋮	⋮
100	0.01	0.01	0.01	0.01	0.01	0.01	0.01	0.01	0.01	0.01	0.01	0.01	0.01	0.01	0.01	0.01

Table 39. $P^{38}_{l,t}$ values for sensor in cell 38

$P^{38}_{l,t}$	Attack time scale, t time steps since the occurrence of the chemical attack															
Location	0	1	2	3	4	5	6	7	8	9	10	11	12	13	14	15
1	0.01	0.01	0.01	0.01	0.01	0.01	0.01	0.01	0.01	0.01	0.01	0.01	0.01	0.01	0.01	0.01
2	0.01	0.01	0.01	0.01	0.01	0.01	0.01	0.01	0.01	0.01	0.01	0.01	0.01	0.01	0.01	0.01
⋮	⋮	⋮	⋮	⋮	⋮	⋮	⋮	⋮	⋮	⋮	⋮	⋮	⋮	⋮	⋮	⋮
⋮	⋮	⋮	⋮	⋮	⋮	⋮	⋮	⋮	⋮	⋮	⋮	⋮	⋮	⋮	⋮	⋮
11	0.01	0.01	0.01	0.01	0.01	0.01	0.50	0.60	0.50	0.01	0.01	0.01	0.01	0.01	0.01	0.01
12	0.01	0.01	0.01	0.01	0.01	0.50	0.50	0.50	0.01	0.01	0.01	0.01	0.01	0.01	0.01	0.01
13	0.01	0.01	0.01	0.01	0.01	0.50	0.01	0.01	0.01	0.01	0.01	0.01	0.01	0.01	0.01	0.01
14	0.01	0.01	0.01	0.01	0.01	0.01	0.01	0.01	0.01	0.01	0.01	0.01	0.01	0.01	0.01	0.01
15	0.01	0.01	0.01	0.01	0.01	0.01	0.01	0.01	0.01	0.01	0.01	0.01	0.01	0.01	0.01	0.01
⋮	⋮	⋮	⋮	⋮	⋮	⋮	⋮	⋮	⋮	⋮	⋮	⋮	⋮	⋮	⋮	⋮
21	0.01	0.01	0.01	0.01	0.01	0.50	0.70	0.80	0.70	0.50	0.01	0.01	0.01	0.01	0.01	0.01
22	0.01	0.01	0.01	0.01	0.50	0.70	0.80	0.70	0.50	0.01	0.01	0.01	0.01	0.01	0.01	0.01
23	0.01	0.01	0.01	0.01	0.60	0.80	0.60	0.01	0.01	0.01	0.01	0.01	0.01	0.01	0.01	0.01
24	0.01	0.01	0.01	0.60	0.70	0.60	0.01	0.01	0.01	0.01	0.01	0.01	0.01	0.01	0.01	0.01
25	0.01	0.01	0.01	0.70	0.01	0.01	0.01	0.01	0.01	0.01	0.01	0.01	0.01	0.01	0.01	0.01
26	0.01	0.01	0.50	0.01	0.01	0.01	0.01	0.01	0.01	0.01	0.01	0.01	0.01	0.01	0.01	0.01
27	0.01	0.01	0.01	0.01	0.01	0.01	0.01	0.01	0.01	0.01	0.01	0.01	0.01	0.01	0.01	0.01
28	0.01	0.01	0.01	0.01	0.01	0.01	0.01	0.01	0.01	0.01	0.01	0.01	0.01	0.01	0.01	0.01
29	0.01	0.01	0.01	0.01	0.01	0.01	0.01	0.01	0.01	0.01	0.01	0.01	0.01	0.01	0.01	0.01
30	0.01	0.01	0.01	0.01	0.01	0.01	0.01	0.01	0.01	0.01	0.01	0.01	0.01	0.01	0.01	0.01
31	0.01	0.01	0.01	0.01	0.01	0.60	0.80	0.80	0.80	0.60	0.01	0.01	0.01	0.01	0.01	0.01
32	0.01	0.01	0.01	0.01	0.50	0.80	0.80	0.80	0.50	0.01	0.01	0.01	0.01	0.01	0.01	0.01
33	0.01	0.01	0.01	0.50	0.80	0.90	0.80	0.50	0.01	0.01	0.01	0.01	0.01	0.01	0.01	0.01
34	0.01	0.01	0.01	0.70	0.90	0.70	0.01	0.01	0.01	0.01	0.01	0.01	0.01	0.01	0.01	0.01
35	0.01	0.01	0.70	1.00	0.70	0.01	0.01	0.01	0.01	0.01	0.01	0.01	0.01	0.01	0.01	0.01
36	0.01	0.50	1.00	0.50	0.01	0.01	0.01	0.01	0.01	0.01	0.01	0.01	0.01	0.01	0.01	0.01
37	0.01	1.00	0.01	0.01	0.01	0.01	0.01	0.01	0.01	0.01	0.01	0.01	0.01	0.01	0.01	0.01
38	1.00	0.01	0.01	0.01	0.01	0.01	0.01	0.01	0.01	0.01	0.01	0.01	0.01	0.01	0.01	0.01
39	0.01	0.01	0.01	0.01	0.01	0.01	0.01	0.01	0.01	0.01	0.01	0.01	0.01	0.01	0.01	0.01
40	0.01	0.01	0.01	0.01	0.01	0.01	0.01	0.01	0.01	0.01	0.01	0.01	0.01	0.01	0.01	0.01
41	0.01	0.01	0.01	0.01	0.01	0.50	0.70	0.80	0.70	0.50	0.01	0.01	0.01	0.01	0.01	0.01
42	0.01	0.01	0.01	0.01	0.50	0.70	0.80	0.70	0.50	0.01	0.01	0.01	0.01	0.01	0.01	0.01
43	0.01	0.01	0.01	0.01	0.60	0.80	0.60	0.01	0.01	0.01	0.01	0.01	0.01	0.01	0.01	0.01
44	0.01	0.01	0.01	0.60	0.70	0.60	0.01	0.01	0.01	0.01	0.01	0.01	0.01	0.01	0.01	0.01

	0	1	2	3	4	5	6	7	8	9	10	11	12	13	14	15
45	0.01	0.01	0.01	0.70	0.01	0.01	0.01	0.01	0.01	0.01	0.01	0.01	0.01	0.01	0.01	0.01
46	0.01	0.01	0.50	0.01	0.01	0.01	0.01	0.01	0.01	0.01	0.01	0.01	0.01	0.01	0.01	0.01
47	0.01	0.01	0.01	0.01	0.01	0.01	0.01	0.01	0.01	0.01	0.01	0.01	0.01	0.01	0.01	0.01
48	0.01	0.01	0.01	0.01	0.01	0.01	0.01	0.01	0.01	0.01	0.01	0.01	0.01	0.01	0.01	0.01
49	0.01	0.01	0.01	0.01	0.01	0.01	0.01	0.01	0.01	0.01	0.01	0.01	0.01	0.01	0.01	0.01
50	0.01	0.01	0.01	0.01	0.01	0.01	0.01	0.01	0.01	0.01	0.01	0.01	0.01	0.01	0.01	0.01
51	0.01	0.01	0.01	0.01	0.01	0.01	0.50	0.60	0.50	0.01	0.01	0.01	0.01	0.01	0.01	0.01
52	0.01	0.01	0.01	0.01	0.01	0.50	0.50	0.50	0.01	0.01	0.01	0.01	0.01	0.01	0.01	0.01
53	0.01	0.01	0.01	0.01	0.01	0.50	0.01	0.01	0.01	0.01	0.01	0.01	0.01	0.01	0.01	0.01
⋮	⋮	⋮	⋮	⋮	⋮	⋮	⋮	⋮	⋮	⋮	⋮	⋮	⋮	⋮	⋮	⋮
⋮	⋮	⋮	⋮	⋮	⋮	⋮	⋮	⋮	⋮	⋮	⋮	⋮	⋮	⋮	⋮	⋮
99	0.01	0.01	0.01	0.01	0.01	0.01	0.01	0.01	0.01	0.01	0.01	0.01	0.01	0.01	0.01	0.01
100	0.01	0.01	0.01	0.01	0.01	0.01	0.01	0.01	0.01	0.01	0.01	0.01	0.01	0.01	0.01	0.01

Table 40. $P_{l,t}^{41}$ values for sensor in cell 41

$P_{l,t}^{41}$	Attack time scale, t time steps since the occurrence of the chemical attack															
Location	0	1	2	3	4	5	6	7	8	9	10	11	12	13	14	15
1	0.01	0.01	0.01	0.01	0.01	0.01	0.01	0.01	0.01	0.01	0.01	0.01	0.01	0.01	0.01	0.01
⋮	⋮	⋮	⋮	⋮	⋮	⋮	⋮	⋮	⋮	⋮	⋮	⋮	⋮	⋮	⋮	⋮
⋮	⋮	⋮	⋮	⋮	⋮	⋮	⋮	⋮	⋮	⋮	⋮	⋮	⋮	⋮	⋮	⋮
41	1.00	0.01	0.01	0.01	0.01	0.01	0.01	0.01	0.01	0.01	0.01	0.01	0.01	0.01	0.01	0.01
42	0.01	0.01	0.01	0.01	0.01	0.01	0.01	0.01	0.01	0.01	0.01	0.01	0.01	0.01	0.01	0.01
⋮	⋮	⋮	⋮	⋮	⋮	⋮	⋮	⋮	⋮	⋮	⋮	⋮	⋮	⋮	⋮	⋮
⋮	⋮	⋮	⋮	⋮	⋮	⋮	⋮	⋮	⋮	⋮	⋮	⋮	⋮	⋮	⋮	⋮
100	0.01	0.01	0.01	0.01	0.01	0.01	0.01	0.01	0.01	0.01	0.01	0.01	0.01	0.01	0.01	0.01

Table 41. $P_{l,t}^{45}$ values for sensor in cell 45

$P_{l,t}^{45}$	Attack time scale, t time steps since the occurrence of the chemical attack															
Location	0	1	2	3	4	5	6	7	8	9	10	11	12	13	14	15
1	0.01	0.01	0.01	0.01	0.01	0.01	0.01	0.01	0.01	0.01	0.01	0.01	0.01	0.01	0.01	0.01
⋮	⋮	⋮	⋮	⋮	⋮	⋮	⋮	⋮	⋮	⋮	⋮	⋮	⋮	⋮	⋮	⋮
31	0.01	0.01	0.01	0.60	0.70	0.60	0.01	0.01	0.01	0.01	0.01	0.01	0.01	0.01	0.01	0.01
32	0.01	0.01	0.01	0.70	0.01	0.01	0.01	0.01	0.01	0.01	0.01	0.01	0.01	0.01	0.01	0.01
33	0.01	0.01	0.50	0.01	0.01	0.01	0.01	0.01	0.01	0.01	0.01	0.01	0.01	0.01	0.01	0.01
34	0.01	0.01	0.01	0.01	0.01	0.01	0.01	0.01	0.01	0.01	0.01	0.01	0.01	0.01	0.01	0.01
35	0.01	0.01	0.01	0.01	0.01	0.01	0.01	0.01	0.01	0.01	0.01	0.01	0.01	0.01	0.01	0.01
36	0.01	0.01	0.01	0.01	0.01	0.01	0.01	0.01	0.01	0.01	0.01	0.01	0.01	0.01	0.01	0.01
37	0.01	0.01	0.01	0.01	0.01	0.01	0.01	0.01	0.01	0.01	0.01	0.01	0.01	0.01	0.01	0.01
38	0.01	0.01	0.01	0.01	0.01	0.01	0.01	0.01	0.01	0.01	0.01	0.01	0.01	0.01	0.01	0.01
39	0.01	0.01	0.01	0.01	0.01	0.01	0.01	0.01	0.01	0.01	0.01	0.01	0.01	0.01	0.01	0.01
40	0.01	0.01	0.01	0.01	0.01	0.01	0.01	0.01	0.01	0.01	0.01	0.01	0.01	0.01	0.01	0.01
41	0.01	0.01	0.01	0.70	0.90	0.70	0.01	0.01	0.01	0.01	0.01	0.01	0.01	0.01	0.01	0.01
42	0.01	0.01	0.70	1.00	0.70	0.01	0.01	0.01	0.01	0.01	0.01	0.01	0.01	0.01	0.01	0.01
43	0.01	0.50	1.00	0.50	0.01	0.01	0.01	0.01	0.01	0.01	0.01	0.01	0.01	0.01	0.01	0.01
44	0.01	1.00	0.01	0.01	0.01	0.01	0.01	0.01	0.01	0.01	0.01	0.01	0.01	0.01	0.01	0.01
45	1.00	0.01	0.01	0.01	0.01	0.01	0.01	0.01	0.01	0.01	0.01	0.01	0.01	0.01	0.01	0.01
46	0.01	0.01	0.01	0.01	0.01	0.01	0.01	0.01	0.01	0.01	0.01	0.01	0.01	0.01	0.01	0.01
47	0.01	0.01	0.01	0.01	0.01	0.01	0.01	0.01	0.01	0.01	0.01	0.01	0.01	0.01	0.01	0.01
48	0.01	0.01	0.01	0.01	0.01	0.01	0.01	0.01	0.01	0.01	0.01	0.01	0.01	0.01	0.01	0.01
49	0.01	0.01	0.01	0.01	0.01	0.01	0.01	0.01	0.01	0.01	0.01	0.01	0.01	0.01	0.01	0.01
50	0.01	0.01	0.01	0.01	0.01	0.01	0.01	0.01	0.01	0.01	0.01	0.01	0.01	0.01	0.01	0.01
51	0.01	0.01	0.01	0.60	0.70	0.60	0.01	0.01	0.01	0.01	0.01	0.01	0.01	0.01	0.01	0.01
52	0.01	0.01	0.01	0.70	0.01	0.01	0.01	0.01	0.01	0.01	0.01	0.01	0.01	0.01	0.01	0.01
53	0.01	0.01	0.50	0.01	0.01	0.01	0.01	0.01	0.01	0.01	0.01	0.01	0.01	0.01	0.01	0.01
54	0.01	0.01	0.01	0.01	0.01	0.01	0.01	0.01	0.01	0.01	0.01	0.01	0.01	0.01	0.01	0.01
⋮	⋮	⋮	⋮	⋮	⋮	⋮	⋮	⋮	⋮	⋮	⋮	⋮	⋮	⋮	⋮	⋮
⋮	⋮	⋮	⋮	⋮	⋮	⋮	⋮	⋮	⋮	⋮	⋮	⋮	⋮	⋮	⋮	⋮
100	0.01	0.01	0.01	0.01	0.01	0.01	0.01	0.01	0.01	0.01	0.01	0.01	0.01	0.01	0.01	0.01

Table 42. $P^{50}_{l,t}$ values for sensor in cell 50

$P^{50}_{l,t}$	Attack time scale, t time steps since the occurrence of the chemical attack															
Location	0	1	2	3	4	5	6	7	8	9	10	11	12	13	14	15
1	0.01	0.01	0.01	0.01	0.01	0.01	0.01	0.01	0.01	0.01	0.01	0.01	0.01	0.01	0.01	0.01
⋮	⋮	⋮	⋮	⋮	⋮	⋮	⋮	⋮	⋮	⋮	⋮	⋮	⋮	⋮	⋮	⋮
⋮	⋮	⋮	⋮	⋮	⋮	⋮	⋮	⋮	⋮	⋮	⋮	⋮	⋮	⋮	⋮	⋮
21	0.01	0.01	0.01	0.01	0.01	0.01	0.01	0.50	0.60	0.60	0.60	0.50	0.01	0.01	0.01	0.01
22	0.01	0.01	0.01	0.01	0.01	0.01	0.50	0.50	0.60	0.50	0.50	0.01	0.01	0.01	0.01	0.01
23	0.01	0.01	0.01	0.01	0.01	0.01	0.50	0.60	0.50	0.01	0.01	0.01	0.01	0.01	0.01	0.01
24	0.01	0.01	0.01	0.01	0.01	0.50	0.50	0.50	0.01	0.01	0.01	0.01	0.01	0.01	0.01	0.01
25	0.01	0.01	0.01	0.01	0.01	0.50	0.01	0.01	0.01	0.01	0.01	0.01	0.01	0.01	0.01	0.01
26	0.01	0.01	0.01	0.01	0.01	0.01	0.01	0.01	0.01	0.01	0.01	0.01	0.01	0.01	0.01	0.01
27	0.01	0.01	0.01	0.01	0.01	0.01	0.01	0.01	0.01	0.01	0.01	0.01	0.01	0.01	0.01	0.01
28	0.01	0.01	0.01	0.01	0.01	0.01	0.01	0.01	0.01	0.01	0.01	0.01	0.01	0.01	0.01	0.01
29	0.01	0.01	0.01	0.01	0.01	0.01	0.01	0.01	0.01	0.01	0.01	0.01	0.01	0.01	0.01	0.01
30	0.01	0.01	0.01	0.01	0.01	0.01	0.01	0.01	0.01	0.01	0.01	0.01	0.01	0.01	0.01	0.01
31	0.01	0.01	0.01	0.01	0.01	0.01	0.01	0.60	0.70	0.70	0.70	0.60	0.01	0.01	0.01	0.01
32	0.01	0.01	0.01	0.01	0.01	0.01	0.50	0.70	0.70	0.70	0.50	0.01	0.01	0.01	0.01	0.01
33	0.01	0.01	0.01	0.01	0.01	0.50	0.70	0.80	0.70	0.50	0.01	0.01	0.01	0.01	0.01	0.01
34	0.01	0.01	0.01	0.01	0.50	0.70	0.80	0.70	0.50	0.01	0.01	0.01	0.01	0.01	0.01	0.01
35	0.01	0.01	0.01	0.01	0.60	0.80	0.60	0.01	0.01	0.01	0.01	0.01	0.01	0.01	0.01	0.01
36	0.01	0.01	0.01	0.60	0.70	0.60	0.01	0.01	0.01	0.01	0.01	0.01	0.01	0.01	0.01	0.01
37	0.01	0.01	0.01	0.70	0.01	0.01	0.01	0.01	0.01	0.01	0.01	0.01	0.01	0.01	0.01	0.01
38	0.01	0.01	0.50	0.01	0.01	0.01	0.01	0.01	0.01	0.01	0.01	0.01	0.01	0.01	0.01	0.01
39	0.01	0.01	0.01	0.01	0.01	0.01	0.01	0.01	0.01	0.01	0.01	0.01	0.01	0.01	0.01	0.01
40	0.01	0.01	0.01	0.01	0.01	0.01	0.01	0.01	0.01	0.01	0.01	0.01	0.01	0.01	0.01	0.01
41	0.01	0.01	0.01	0.01	0.01	0.01	0.50	0.60	0.70	0.80	0.70	0.60	0.50	0.01	0.01	0.01
42	0.01	0.01	0.01	0.01	0.01	0.01	0.60	0.70	0.80	0.70	0.60	0.01	0.01	0.01	0.01	0.01
43	0.01	0.01	0.01	0.01	0.01	0.60	0.80	0.80	0.80	0.60	0.01	0.01	0.01	0.01	0.01	0.01
44	0.01	0.01	0.01	0.01	0.50	0.80	0.80	0.80	0.50	0.01	0.01	0.01	0.01	0.01	0.01	0.01
45	0.01	0.01	0.01	0.50	0.80	0.90	0.80	0.50	0.01	0.01	0.01	0.01	0.01	0.01	0.01	0.01
46	0.01	0.01	0.01	0.70	0.90	0.70	0.01	0.01	0.01	0.01	0.01	0.01	0.01	0.01	0.01	0.01
47	0.01	0.01	0.70	1.00	0.70	0.01	0.01	0.01	0.01	0.01	0.01	0.01	0.01	0.01	0.01	0.01
48	0.01	0.50	1.00	0.50	0.01	0.01	0.01	0.01	0.01	0.01	0.01	0.01	0.01	0.01	0.01	0.01
49	0.01	1.00	0.01	0.01	0.01	0.01	0.01	0.01	0.01	0.01	0.01	0.01	0.01	0.01	0.01	0.01
50	1.00	0.01	0.01	0.01	0.01	0.01	0.01	0.01	0.01	0.01	0.01	0.01	0.01	0.01	0.01	0.01
51	0.01	0.01	0.01	0.01	0.01	0.01	0.01	0.60	0.70	0.70	0.70	0.60	0.01	0.01	0.01	0.01

52	0.01	0.01	0.01	0.01	0.01	0.01	0.50	0.70	0.70	0.70	0.50	0.01	0.01	0.01	0.01	0.01
53	0.01	0.01	0.01	0.01	0.01	0.50	0.70	0.80	0.70	0.50	0.01	0.01	0.01	0.01	0.01	0.01
54	0.01	0.01	0.01	0.01	0.50	0.70	0.80	0.70	0.50	0.01	0.01	0.01	0.01	0.01	0.01	0.01
55	0.01	0.01	0.01	0.01	0.60	0.80	0.60	0.01	0.01	0.01	0.01	0.01	0.01	0.01	0.01	0.01
56	0.01	0.01	0.01	0.60	0.70	0.60	0.01	0.01	0.01	0.01	0.01	0.01	0.01	0.01	0.01	0.01
57	0.01	0.01	0.01	0.70	0.01	0.01	0.01	0.01	0.01	0.01	0.01	0.01	0.01	0.01	0.01	0.01
58	0.01	0.01	0.50	0.01	0.01	0.01	0.01	0.01	0.01	0.01	0.01	0.01	0.01	0.01	0.01	0.01
59	0.01	0.01	0.01	0.01	0.01	0.01	0.01	0.01	0.01	0.01	0.01	0.01	0.01	0.01	0.01	0.01
60	0.01	0.01	0.01	0.01	0.01	0.01	0.01	0.01	0.01	0.01	0.01	0.01	0.01	0.01	0.01	0.01
61	0.01	0.01	0.01	0.01	0.01	0.01	0.01	0.50	0.60	0.60	0.60	0.50	0.01	0.01	0.01	0.01
62	0.01	0.01	0.01	0.01	0.01	0.01	0.50	0.50	0.60	0.50	0.50	0.01	0.01	0.01	0.01	0.01
63	0.01	0.01	0.01	0.01	0.01	0.01	0.50	0.60	0.50	0.01	0.01	0.01	0.01	0.01	0.01	0.01
64	0.01	0.01	0.01	0.01	0.01	0.50	0.50	0.50	0.01	0.01	0.01	0.01	0.01	0.01	0.01	0.01
65	0.01	0.01	0.01	0.01	0.01	0.50	0.01	0.01	0.01	0.01	0.01	0.01	0.01	0.01	0.01	0.01
66	0.01	0.01	0.01	0.01	0.01	0.01	0.01	0.01	0.01	0.01	0.01	0.01	0.01	0.01	0.01	0.01
67	0.01	0.01	0.01	0.01	0.01	0.01	0.01	0.01	0.01	0.01	0.01	0.01	0.01	0.01	0.01	0.01
68	0.01	0.01	0.01	0.01	0.01	0.01	0.01	0.01	0.01	0.01	0.01	0.01	0.01	0.01	0.01	0.01
69	0.01	0.01	0.01	0.01	0.01	0.01	0.01	0.01	0.01	0.01	0.01	0.01	0.01	0.01	0.01	0.01
70	0.01	0.01	0.01	0.01	0.01	0.01	0.01	0.01	0.01	0.01	0.01	0.01	0.01	0.01	0.01	0.01
100	0.01	0.01	0.01	0.01	0.01	0.01	0.01	0.01	0.01	0.01	0.01	0.01	0.01	0.01	0.01	0.01

Table 43. $P_{l,t}^{56}$ values for sensor in cell 56

$P_{l,t}^{56}$	Attack time scale, t time steps since the occurrence of the chemical attack															
Location	0	1	2	3	4	5	6	7	8	9	10	11	12	13	14	15
1	0.01	0.01	0.01	0.01	0.01	0.01	0.01	0.01	0.01	0.01	0.01	0.01	0.01	0.01	0.01	0.01
⋮	⋮	⋮	⋮	⋮	⋮	⋮	⋮	⋮	⋮	⋮	⋮	⋮	⋮	⋮	⋮	⋮
⋮	⋮	⋮	⋮	⋮	⋮	⋮	⋮	⋮	⋮	⋮	⋮	⋮	⋮	⋮	⋮	⋮
31	0.01	0.01	0.01	0.01	0.01	0.50	0.01	0.01	0.01	0.01	0.01	0.01	0.01	0.01	0.01	0.01
32	0.01	0.01	0.01	0.01	0.01	0.01	0.01	0.01	0.01	0.01	0.01	0.01	0.01	0.01	0.01	0.01
⋮	⋮	⋮	⋮	⋮	⋮	⋮	⋮	⋮	⋮	⋮	⋮	⋮	⋮	⋮	⋮	⋮
41	0.01	0.01	0.01	0.01	0.60	0.80	0.60	0.01	0.01	0.01	0.01	0.01	0.01	0.01	0.01	0.01
42	0.01	0.01	0.01	0.60	0.70	0.60	0.01	0.01	0.01	0.01	0.01	0.01	0.01	0.01	0.01	0.01
43	0.01	0.01	0.01	0.70	0.01	0.01	0.01	0.01	0.01	0.01	0.01	0.01	0.01	0.01	0.01	0.01
44	0.01	0.01	0.50	0.01	0.01	0.01	0.01	0.01	0.01	0.01	0.01	0.01	0.01	0.01	0.01	0.01
45	0.01	0.01	0.01	0.01	0.01	0.01	0.01	0.01	0.01	0.01	0.01	0.01	0.01	0.01	0.01	0.01
46	0.01	0.01	0.01	0.01	0.01	0.01	0.01	0.01	0.01	0.01	0.01	0.01	0.01	0.01	0.01	0.01
47	0.01	0.01	0.01	0.01	0.01	0.01	0.01	0.01	0.01	0.01	0.01	0.01	0.01	0.01	0.01	0.01

48	0.01	0.01	0.01	0.01	0.01	0.01	0.01	0.01	0.01	0.01	0.01	0.01	0.01	0.01	0.01	0.01
49	0.01	0.01	0.01	0.01	0.01	0.01	0.01	0.01	0.01	0.01	0.01	0.01	0.01	0.01	0.01	0.01
50	0.01	0.01	0.01	0.01	0.01	0.01	0.01	0.01	0.01	0.01	0.01	0.01	0.01	0.01	0.01	0.01
51	0.01	0.01	0.01	0.50	0.80	0.90	0.80	0.50	0.01	0.01	0.01	0.01	0.01	0.01	0.01	0.01
52	0.01	0.01	0.01	0.70	0.90	0.70	0.01	0.01	0.01	0.01	0.01	0.01	0.01	0.01	0.01	0.01
53	0.01	0.01	0.70	1.00	0.70	0.01	0.01	0.01	0.01	0.01	0.01	0.01	0.01	0.01	0.01	0.01
54	0.01	0.50	1.00	0.50	0.01	0.01	0.01	0.01	0.01	0.01	0.01	0.01	0.01	0.01	0.01	0.01
55	0.01	1.00	0.01	0.01	0.01	0.01	0.01	0.01	0.01	0.01	0.01	0.01	0.01	0.01	0.01	0.01
56	1.00	0.01	0.01	0.01	0.01	0.01	0.01	0.01	0.01	0.01	0.01	0.01	0.01	0.01	0.01	0.01
57	0.01	0.01	0.01	0.01	0.01	0.01	0.01	0.01	0.01	0.01	0.01	0.01	0.01	0.01	0.01	0.01
58	0.01	0.01	0.01	0.01	0.01	0.01	0.01	0.01	0.01	0.01	0.01	0.01	0.01	0.01	0.01	0.01
59	0.01	0.01	0.01	0.01	0.01	0.01	0.01	0.01	0.01	0.01	0.01	0.01	0.01	0.01	0.01	0.01
60	0.01	0.01	0.01	0.01	0.01	0.01	0.01	0.01	0.01	0.01	0.01	0.01	0.01	0.01	0.01	0.01
61	0.01	0.01	0.01	0.01	0.60	0.80	0.60	0.01	0.01	0.01	0.01	0.01	0.01	0.01	0.01	0.01
62	0.01	0.01	0.01	0.60	0.70	0.60	0.01	0.01	0.01	0.01	0.01	0.01	0.01	0.01	0.01	0.01
63	0.01	0.01	0.01	0.70	0.01	0.01	0.01	0.01	0.01	0.01	0.01	0.01	0.01	0.01	0.01	0.01
64	0.01	0.01	0.50	0.01	0.01	0.01	0.01	0.01	0.01	0.01	0.01	0.01	0.01	0.01	0.01	0.01
65	0.01	0.01	0.01	0.01	0.01	0.01	0.01	0.01	0.01	0.01	0.01	0.01	0.01	0.01	0.01	0.01
66	0.01	0.01	0.01	0.01	0.01	0.01	0.01	0.01	0.01	0.01	0.01	0.01	0.01	0.01	0.01	0.01
67	0.01	0.01	0.01	0.01	0.01	0.01	0.01	0.01	0.01	0.01	0.01	0.01	0.01	0.01	0.01	0.01
68	0.01	0.01	0.01	0.01	0.01	0.01	0.01	0.01	0.01	0.01	0.01	0.01	0.01	0.01	0.01	0.01
69	0.01	0.01	0.01	0.01	0.01	0.01	0.01	0.01	0.01	0.01	0.01	0.01	0.01	0.01	0.01	0.01
70	0.01	0.01	0.01	0.01	0.01	0.01	0.01	0.01	0.01	0.01	0.01	0.01	0.01	0.01	0.01	0.01
71	0.01	0.01	0.01	0.01	0.01	0.50	0.01	0.01	0.01	0.01	0.01	0.01	0.01	0.01	0.01	0.01
72	0.01	0.01	0.01	0.01	0.01	0.01	0.01	0.01	0.01	0.01	0.01	0.01	0.01	0.01	0.01	0.01
⋮	⋮	⋮	⋮	⋮	⋮	⋮	⋮	⋮	⋮	⋮	⋮	⋮	⋮	⋮	⋮	⋮
100	0.01	0.01	0.01	0.01	0.01	0.01	0.01	0.01	0.01	0.01	0.01	0.01	0.01	0.01	0.01	0.01

Table 44. $P_{l,t}^{63}$ values for sensor in cell 63

$P_{l,t}^{63}$	Attack time scale, t time steps since the occurrence of the chemical attack															
Location	0	1	2	3	4	5	6	7	8	9	10	11	12	13	14	15
1	0.01	0.01	0.01	0.01	0.01	0.01	0.01	0.01	0.01	0.01	0.01	0.01	0.01	0.01	0.01	0.01
⋮	⋮	⋮	⋮	⋮	⋮	⋮	⋮	⋮	⋮	⋮	⋮	⋮	⋮	⋮	⋮	⋮
⋮	⋮	⋮	⋮	⋮	⋮	⋮	⋮	⋮	⋮	⋮	⋮	⋮	⋮	⋮	⋮	⋮
51	0.01	0.01	0.50	0.01	0.01	0.01	0.01	0.01	0.01	0.01	0.01	0.01	0.01	0.01	0.01	0.01
52	0.01	0.01	0.01	0.01	0.01	0.01	0.01	0.01	0.01	0.01	0.01	0.01	0.01	0.01	0.01	0.01
53	0.01	0.01	0.01	0.01	0.01	0.01	0.01	0.01	0.01	0.01	0.01	0.01	0.01	0.01	0.01	0.01
54	0.01	0.01	0.01	0.01	0.01	0.01	0.01	0.01	0.01	0.01	0.01	0.01	0.01	0.01	0.01	0.01
55	0.01	0.01	0.01	0.01	0.01	0.01	0.01	0.01	0.01	0.01	0.01	0.01	0.01	0.01	0.01	0.01
56	0.01	0.01	0.01	0.01	0.01	0.01	0.01	0.01	0.01	0.01	0.01	0.01	0.01	0.01	0.01	0.01
57	0.01	0.01	0.01	0.01	0.01	0.01	0.01	0.01	0.01	0.01	0.01	0.01	0.01	0.01	0.01	0.01
58	0.01	0.01	0.01	0.01	0.01	0.01	0.01	0.01	0.01	0.01	0.01	0.01	0.01	0.01	0.01	0.01
59	0.01	0.01	0.01	0.01	0.01	0.01	0.01	0.01	0.01	0.01	0.01	0.01	0.01	0.01	0.01	0.01
60	0.01	0.01	0.01	0.01	0.01	0.01	0.01	0.01	0.01	0.01	0.01	0.01	0.01	0.01	0.01	0.01
61	0.01	0.50	1.00	0.50	0.01	0.01	0.01	0.01	0.01	0.01	0.01	0.01	0.01	0.01	0.01	0.01
62	0.01	1.00	0.01	0.01	0.01	0.01	0.01	0.01	0.01	0.01	0.01	0.01	0.01	0.01	0.01	0.01
63	1.00	0.01	0.01	0.01	0.01	0.01	0.01	0.01	0.01	0.01	0.01	0.01	0.01	0.01	0.01	0.01
64	0.01	0.01	0.01	0.01	0.01	0.01	0.01	0.01	0.01	0.01	0.01	0.01	0.01	0.01	0.01	0.01
65	0.01	0.01	0.01	0.01	0.01	0.01	0.01	0.01	0.01	0.01	0.01	0.01	0.01	0.01	0.01	0.01
66	0.01	0.01	0.01	0.01	0.01	0.01	0.01	0.01	0.01	0.01	0.01	0.01	0.01	0.01	0.01	0.01
67	0.01	0.01	0.01	0.01	0.01	0.01	0.01	0.01	0.01	0.01	0.01	0.01	0.01	0.01	0.01	0.01
68	0.01	0.01	0.01	0.01	0.01	0.01	0.01	0.01	0.01	0.01	0.01	0.01	0.01	0.01	0.01	0.01
69	0.01	0.01	0.01	0.01	0.01	0.01	0.01	0.01	0.01	0.01	0.01	0.01	0.01	0.01	0.01	0.01
70	0.01	0.01	0.01	0.01	0.01	0.01	0.01	0.01	0.01	0.01	0.01	0.01	0.01	0.01	0.01	0.01
71	0.01	0.01	0.50	0.01	0.01	0.01	0.01	0.01	0.01	0.01	0.01	0.01	0.01	0.01	0.01	0.01
72	0.01	0.01	0.01	0.01	0.01	0.01	0.01	0.01	0.01	0.01	0.01	0.01	0.01	0.01	0.01	0.01
⋮	⋮	⋮	⋮	⋮	⋮	⋮	⋮	⋮	⋮	⋮	⋮	⋮	⋮	⋮	⋮	⋮
⋮	⋮	⋮	⋮	⋮	⋮	⋮	⋮	⋮	⋮	⋮	⋮	⋮	⋮	⋮	⋮	⋮
100	0.01	0.01	0.01	0.01	0.01	0.01	0.01	0.01	0.01	0.01	0.01	0.01	0.01	0.01	0.01	0.01

<p align="center">Table 45. $P_{l,t}^{68}$ values for sensor in cell 68</p>

$P_{l,t}^{68}$	Attack time scale, t time steps since the occurrence of the chemical attack															
Location	0	1	2	3	4	5	6	7	8	9	10	11	12	13	14	15
1	0.01	0.01	0.01	0.01	0.01	0.01	0.01	0.01	0.01	0.01	0.01	0.01	0.01	0.01	0.01	0.01
⋮	⋮	⋮	⋮	⋮	⋮	⋮	⋮	⋮	⋮	⋮	⋮	⋮	⋮	⋮	⋮	⋮
⋮	⋮	⋮	⋮	⋮	⋮	⋮	⋮	⋮	⋮	⋮	⋮	⋮	⋮	⋮	⋮	⋮
41	0.01	0.01	0.01	0.01	0.01	0.01	0.50	0.60	0.50	0.01	0.01	0.01	0.01	0.01	0.01	0.01
42	0.01	0.01	0.01	0.01	0.01	0.50	0.50	0.50	0.01	0.01	0.01	0.01	0.01	0.01	0.01	0.01
43	0.01	0.01	0.01	0.01	0.01	0.50	0.01	0.01	0.01	0.01	0.01	0.01	0.01	0.01	0.01	0.01
44	0.01	0.01	0.01	0.01	0.01	0.01	0.01	0.01	0.01	0.01	0.01	0.01	0.01	0.01	0.01	0.01
45	0.01	0.01	0.01	0.01	0.01	0.01	0.01	0.01	0.01	0.01	0.01	0.01	0.01	0.01	0.01	0.01
46	0.01	0.01	0.01	0.01	0.01	0.01	0.01	0.01	0.01	0.01	0.01	0.01	0.01	0.01	0.01	0.01
47	0.01	0.01	0.01	0.01	0.01	0.01	0.01	0.01	0.01	0.01	0.01	0.01	0.01	0.01	0.01	0.01
48	0.01	0.01	0.01	0.01	0.01	0.01	0.01	0.01	0.01	0.01	0.01	0.01	0.01	0.01	0.01	0.01
49	0.01	0.01	0.01	0.01	0.01	0.01	0.01	0.01	0.01	0.01	0.01	0.01	0.01	0.01	0.01	0.01
50	0.01	0.01	0.01	0.01	0.01	0.01	0.01	0.01	0.01	0.01	0.01	0.01	0.01	0.01	0.01	0.01
51	0.01	0.01	0.01	0.01	0.01	0.50	0.70	0.80	0.70	0.50	0.01	0.01	0.01	0.01	0.01	0.01
52	0.01	0.01	0.01	0.01	0.50	0.70	0.80	0.70	0.50	0.01	0.01	0.01	0.01	0.01	0.01	0.01
53	0.01	0.01	0.01	0.01	0.60	0.80	0.60	0.01	0.01	0.01	0.01	0.01	0.01	0.01	0.01	0.01
54	0.01	0.01	0.01	0.60	0.70	0.60	0.01	0.01	0.01	0.01	0.01	0.01	0.01	0.01	0.01	0.01
55	0.01	0.01	0.01	0.70	0.01	0.01	0.01	0.01	0.01	0.01	0.01	0.01	0.01	0.01	0.01	0.01
56	0.01	0.01	0.50	0.01	0.01	0.01	0.01	0.01	0.01	0.01	0.01	0.01	0.01	0.01	0.01	0.01
57	0.01	0.01	0.01	0.01	0.01	0.01	0.01	0.01	0.01	0.01	0.01	0.01	0.01	0.01	0.01	0.01
58	0.01	0.01	0.01	0.01	0.01	0.01	0.01	0.01	0.01	0.01	0.01	0.01	0.01	0.01	0.01	0.01
59	0.01	0.01	0.01	0.01	0.01	0.01	0.01	0.01	0.01	0.01	0.01	0.01	0.01	0.01	0.01	0.01
60	0.01	0.01	0.01	0.01	0.01	0.01	0.01	0.01	0.01	0.01	0.01	0.01	0.01	0.01	0.01	0.01
61	0.01	0.01	0.01	0.01	0.01	0.60	0.80	0.80	0.80	0.60	0.01	0.01	0.01	0.01	0.01	0.01
62	0.01	0.01	0.01	0.01	0.50	0.80	0.80	0.80	0.50	0.01	0.01	0.01	0.01	0.01	0.01	0.01
63	0.01	0.01	0.01	0.50	0.80	0.90	0.80	0.50	0.01	0.01	0.01	0.01	0.01	0.01	0.01	0.01
64	0.01	0.01	0.01	0.70	0.90	0.70	0.01	0.01	0.01	0.01	0.01	0.01	0.01	0.01	0.01	0.01
65	0.01	0.01	0.70	1.00	0.70	0.01	0.01	0.01	0.01	0.01	0.01	0.01	0.01	0.01	0.01	0.01
66	0.01	0.50	1.00	0.50	0.01	0.01	0.01	0.01	0.01	0.01	0.01	0.01	0.01	0.01	0.01	0.01
67	0.01	1.00	0.01	0.01	0.01	0.01	0.01	0.01	0.01	0.01	0.01	0.01	0.01	0.01	0.01	0.01
68	1.00	0.01	0.01	0.01	0.01	0.01	0.01	0.01	0.01	0.01	0.01	0.01	0.01	0.01	0.01	0.01
69	0.01	0.01	0.01	0.01	0.01	0.01	0.01	0.01	0.01	0.01	0.01	0.01	0.01	0.01	0.01	0.01
70	0.01	0.01	0.01	0.01	0.01	0.01	0.01	0.01	0.01	0.01	0.01	0.01	0.01	0.01	0.01	0.01
71	0.01	0.01	0.01	0.01	0.01	0.50	0.70	0.80	0.70	0.50	0.01	0.01	0.01	0.01	0.01	0.01

Location																
72	0.01	0.01	0.01	0.01	0.50	0.70	0.80	0.70	0.50	0.01	0.01	0.01	0.01	0.01	0.01	0.01
73	0.01	0.01	0.01	0.01	0.60	0.80	0.60	0.01	0.01	0.01	0.01	0.01	0.01	0.01	0.01	0.01
74	0.01	0.01	0.01	0.60	0.70	0.60	0.01	0.01	0.01	0.01	0.01	0.01	0.01	0.01	0.01	0.01
75	0.01	0.01	0.01	0.70	0.01	0.01	0.01	0.01	0.01	0.01	0.01	0.01	0.01	0.01	0.01	0.01
76	0.01	0.01	0.50	0.01	0.01	0.01	0.01	0.01	0.01	0.01	0.01	0.01	0.01	0.01	0.01	0.01
77	0.01	0.01	0.01	0.01	0.01	0.01	0.01	0.01	0.01	0.01	0.01	0.01	0.01	0.01	0.01	0.01
78	0.01	0.01	0.01	0.01	0.01	0.01	0.01	0.01	0.01	0.01	0.01	0.01	0.01	0.01	0.01	0.01
79	0.01	0.01	0.01	0.01	0.01	0.01	0.01	0.01	0.01	0.01	0.01	0.01	0.01	0.01	0.01	0.01
80	0.01	0.01	0.01	0.01	0.01	0.01	0.01	0.01	0.01	0.01	0.01	0.01	0.01	0.01	0.01	0.01
81	0.01	0.01	0.01	0.01	0.01	0.01	0.50	0.60	0.50	0.01	0.01	0.01	0.01	0.01	0.01	0.01
82	0.01	0.01	0.01	0.01	0.01	0.50	0.50	0.50	0.01	0.01	0.01	0.01	0.01	0.01	0.01	0.01
83	0.01	0.01	0.01	0.01	0.01	0.50	0.01	0.01	0.01	0.01	0.01	0.01	0.01	0.01	0.01	0.01
84	0.01	0.01	0.01	0.01	0.01	0.01	0.01	0.01	0.01	0.01	0.01	0.01	0.01	0.01	0.01	0.01
⋮	⋮	⋮	⋮	⋮	⋮	⋮	⋮	⋮	⋮	⋮	⋮	⋮	⋮	⋮	⋮	⋮
⋮	⋮	⋮	⋮	⋮	⋮	⋮	⋮	⋮	⋮	⋮	⋮	⋮	⋮	⋮	⋮	⋮
100	0.01	0.01	0.01	0.01	0.01	0.01	0.01	0.01	0.01	0.01	0.01	0.01	0.01	0.01	0.01	0.01

Table 46. $P_{l,t}^{84}$ values for sensor in cell 84

$P_{l,t}^{83}$	Attack time scale, t time steps since the occurrence of the chemical attack															
Location	0	1	2	3	4	5	6	7	8	9	10	11	12	13	14	15
1	0.01	0.01	0.01	0.01	0.01	0.01	0.01	0.01	0.01	0.01	0.01	0.01	0.01	0.01	0.01	0.01
⋮	⋮	⋮	⋮	⋮	⋮	⋮	⋮	⋮	⋮	⋮	⋮	⋮	⋮	⋮	⋮	⋮
⋮	⋮	⋮	⋮	⋮	⋮	⋮	⋮	⋮	⋮	⋮	⋮	⋮	⋮	⋮	⋮	⋮
71	0.01	0.01	0.01	0.70	0.01	0.01	0.01	0.01	0.01	0.01	0.01	0.01	0.01	0.01	0.01	0.01
72	0.01	0.01	0.50	0.01	0.01	0.01	0.01	0.01	0.01	0.01	0.01	0.01	0.01	0.01	0.01	0.01
73	0.01	0.01	0.01	0.01	0.01	0.01	0.01	0.01	0.01	0.01	0.01	0.01	0.01	0.01	0.01	0.01
74	0.01	0.01	0.01	0.01	0.01	0.01	0.01	0.01	0.01	0.01	0.01	0.01	0.01	0.01	0.01	0.01
75	0.01	0.01	0.01	0.01	0.01	0.01	0.01	0.01	0.01	0.01	0.01	0.01	0.01	0.01	0.01	0.01
76	0.01	0.01	0.01	0.01	0.01	0.01	0.01	0.01	0.01	0.01	0.01	0.01	0.01	0.01	0.01	0.01
77	0.01	0.01	0.01	0.01	0.01	0.01	0.01	0.01	0.01	0.01	0.01	0.01	0.01	0.01	0.01	0.01
78	0.01	0.01	0.01	0.01	0.01	0.01	0.01	0.01	0.01	0.01	0.01	0.01	0.01	0.01	0.01	0.01
79	0.01	0.01	0.01	0.01	0.01	0.01	0.01	0.01	0.01	0.01	0.01	0.01	0.01	0.01	0.01	0.01
80	0.01	0.01	0.01	0.01	0.01	0.01	0.01	0.01	0.01	0.01	0.01	0.01	0.01	0.01	0.01	0.01
81	0.01	0.01	0.70	1.00	0.70	0.01	0.01	0.01	0.01	0.01	0.01	0.01	0.01	0.01	0.01	0.01
82	0.01	0.50	1.00	0.50	0.01	0.01	0.01	0.01	0.01	0.01	0.01	0.01	0.01	0.01	0.01	0.01
83	0.01	1.00	0.01	0.01	0.01	0.01	0.01	0.01	0.01	0.01	0.01	0.01	0.01	0.01	0.01	0.01
84	1.00	0.01	0.01	0.01	0.01	0.01	0.01	0.01	0.01	0.01	0.01	0.01	0.01	0.01	0.01	0.01

85	0.01	0.01	0.01	0.01	0.01	0.01	0.01	0.01	0.01	0.01	0.01	0.01	0.01	0.01	0.01	0.01
86	0.01	0.01	0.01	0.01	0.01	0.01	0.01	0.01	0.01	0.01	0.01	0.01	0.01	0.01	0.01	0.01
87	0.01	0.01	0.01	0.01	0.01	0.01	0.01	0.01	0.01	0.01	0.01	0.01	0.01	0.01	0.01	0.01
88	0.01	0.01	0.01	0.01	0.01	0.01	0.01	0.01	0.01	0.01	0.01	0.01	0.01	0.01	0.01	0.01
89	0.01	0.01	0.01	0.01	0.01	0.01	0.01	0.01	0.01	0.01	0.01	0.01	0.01	0.01	0.01	0.01
90	0.01	0.01	0.01	0.01	0.01	0.01	0.01	0.01	0.01	0.01	0.01	0.01	0.01	0.01	0.01	0.01
91	0.01	0.01	0.01	0.70	0.01	0.01	0.01	0.01	0.01	0.01	0.01	0.01	0.01	0.01	0.01	0.01
92	0.01	0.01	0.50	0.01	0.01	0.01	0.01	0.01	0.01	0.01	0.01	0.01	0.01	0.01	0.01	0.01
93	0.01	0.01	0.01	0.01	0.01	0.01	0.01	0.01	0.01	0.01	0.01	0.01	0.01	0.01	0.01	0.01
⋮	⋮	⋮	⋮	⋮	⋮	⋮	⋮	⋮	⋮	⋮	⋮	⋮	⋮	⋮	⋮	⋮
100	0.01	0.01	0.01	0.01	0.01	0.01	0.01	0.01	0.01	0.01	0.01	0.01	0.01	0.01	0.01	0.01

Table 47. $P_{l,t}^{87}$ values for sensor in cell 87

$P_{l,t}^{87}$	Attack time scale, t time steps since the occurrence of the chemical attack															
Location	0	1	2	3	4	5	6	7	8	9	10	11	12	13	14	15
1	0.01	0.01	0.01	0.01	0.01	0.01	0.01	0.01	0.01	0.01	0.01	0.01	0.01	0.01	0.01	0.01
⋮	⋮	⋮	⋮	⋮	⋮	⋮	⋮	⋮	⋮	⋮	⋮	⋮	⋮	⋮	⋮	⋮
⋮	⋮	⋮	⋮	⋮	⋮	⋮	⋮	⋮	⋮	⋮	⋮	⋮	⋮	⋮	⋮	⋮
61	0.01	0.01	0.01	0.01	0.01	0.50	0.50	0.50	0.01	0.01	0.01	0.01	0.01	0.01	0.01	0.01
62	0.01	0.01	0.01	0.01	0.01	0.50	0.01	0.01	0.01	0.01	0.01	0.01	0.01	0.01	0.01	0.01
63	0.01	0.01	0.01	0.01	0.01	0.01	0.01	0.01	0.01	0.01	0.01	0.01	0.01	0.01	0.01	0.01
64	0.01	0.01	0.01	0.01	0.01	0.01	0.01	0.01	0.01	0.01	0.01	0.01	0.01	0.01	0.01	0.01
65	0.01	0.01	0.01	0.01	0.01	0.01	0.01	0.01	0.01	0.01	0.01	0.01	0.01	0.01	0.01	0.01
66	0.01	0.01	0.01	0.01	0.01	0.01	0.01	0.01	0.01	0.01	0.01	0.01	0.01	0.01	0.01	0.01
67	0.01	0.01	0.01	0.01	0.01	0.01	0.01	0.01	0.01	0.01	0.01	0.01	0.01	0.01	0.01	0.01
68	0.01	0.01	0.01	0.01	0.01	0.01	0.01	0.01	0.01	0.01	0.01	0.01	0.01	0.01	0.01	0.01
69	0.01	0.01	0.01	0.01	0.01	0.01	0.01	0.01	0.01	0.01	0.01	0.01	0.01	0.01	0.01	0.01
70	0.01	0.01	0.01	0.01	0.01	0.01	0.01	0.01	0.01	0.01	0.01	0.01	0.01	0.01	0.01	0.01
71	0.01	0.01	0.01	0.01	0.50	0.70	0.80	0.70	0.50	0.01	0.01	0.01	0.01	0.01	0.01	0.01
72	0.01	0.01	0.01	0.01	0.60	0.80	0.60	0.01	0.01	0.01	0.01	0.01	0.01	0.01	0.01	0.01
73	0.01	0.01	0.01	0.60	0.70	0.60	0.01	0.01	0.01	0.01	0.01	0.01	0.01	0.01	0.01	0.01
74	0.01	0.01	0.01	0.70	0.01	0.01	0.01	0.01	0.01	0.01	0.01	0.01	0.01	0.01	0.01	0.01
75	0.01	0.01	0.50	0.01	0.01	0.01	0.01	0.01	0.01	0.01	0.01	0.01	0.01	0.01	0.01	0.01
76	0.01	0.01	0.01	0.01	0.01	0.01	0.01	0.01	0.01	0.01	0.01	0.01	0.01	0.01	0.01	0.01
77	0.01	0.01	0.01	0.01	0.01	0.01	0.01	0.01	0.01	0.01	0.01	0.01	0.01	0.01	0.01	0.01
78	0.01	0.01	0.01	0.01	0.01	0.01	0.01	0.01	0.01	0.01	0.01	0.01	0.01	0.01	0.01	0.01
79	0.01	0.01	0.01	0.01	0.01	0.01	0.01	0.01	0.01	0.01	0.01	0.01	0.01	0.01	0.01	0.01

80	0.01	0.01	0.01	0.01	0.01	0.01	0.01	0.01	0.01	0.01	0.01	0.01	0.01	0.01	0.01	0.01
81	0.01	0.01	0.01	0.01	0.50	0.80	0.80	0.80	0.50	0.01	0.01	0.01	0.01	0.01	0.01	0.01
82	0.01	0.01	0.01	0.50	0.80	0.90	0.80	0.50	0.01	0.01	0.01	0.01	0.01	0.01	0.01	0.01
83	0.01	0.01	0.01	0.70	0.90	0.70	0.01	0.01	0.01	0.01	0.01	0.01	0.01	0.01	0.01	0.01
84	0.01	0.01	0.70	1.00	0.70	0.01	0.01	0.01	0.01	0.01	0.01	0.01	0.01	0.01	0.01	0.01
85	0.01	0.50	1.00	0.50	0.01	0.01	0.01	0.01	0.01	0.01	0.01	0.01	0.01	0.01	0.01	0.01
86	0.01	1.00	0.01	0.01	0.01	0.01	0.01	0.01	0.01	0.01	0.01	0.01	0.01	0.01	0.01	0.01
87	1.00	0.01	0.01	0.01	0.01	0.01	0.01	0.01	0.01	0.01	0.01	0.01	0.01	0.01	0.01	0.01
88	0.01	0.01	0.01	0.01	0.01	0.01	0.01	0.01	0.01	0.01	0.01	0.01	0.01	0.01	0.01	0.01
89	0.01	0.01	0.01	0.01	0.01	0.01	0.01	0.01	0.01	0.01	0.01	0.01	0.01	0.01	0.01	0.01
90	0.01	0.01	0.01	0.01	0.01	0.01	0.01	0.01	0.01	0.01	0.01	0.01	0.01	0.01	0.01	0.01
91	0.01	0.01	0.01	0.01	0.50	0.70	0.80	0.70	0.50	0.01	0.01	0.01	0.01	0.01	0.01	0.01
92	0.01	0.01	0.01	0.01	0.60	0.80	0.60	0.01	0.01	0.01	0.01	0.01	0.01	0.01	0.01	0.01
93	0.01	0.01	0.01	0.60	0.70	0.60	0.01	0.01	0.01	0.01	0.01	0.01	0.01	0.01	0.01	0.01
94	0.01	0.01	0.01	0.70	0.01	0.01	0.01	0.01	0.01	0.01	0.01	0.01	0.01	0.01	0.01	0.01
95	0.01	0.01	0.50	0.01	0.01	0.01	0.01	0.01	0.01	0.01	0.01	0.01	0.01	0.01	0.01	0.01
96	0.01	0.01	0.01	0.01	0.01	0.01	0.01	0.01	0.01	0.01	0.01	0.01	0.01	0.01	0.01	0.01
97	0.01	0.01	0.01	0.01	0.01	0.01	0.01	0.01	0.01	0.01	0.01	0.01	0.01	0.01	0.01	0.01
98	0.01	0.01	0.01	0.01	0.01	0.01	0.01	0.01	0.01	0.01	0.01	0.01	0.01	0.01	0.01	0.01
99	0.01	0.01	0.01	0.01	0.01	0.01	0.01	0.01	0.01	0.01	0.01	0.01	0.01	0.01	0.01	0.01
100	0.01	0.01	0.01	0.01	0.01	0.01	0.01	0.01	0.01	0.01	0.01	0.01	0.01	0.01	0.01	0.01

Table 48. $P_{l,t}^{91}$ values for sensor in cell 91

$P_{l,t}^{91}$	Attack time scale, t time steps since the occurrence of the chemical attack															
Location	0	1	2	3	4	5	6	7	8	9	10	11	12	13	14	15
1	0.01	0.01	0.01	0.01	0.01	0.01	0.01	0.01	0.01	0.01	0.01	0.01	0.01	0.01	0.01	0.01
⋮	⋮	⋮	⋮	⋮	⋮	⋮	⋮	⋮	⋮	⋮	⋮	⋮	⋮	⋮	⋮	⋮
⋮	⋮	⋮	⋮	⋮	⋮	⋮	⋮	⋮	⋮	⋮	⋮	⋮	⋮	⋮	⋮	⋮
91	1.00	0.01	0.01	0.01	0.01	0.01	0.01	0.01	0.01	0.01	0.01	0.01	0.01	0.01	0.01	0.01
92	0.01	0.01	0.01	0.01	0.01	0.01	0.01	0.01	0.01	0.01	0.01	0.01	0.01	0.01	0.01	0.01
⋮	⋮	⋮	⋮	⋮	⋮	⋮	⋮	⋮	⋮	⋮	⋮	⋮	⋮	⋮	⋮	⋮
⋮	⋮	⋮	⋮	⋮	⋮	⋮	⋮	⋮	⋮	⋮	⋮	⋮	⋮	⋮	⋮	⋮
100	0.01	0.01	0.01	0.01	0.01	0.01	0.01	0.01	0.01	0.01	0.01	0.01	0.01	0.01	0.01	0.01

Table 49. $P_{l,t}^{100}$ values for sensor in cell 100

$P_{l,t}^{100}$	Attack time scale, t time steps since the occurrence of the chemical attack															
Location	0	1	2	3	4	5	6	7	8	9	10	11	12	13	14	15
1	0.01	0.01	0.01	0.01	0.01	0.01	0.01	0.01	0.01	0.01	0.01	0.01	0.01	0.01	0.01	0.01
⋮	⋮	⋮	⋮	⋮	⋮	⋮	⋮	⋮	⋮	⋮	⋮	⋮	⋮	⋮	⋮	⋮
61	0.01	0.01	0.01	0.01	0.01	0.01	0.01	0.01	0.01	0.50	0.01	0.01	0.01	0.01	0.01	0.01
62	0.01	0.01	0.01	0.01	0.01	0.01	0.01	0.01	0.01	0.01	0.01	0.01	0.01	0.01	0.01	0.01
⋮	⋮	⋮	⋮	⋮	⋮	⋮	⋮	⋮	⋮	⋮	⋮	⋮	⋮	⋮	⋮	⋮
71	0.01	0.01	0.01	0.01	0.01	0.01	0.01	0.50	0.60	0.60	0.60	0.50	0.01	0.01	0.01	0.01
72	0.01	0.01	0.01	0.01	0.01	0.01	0.50	0.50	0.60	0.50	0.50	0.01	0.01	0.01	0.01	0.01
73	0.01	0.01	0.01	0.01	0.01	0.01	0.50	0.60	0.50	0.01	0.01	0.01	0.01	0.01	0.01	0.01
74	0.01	0.01	0.01	0.01	0.01	0.50	0.50	0.50	0.01	0.01	0.01	0.01	0.01	0.01	0.01	0.01
75	0.01	0.01	0.01	0.01	0.01	0.50	0.01	0.01	0.01	0.01	0.01	0.01	0.01	0.01	0.01	0.01
76	0.01	0.01	0.01	0.01	0.01	0.01	0.01	0.01	0.01	0.01	0.01	0.01	0.01	0.01	0.01	0.01
77	0.01	0.01	0.01	0.01	0.01	0.01	0.01	0.01	0.01	0.01	0.01	0.01	0.01	0.01	0.01	0.01
78	0.01	0.01	0.01	0.01	0.01	0.01	0.01	0.01	0.01	0.01	0.01	0.01	0.01	0.01	0.01	0.01
79	0.01	0.01	0.01	0.01	0.01	0.01	0.01	0.01	0.01	0.01	0.01	0.01	0.01	0.01	0.01	0.01
80	0.01	0.01	0.01	0.01	0.01	0.01	0.01	0.01	0.01	0.01	0.01	0.01	0.01	0.01	0.01	0.01
81	0.01	0.01	0.01	0.01	0.01	0.01	0.01	0.60	0.70	0.70	0.70	0.60	0.01	0.01	0.01	0.01
82	0.01	0.01	0.01	0.01	0.01	0.01	0.50	0.70	0.70	0.70	0.50	0.01	0.01	0.01	0.01	0.01
83	0.01	0.01	0.01	0.01	0.01	0.50	0.70	0.80	0.70	0.50	0.01	0.01	0.01	0.01	0.01	0.01
84	0.01	0.01	0.01	0.01	0.50	0.70	0.80	0.70	0.50	0.01	0.01	0.01	0.01	0.01	0.01	0.01
85	0.01	0.01	0.01	0.01	0.60	0.80	0.60	0.01	0.01	0.01	0.01	0.01	0.01	0.01	0.01	0.01
86	0.01	0.01	0.01	0.60	0.70	0.60	0.01	0.01	0.01	0.01	0.01	0.01	0.01	0.01	0.01	0.01
87	0.01	0.01	0.01	0.70	0.01	0.01	0.01	0.01	0.01	0.01	0.01	0.01	0.01	0.01	0.01	0.01
88	0.01	0.01	0.50	0.01	0.01	0.01	0.01	0.01	0.01	0.01	0.01	0.01	0.01	0.01	0.01	0.01
89	0.01	0.01	0.01	0.01	0.01	0.01	0.01	0.01	0.01	0.01	0.01	0.01	0.01	0.01	0.01	0.01
90	0.01	0.01	0.01	0.01	0.01	0.01	0.01	0.01	0.01	0.01	0.01	0.01	0.01	0.01	0.01	0.01
91	0.01	0.01	0.01	0.01	0.01	0.01	0.50	0.60	0.70	0.80	0.70	0.60	0.50	0.01	0.01	0.01
92	0.01	0.01	0.01	0.01	0.01	0.01	0.60	0.70	0.80	0.70	0.60	0.01	0.01	0.01	0.01	0.01
93	0.01	0.01	0.01	0.01	0.01	0.60	0.80	0.80	0.80	0.60	0.01	0.01	0.01	0.01	0.01	0.01
94	0.01	0.01	0.01	0.01	0.50	0.80	0.80	0.80	0.50	0.01	0.01	0.01	0.01	0.01	0.01	0.01
95	0.01	0.01	0.01	0.50	0.80	0.90	0.80	0.50	0.01	0.01	0.01	0.01	0.01	0.01	0.01	0.01
96	0.01	0.01	0.01	0.70	0.90	0.70	0.01	0.01	0.01	0.01	0.01	0.01	0.01	0.01	0.01	0.01
97	0.01	0.01	0.70	1.00	0.70	0.01	0.01	0.01	0.01	0.01	0.01	0.01	0.01	0.01	0.01	0.01
98	0.01	0.50	1.00	0.50	0.01	0.01	0.01	0.01	0.01	0.01	0.01	0.01	0.01	0.01	0.01	0.01
99	0.01	1.00	0.01	0.01	0.01	0.01	0.01	0.01	0.01	0.01	0.01	0.01	0.01	0.01	0.01	0.01
100	1.00	0.01	0.01	0.01	0.01	0.01	0.01	0.01	0.01	0.01	0.01	0.01	0.01	0.01	0.01	0.01

LIST OF REFERENCES

Bagtzoglou, A.C., and Baun, S.A. (2004). An efficient inverse method for real-time atmospheric contamination. Proceedings from: *Inverse Problems, Design and Optimization Symposium 2004.* Rio de Janeiro, Brazil.

Chan, R., and Yee, E. (1997). A simple model for the probability density function of concentration flunctuations in atmospheric plumes. *Journal of Atmospheric Environment*, 31, 991-1002.

Crowl, D.A., and Louvar, J.F. (2002). *Chemical process safety: Fundamental with applications* (2nd ed.). Upper Saddle River, NJ: Prentice Hall.

Fry, R., Sykes, R.I., and Koble. R. (2005). Chemical/Biological Source Characterization. Proceedings from: *Science and Technology for Chem-Bio Information Systems 2005.* Texas, USA.

Liu, H.F. (1997). *Environmental engineers's handbook* (2nd ed.). Boca Raton, Fla: Lewis Publishers.

Montgomery, D.C. (2009). *Design and analysis of experiments* (7th ed.). New York: John Wiley and Sons.

Myers, R.H., Montgomery, D.C. and Vining, G.G (2002). *Generalized linear models: With applications in engineering and the sciences*. New York: John Wiley and Sons.

Proengin. (2009). *AP4C* chemical detection. Retrieved: June 12, 2009, from Proengin Web site: http://www.proengin.com/images/pdf/ proengin%20fiche%20ap4c.pdf

Rajah, I. (1995, July 20). Emergency prepardness contigency plans for hospitals. Retrieved: November 10, 2009, from Ministry of Health Singapore: http://www.moh.gov.sg/mohcorp/parliamentaryqa.aspx?id=4694

Rapley, V., Robins P., and Thomas P. (2005). A probabilistic chemical sensor model for data fusion. Proceedings from: *7th International Conference on Information Fusion 2005*. Philadelphia, USA.

Sohn, M.D., Reynolds, N., Singh and Gadgil A.J. (2002). Rapidly locating and characterizing pollutant releases in buildings. *Journal of the Air and Waste Management Association,* 2002 , 52, 1422–1432.

THIS PAGE INTENTIONALLY LEFT BLANK

INITIAL DISTRIBUTION LIST

1.   Defense Technical Information Center
          Ft. Belvoir, Virginia

2.   Dudley Knox Library
          Naval Postgraduate School
          Monterey, California

3.   Professor Moshe Kress
          Naval Postgraduate School
          Monterey, California

4.   Professor Rachel Johnson
          Naval Postgraduate School
          Monterey, California

5.   Miss Sng Mui Tiang
          DSO National Laboratories
          Singapore

6.   Miss Elaine See Mei Eng
          DSO National Laboratories
          Singapore

7.   Professor Yeo Tat Soon, Director
          Temasek Defence Systems Institute
          National University of Singapore
          Republic of Singapore

8.   Tan Lai Poh (Ms), Assistant Manager
          Temasek Defence Systems Institute
          National University of Singapore
          Republic of Singapore